DETECTION AND CHARACTERISATION OF EXOPLANETARY SYSTEMS

The contribution of high angular resolution

ROXANNE LIGI

INAF-Osservatorio Astronomico di Brera
Marie Skłodowska-Curie/AstroFIt2 Fellow

Seminar at OCA - 20 February 2018

In collaboration with:

Mickaël Bonnefoy (IPAG)
Orlagh Creevey (OCA)
Aurélien Crida (OCA)
Caroline Dorn (Univ. Zurich)
Yveline Lebreton (Univ. Rennes/OBSPM)
Denis Mourard (OCA)
Nicolas Nardetto (OCA)
Mathias Schultheis (OCA)
SPHERE consortium
VEGA team
...

Osservatorio Astronomico di Brera INAF

AstroFIt 2 Astronomy Fellowships in Italy

FROM THE FORMATION TO THE CHARACTERISATION OF EXOPLANETS

Planetary formation: 2 scenarios

Gravitational instability

- Giant planets, large separation (> 50 au)

Core Accretion

- Rocky planets
- Giant planets close to the star (<50 au)

FROM THE FORMATION TO THE CHARACTERISATION OF EXOPLANETS

Planetary formation: 2 scenarios

Direct Imaging: detection of disks and planets

Gravitational instability

- Giant planets, large separation (> 50 au)

Core Accretion

- Rocky planets
- Giant planets close to the star (<50 au)

Direct Imaging: detection of disks and planets

FROM THE FORMATION TO THE CHARACTERISATION OF EXOPLANETS

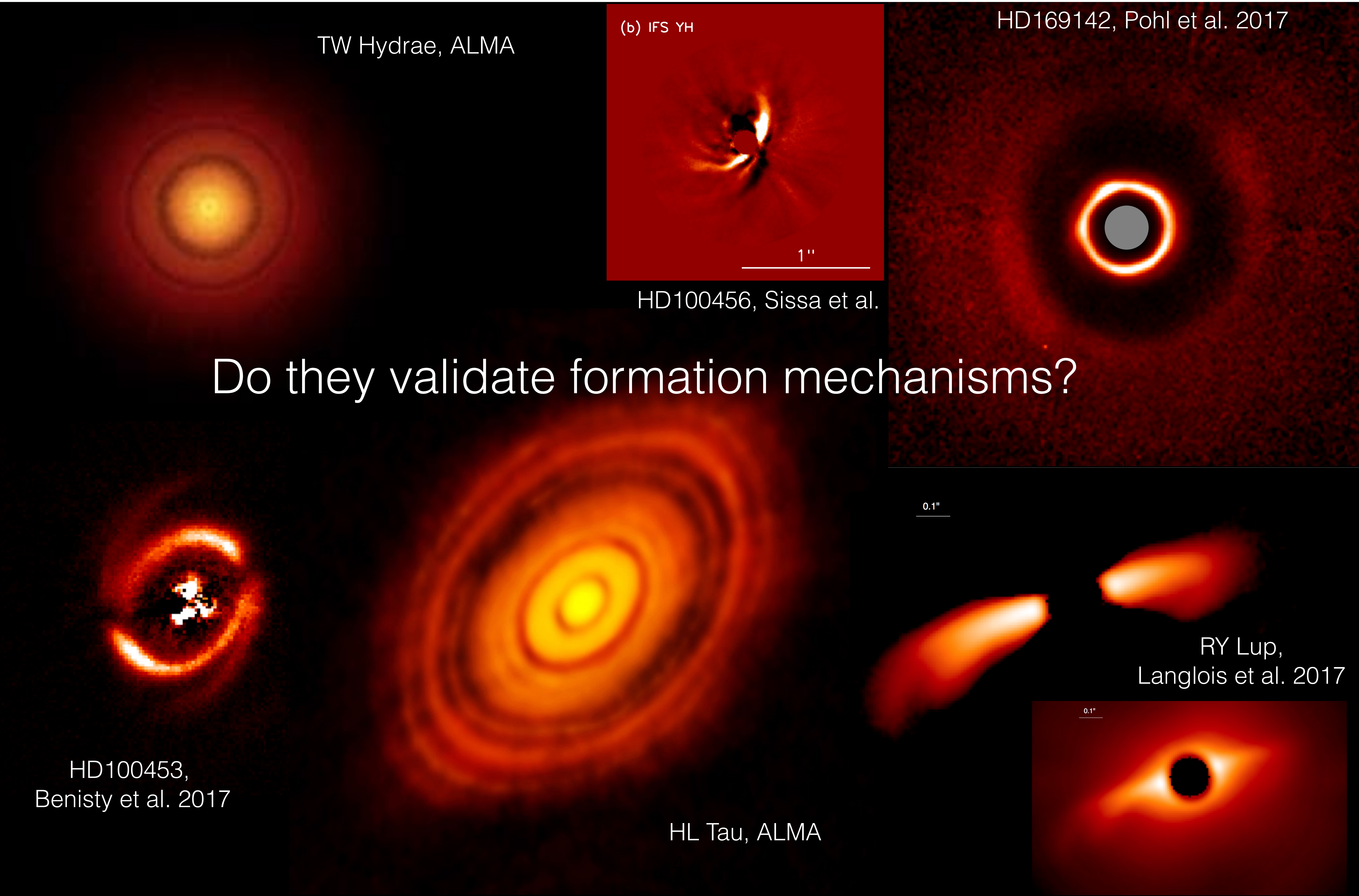

Do they validate formation mechanisms?

FROM THE FORMATION TO THE CHARACTERISATION OF EXOPLANETS

Planetary formation: 2 scenarios

Direct Imaging: detection of disks and planets

Gravitational instability

- Giant planets, large separation (> 50 au)

Core Accretion

- Rocky planets
- Giant planets close to the star (<50 au)

Direct Imaging: detection of disks and planets

Physical properties

m_p, R_p, ρ_p

FROM THE FORMATION TO THE CHARACTERISATION OF EXOPLANETS

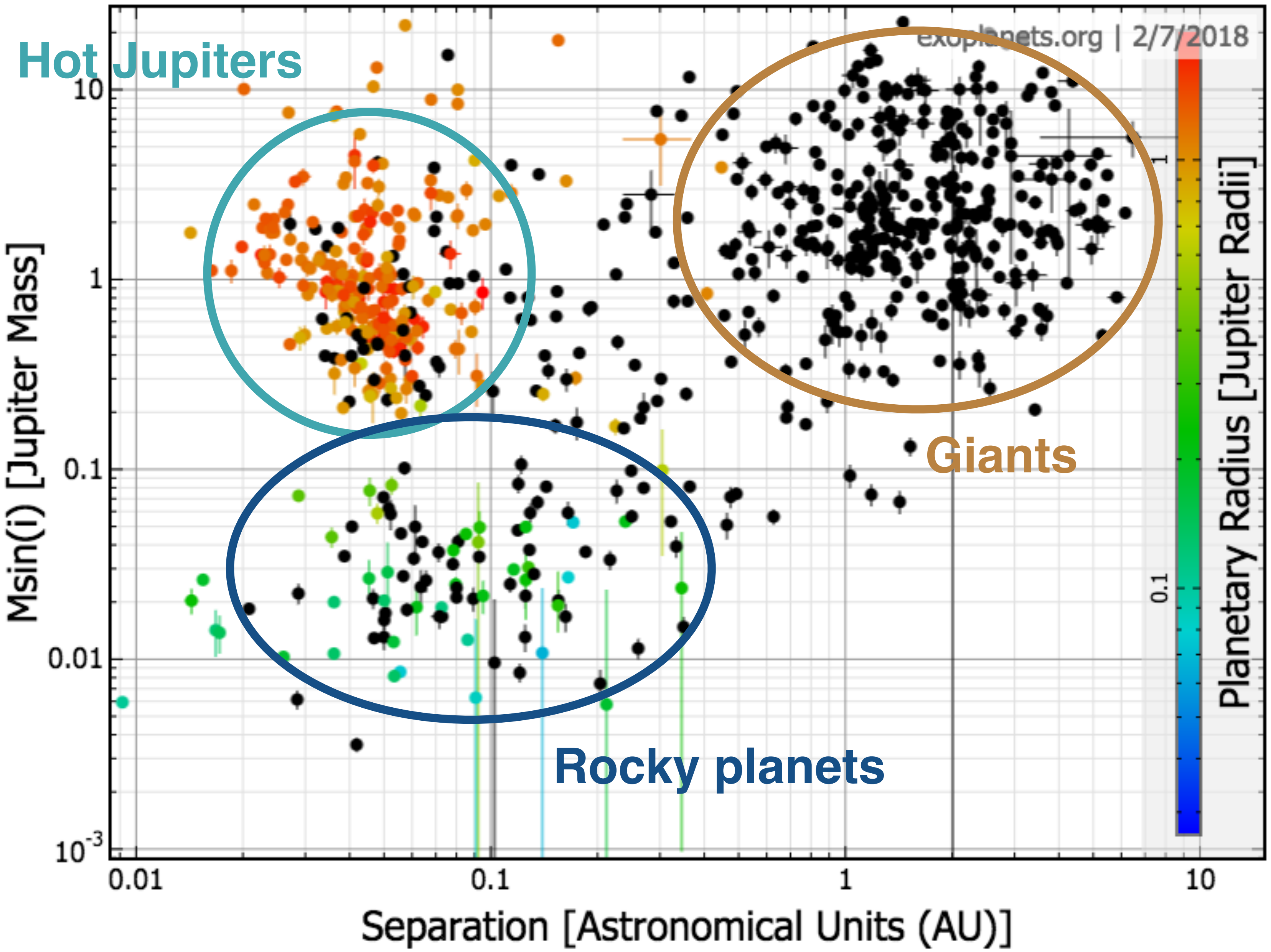

- 3 groups of exoplanets
- instrumental bias?

A majority of Super-Earths and mini neptune

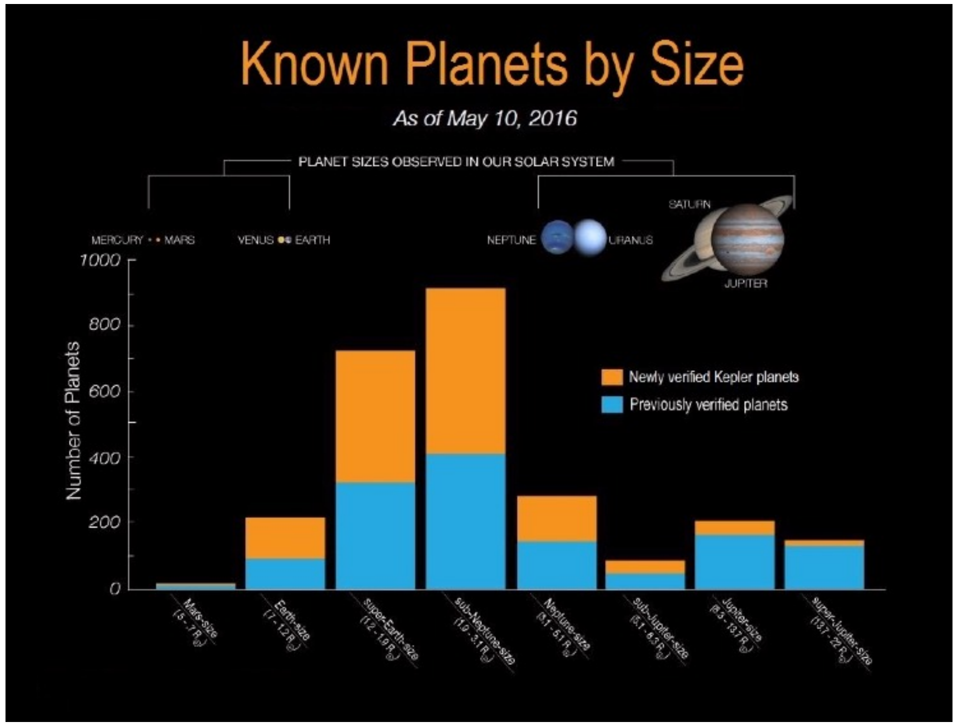

FROM THE FORMATION TO THE CHARACTERISATION OF EXOPLANETS

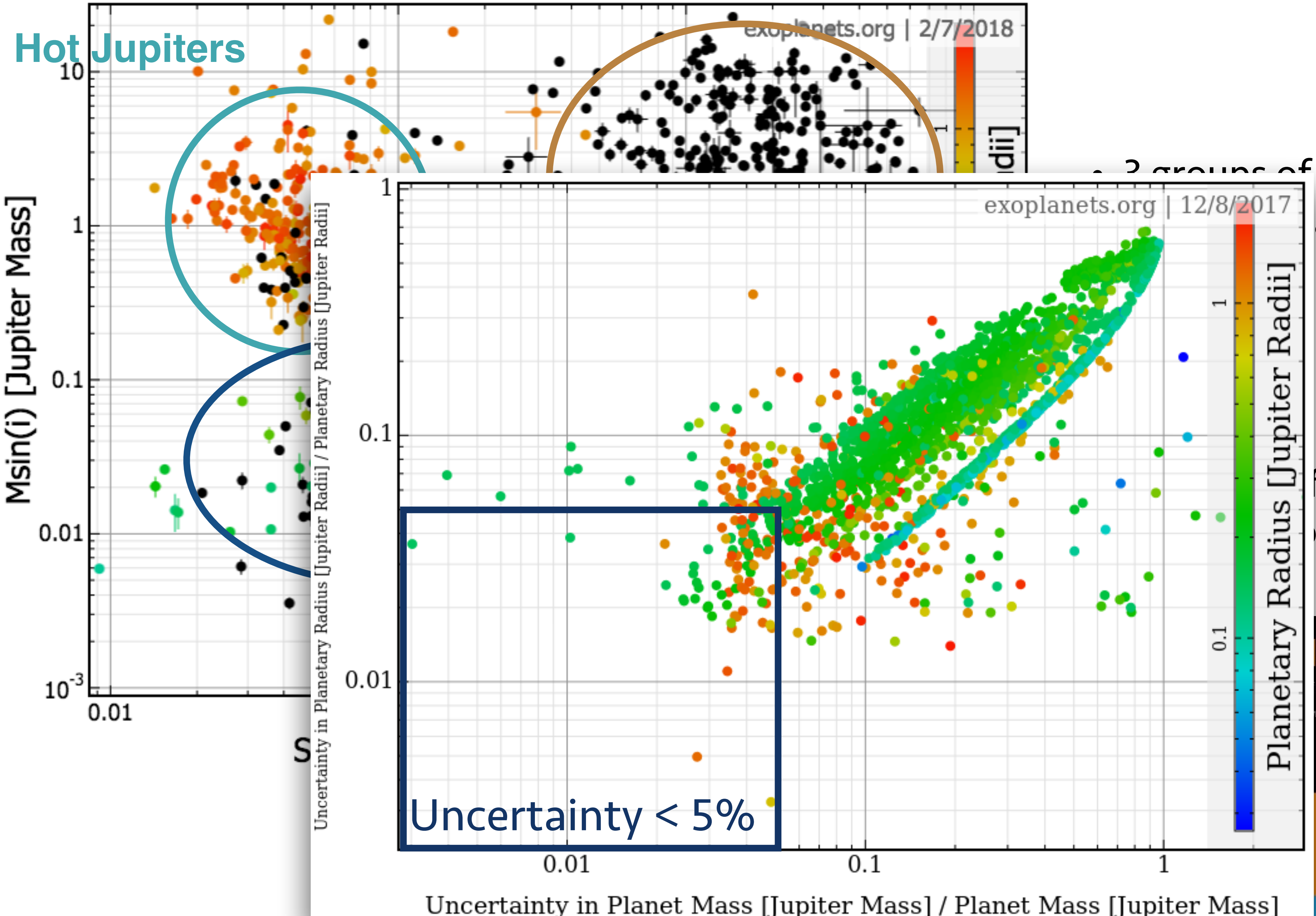

- 3 groups of exoplanets
- al bias?

f Super-Earths
tune

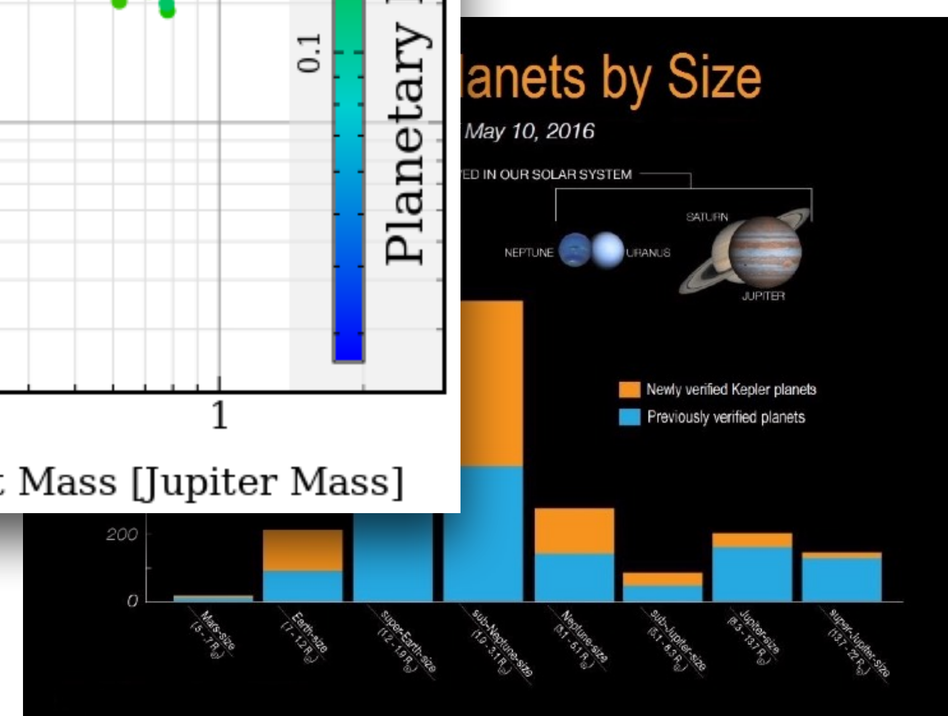

FROM THE FORMATION TO THE CHARACTERISATION OF EXOPLANETS

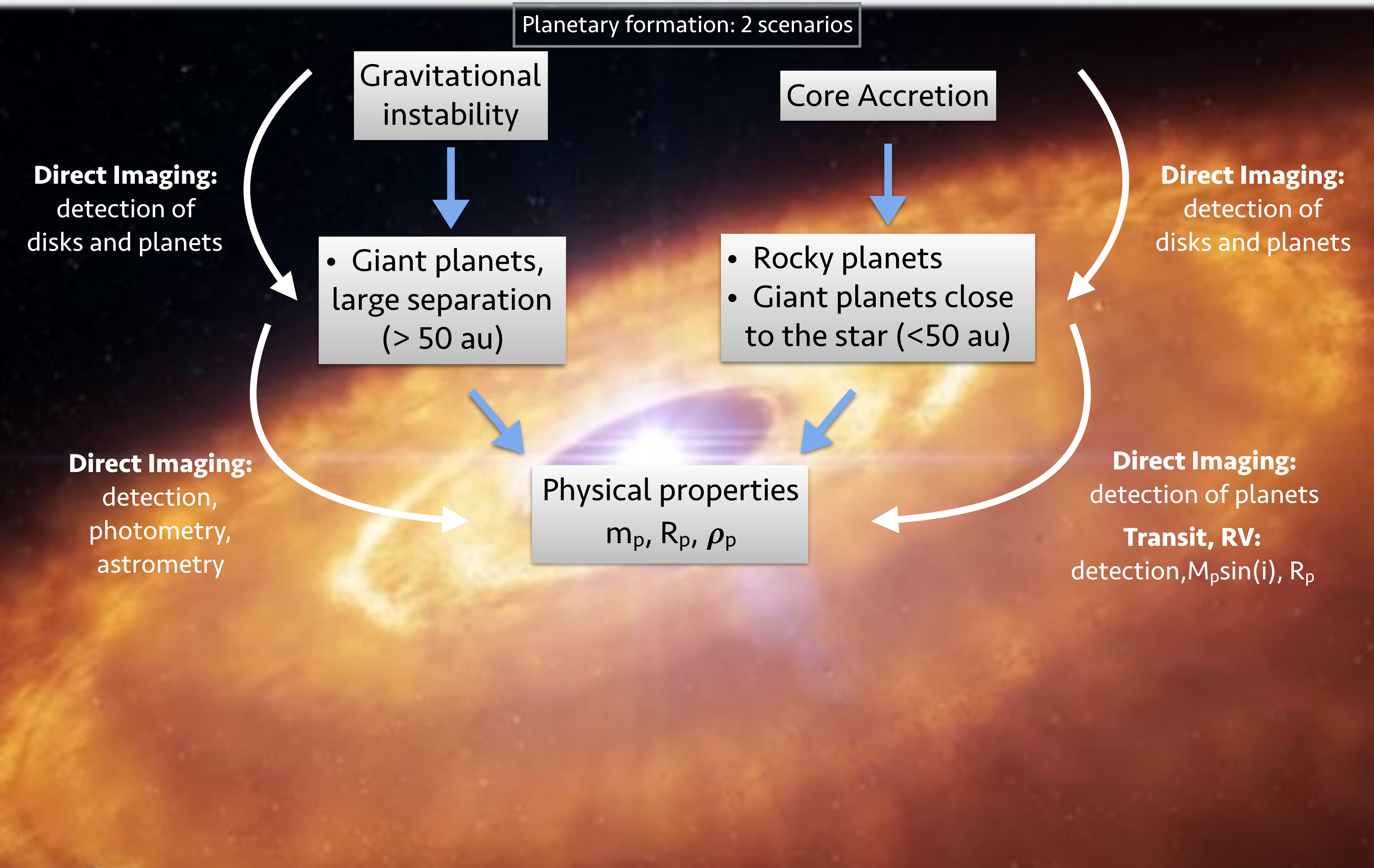

FROM THE FORMATION TO THE CHARACTERISATION OF EXOPLANETS

Planetary formation: 2 scenarios

Gravitational instability

- Giant planets, large separation (> 50 au)

Core Accretion

- Rocky planets
- Giant planets close to the star (<50 au)

Direct Imaging: detection of disks and planets

Direct Imaging: detection of disks and planets

Direct Imaging: detection, photometry, astrometry

Direct Imaging: detection of planets

Transit, RV: detection, $M_p \sin(i)$, R_p

Physical properties

m_p, R_p, ρ_p

$R_\star$, $M_\star$, $\rho_\star$

FROM THE FORMATION TO THE CHARACTERISATION OF EXOPLANETS

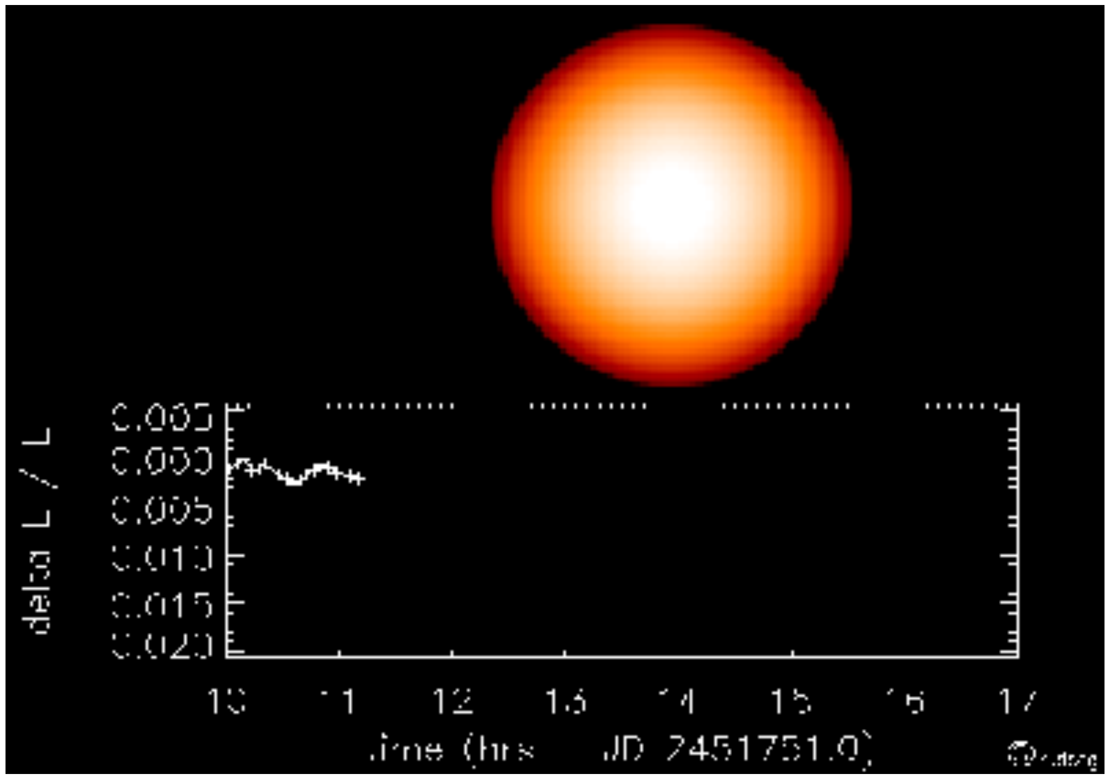

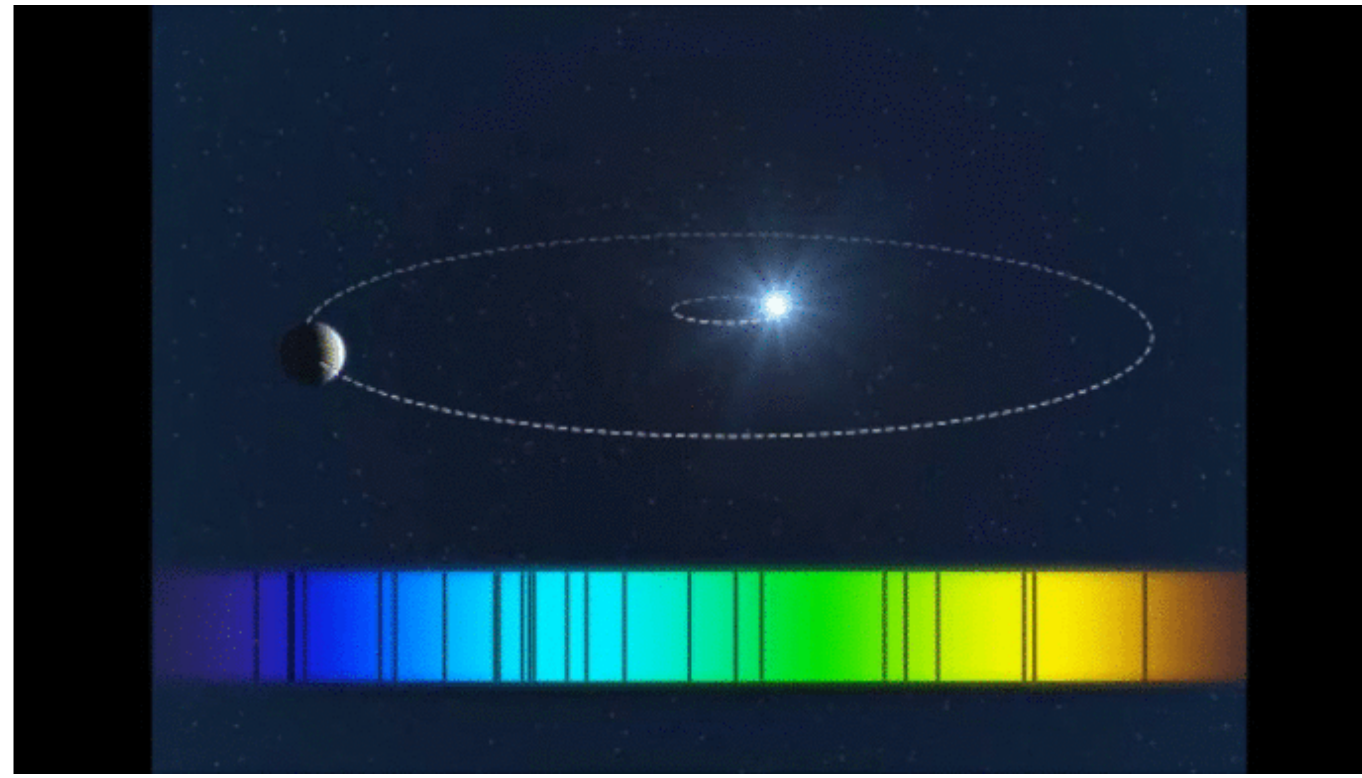

$$\frac{\Delta F}{F} = \left(\frac{R_P}{R_\star}\right)^2$$

$$\frac{(m_p \sin i)^3}{(M_\star + m_p)^2} = \frac{P}{2\pi G} K^3 (1-e)^{3/2}$$

→ Dependent on **R★** and **M★**

FROM THE FORMATION TO THE CHARACTERISATION OF EXOPLANETS

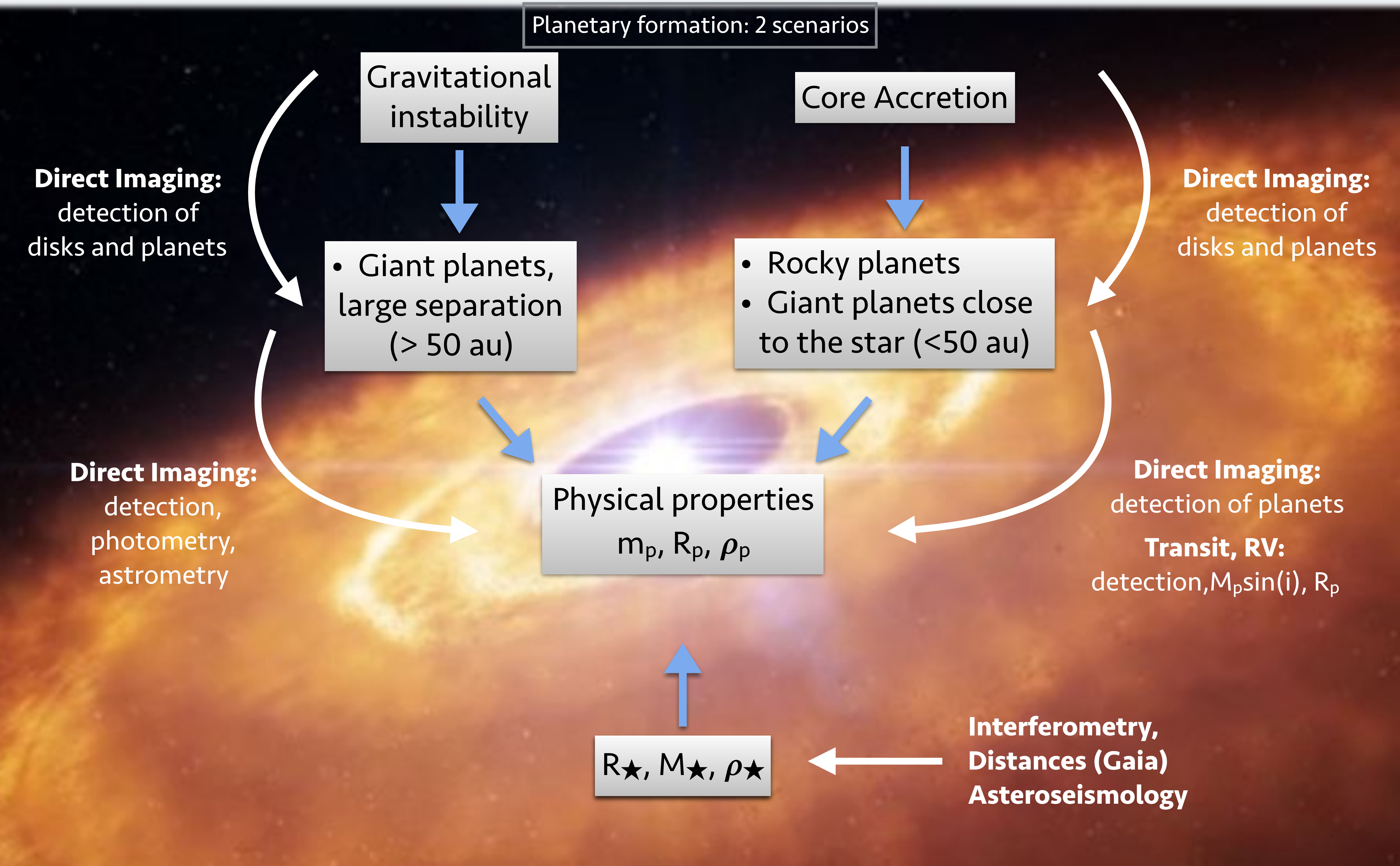

FROM THE FORMATION TO THE CHARACTERISATION OF EXOPLANETS

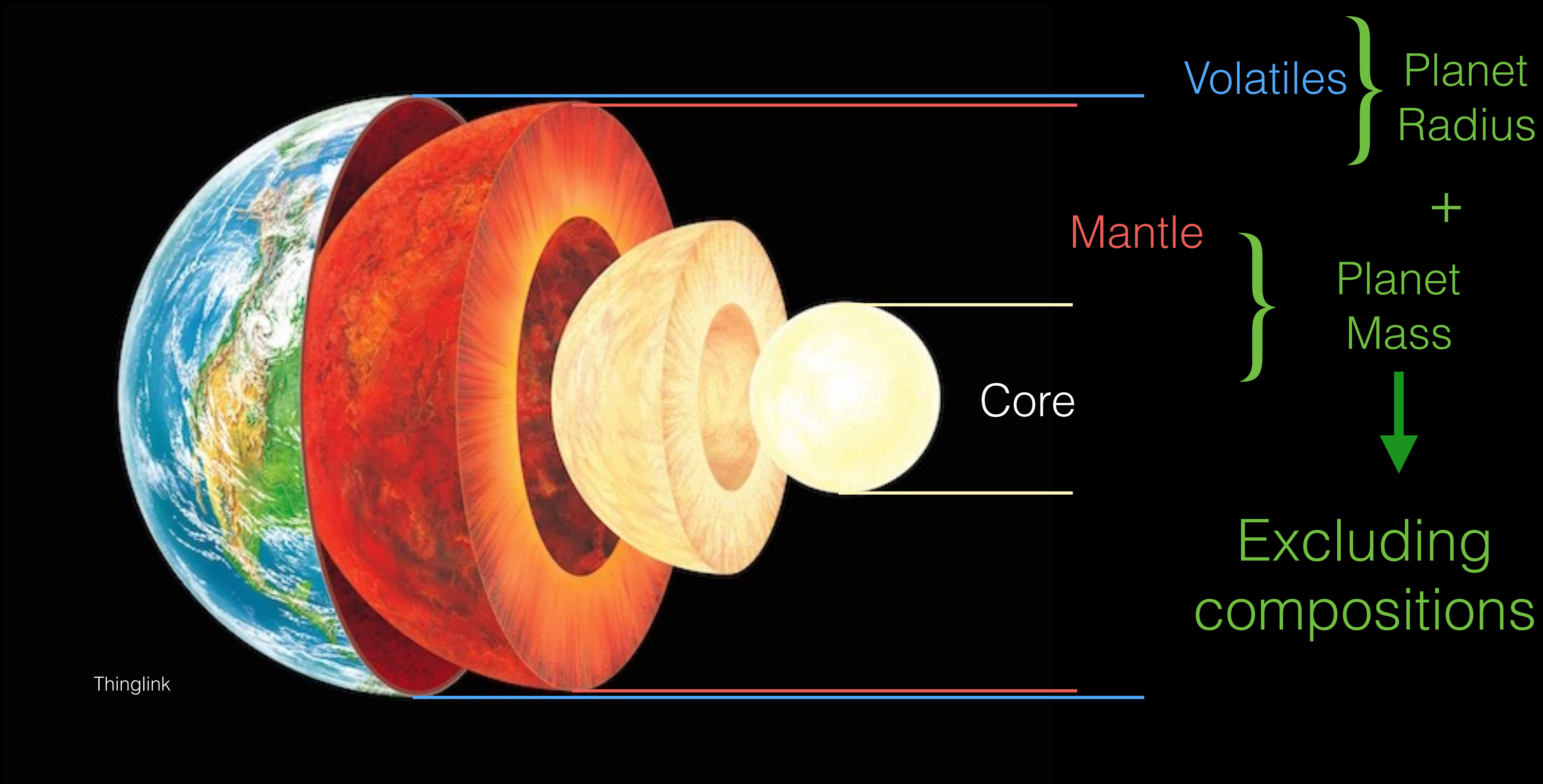

FROM THE FORMATION TO THE CHARACTERISATION OF EXOPLANETS

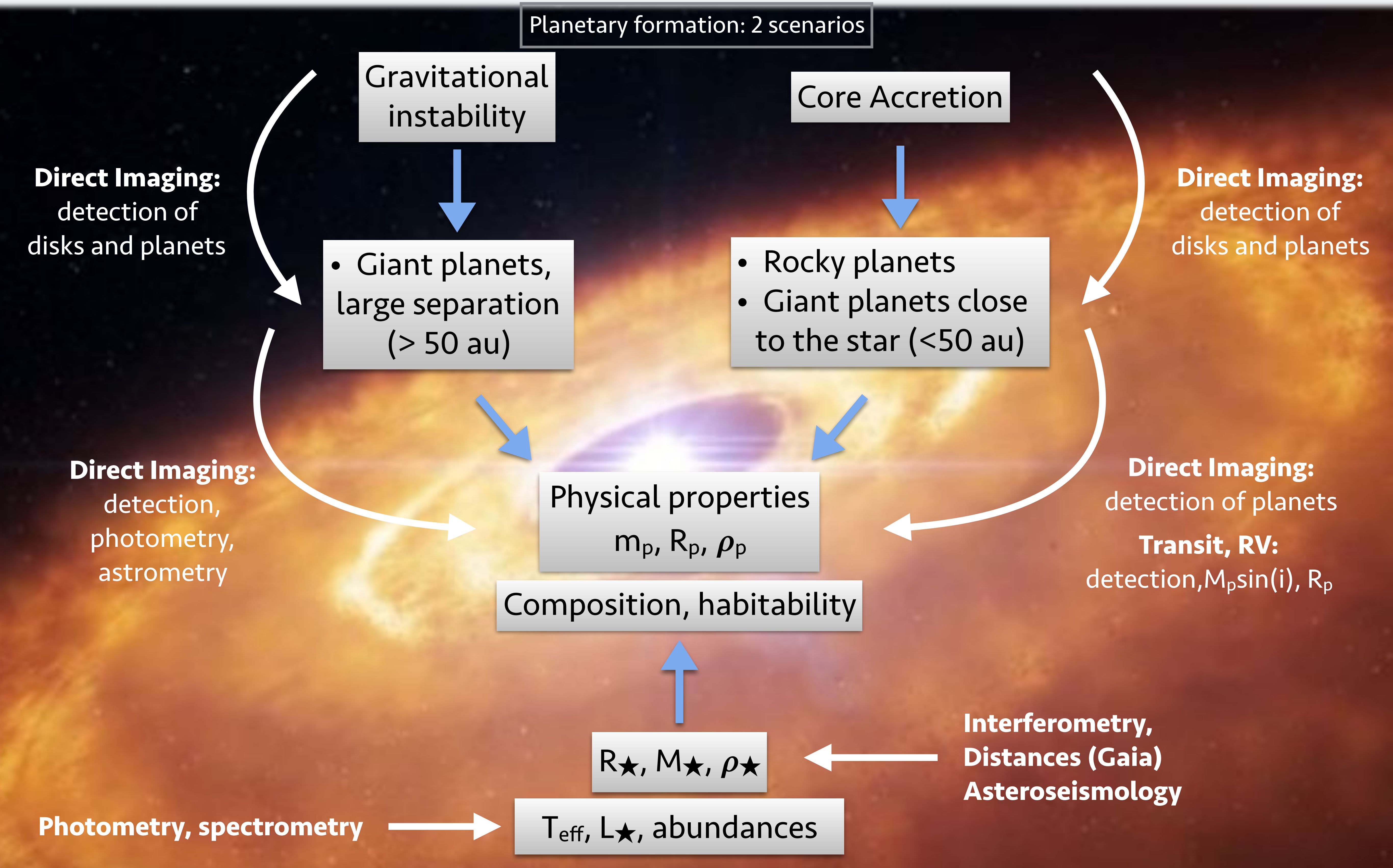

FROM THE FORMATION TO THE CHARACTERISATION OF EXOPLANETS

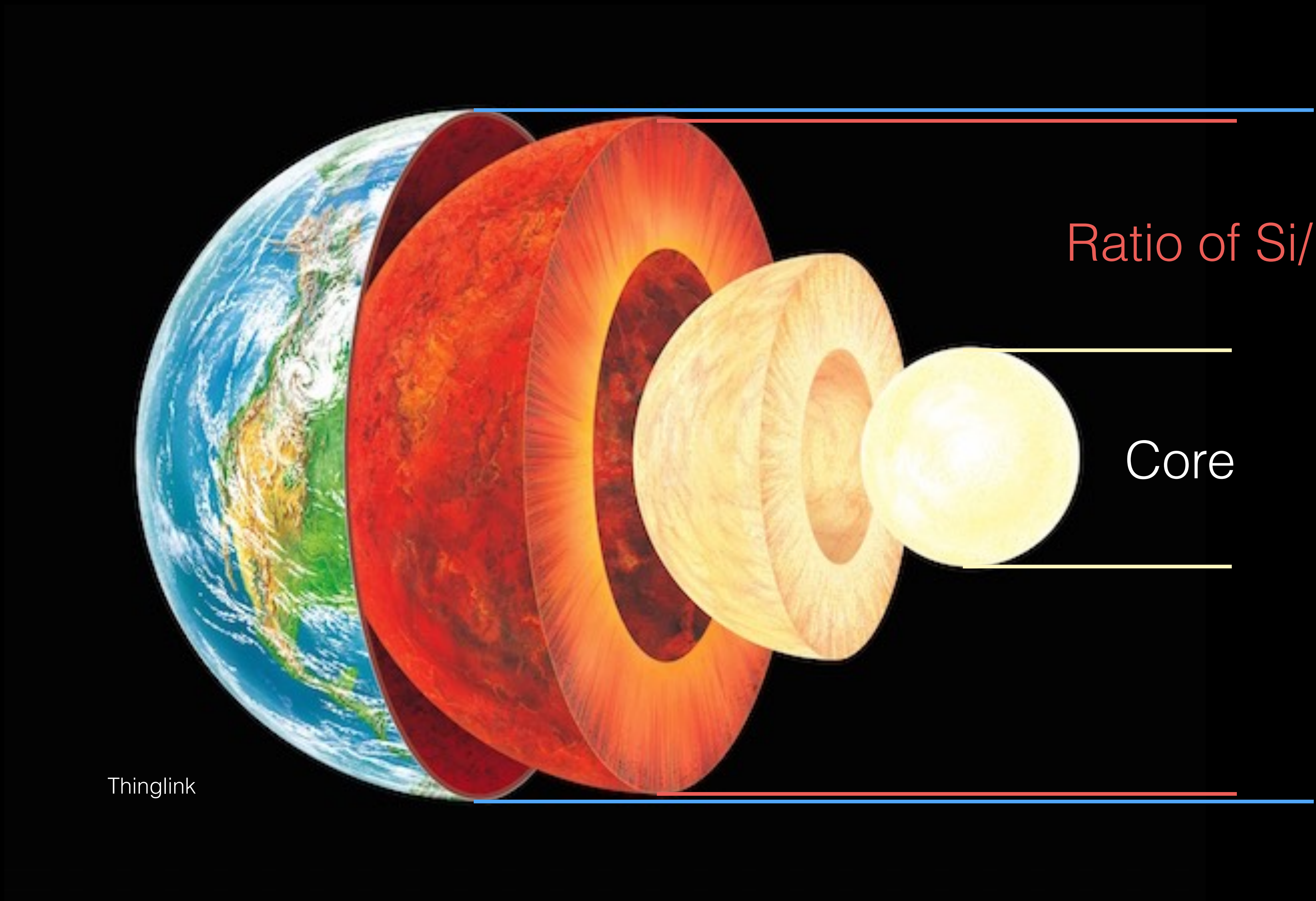

Volatiles

Ratio of Si/Fe and Si/Mg

Core

Excluding compositions

FROM THE FORMATION TO THE CHARACTERISATION OF EXOPLANETS

Planetary formation: 2 scenarios

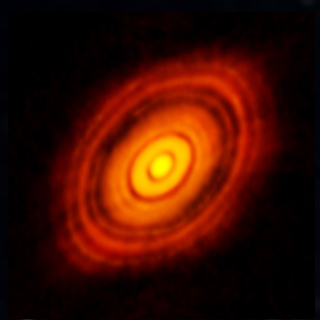

Gravitational instability

- Giant planets, large separation (> 50 au)

Core Accretion

- Rocky planets
- Giant planets close to the star (<50 au)

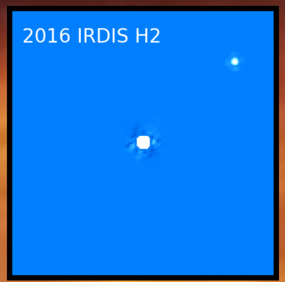

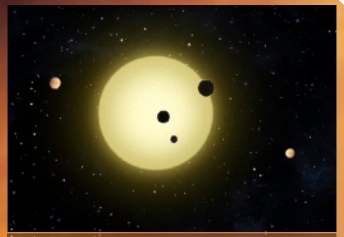

Physical properties

m_p, R_p, ρ_p

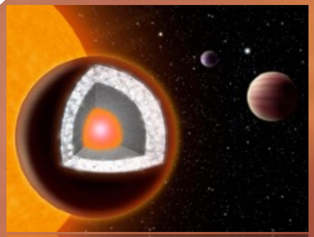

Composition, habitability

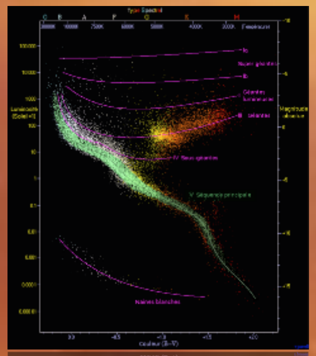

$R_\star$, $M_\star$, $\rho_\star$

T_{eff}, $L_\star$, abundances

FROM THE FORMATION TO THE CHARACTERISATION OF EXOPLANETS

Planetary formation: 2 scenarios

Gravitational instability

- Giant planets, large separation (> 50 au)

Core Accretion

- Rocky planets
- Giant planets close to the star (<50 au)

Physical properties
m_p, R_p, ρ_p

Composition, habitability

$R_\star$, $M_\star$, $\rho_\star$

T_{eff}, $L_\star$, abundances

Limitations

- Reserved to bright stars
- Difficult to mix techniques because of stellar properties/ instrumental specificities

High Angular Resolution:

- Interferometry
- Direct imaging

Appropriate for exoplanetary detection and characterisation

OUTLINE

- Introduction: from the formation to the characterisation of exoplanets

- Characterisation of exoplanetary systems with interferometry

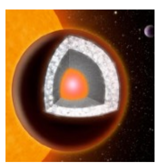

- Getting the most out of it: 55 Cnc

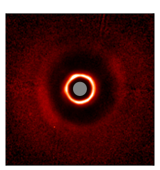

- Detection of exoplanets with direct imaging:
  insights in the system of HD169142

- Formation mechanisms: the challenging case of GJ504

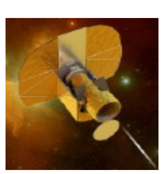

- Conclusion and perspectives

DIRECT MEASUREMENTS OF ANGULAR DIAMETERS

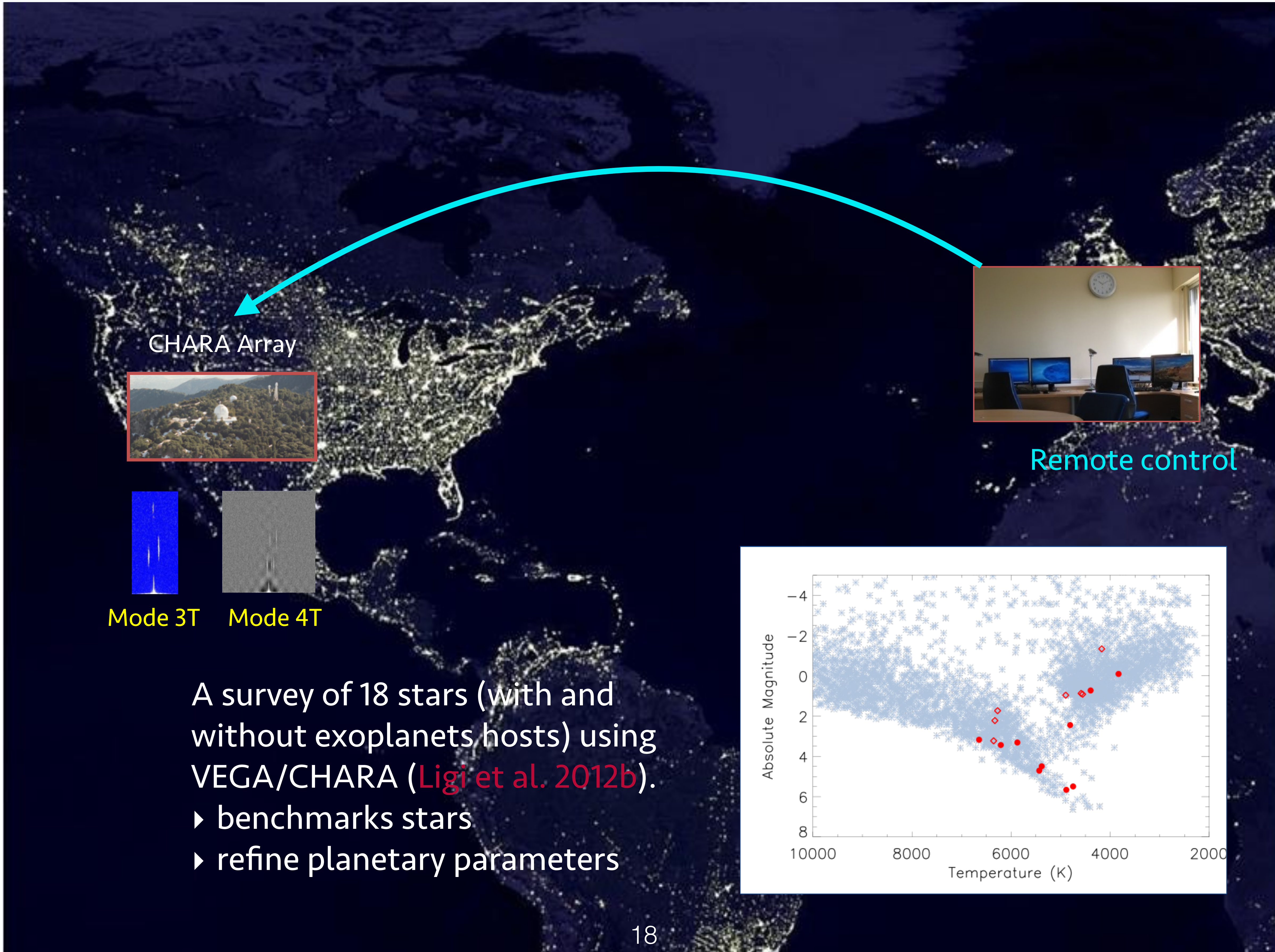

A survey of 18 stars (with and without exoplanets hosts) using VEGA/CHARA (Ligi et al. 2012b).

- benchmarks stars
- refine planetary parameters

DIRECT MEASUREMENTS OF ANGULAR DIAMETERS

Interferometric angular diameter → ← Hipparcos distance

$$R_{\star[R_\odot]} = \frac{\theta_{\mathrm{LD[mas]}} \times d_{\mathrm{[pc]}}}{9.305} \; .$$

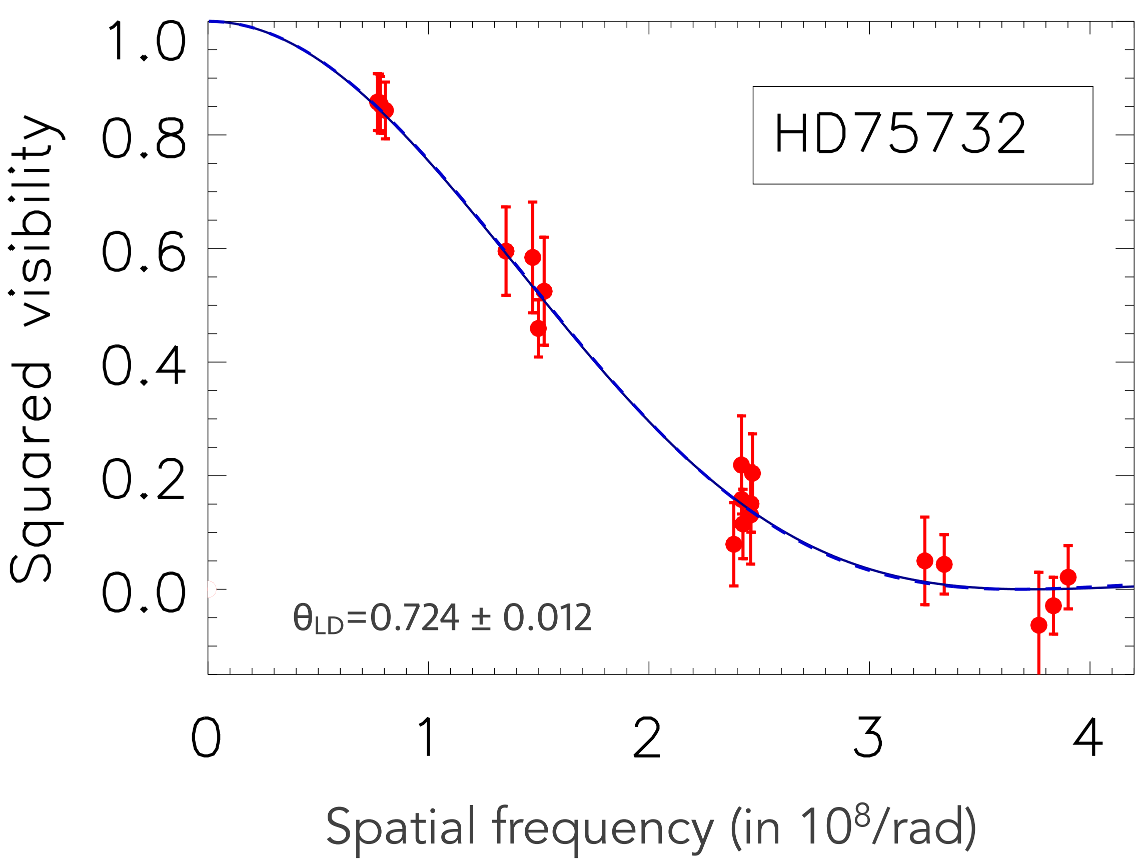

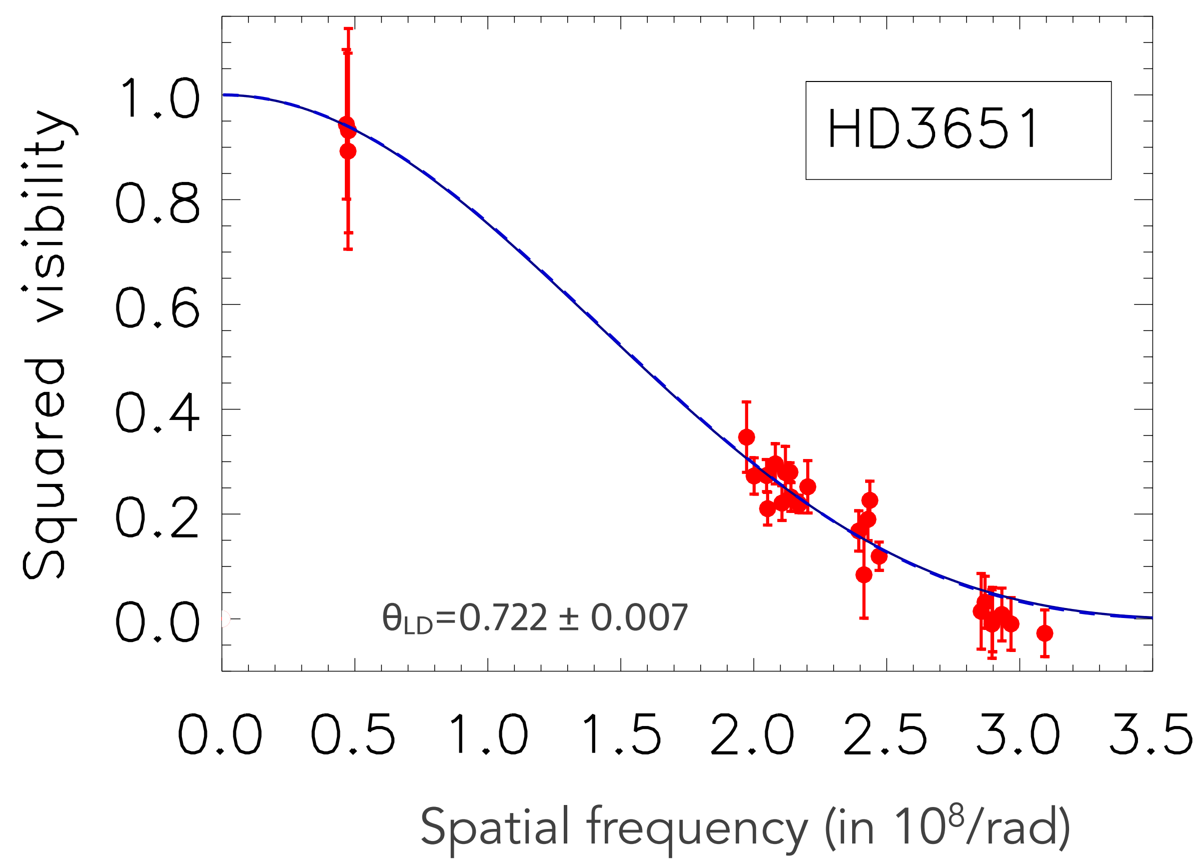

- Examples of visibility curves from VEGA instrument
- Average accuracy: 1.9 % on diameters (θ_{LD}) and 3% on radii ($R_\star$).

Ligi et al. (2012a, 2016)

FROM ANGULAR DIAMETERS TO LUMINOSITY

- Photometry from VizieR Photometry Viewer
- Fit from BASEL library spectra
- Take into account log(g), Av, [Fe/H]
- Average accuracy on $T_{\mathrm{eff},\star}$: 57K in average

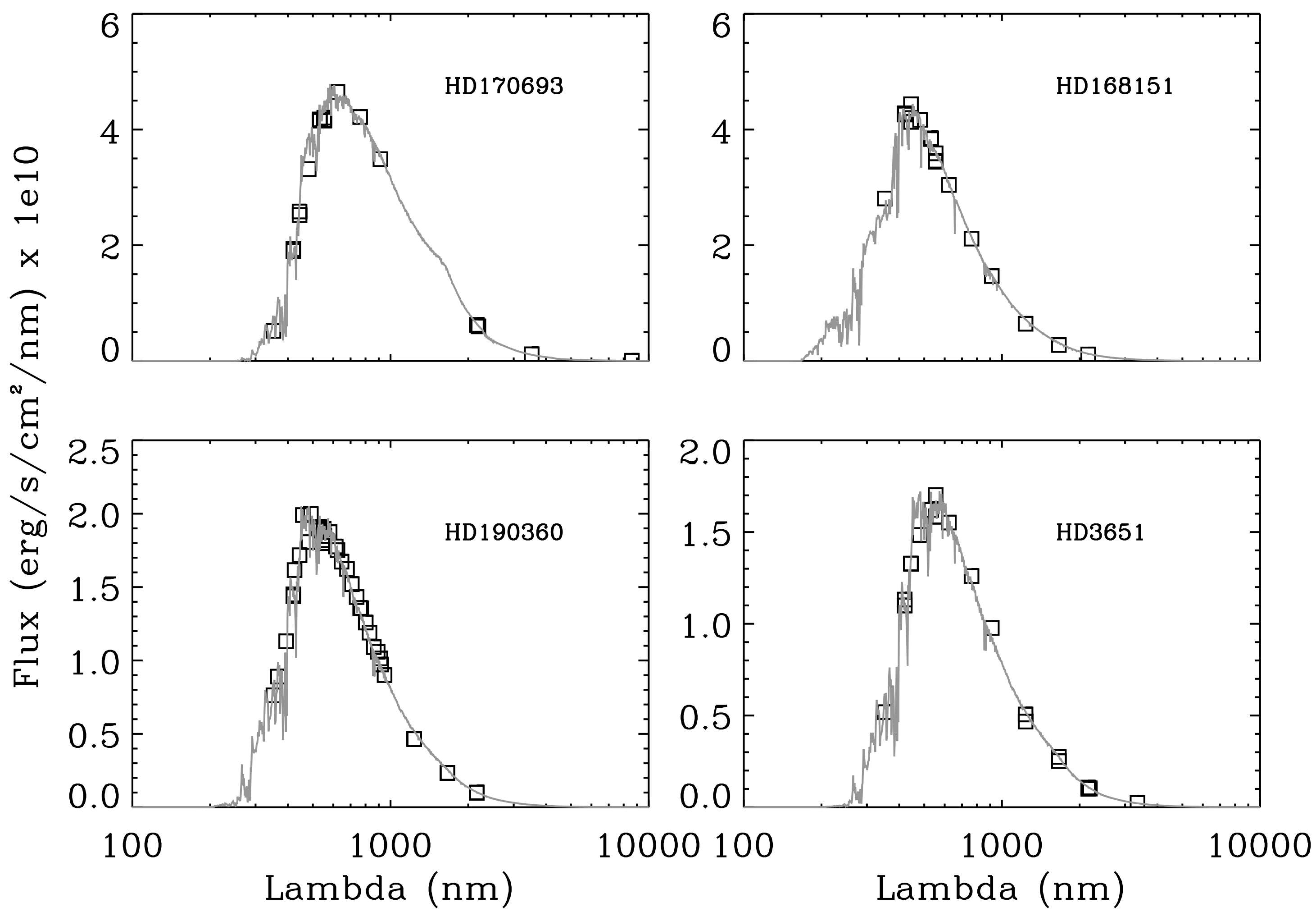

SED

$$T_{\mathrm{eff},\star} = \left(\frac{4 \times F_{\mathrm{bol}}}{\sigma_{\mathrm{SB}} \theta_{\mathrm{LD}}^2} \right)^{0.25} \rightarrow L_\star = 4\pi d^2 F_{\mathrm{bol}}$$

Interferometric angular diameter

DETERMINATION OF STELLAR MASSES AND AGES

Method: Interpolation of PARSEC stellar models (*Bressan et al. 2012*).

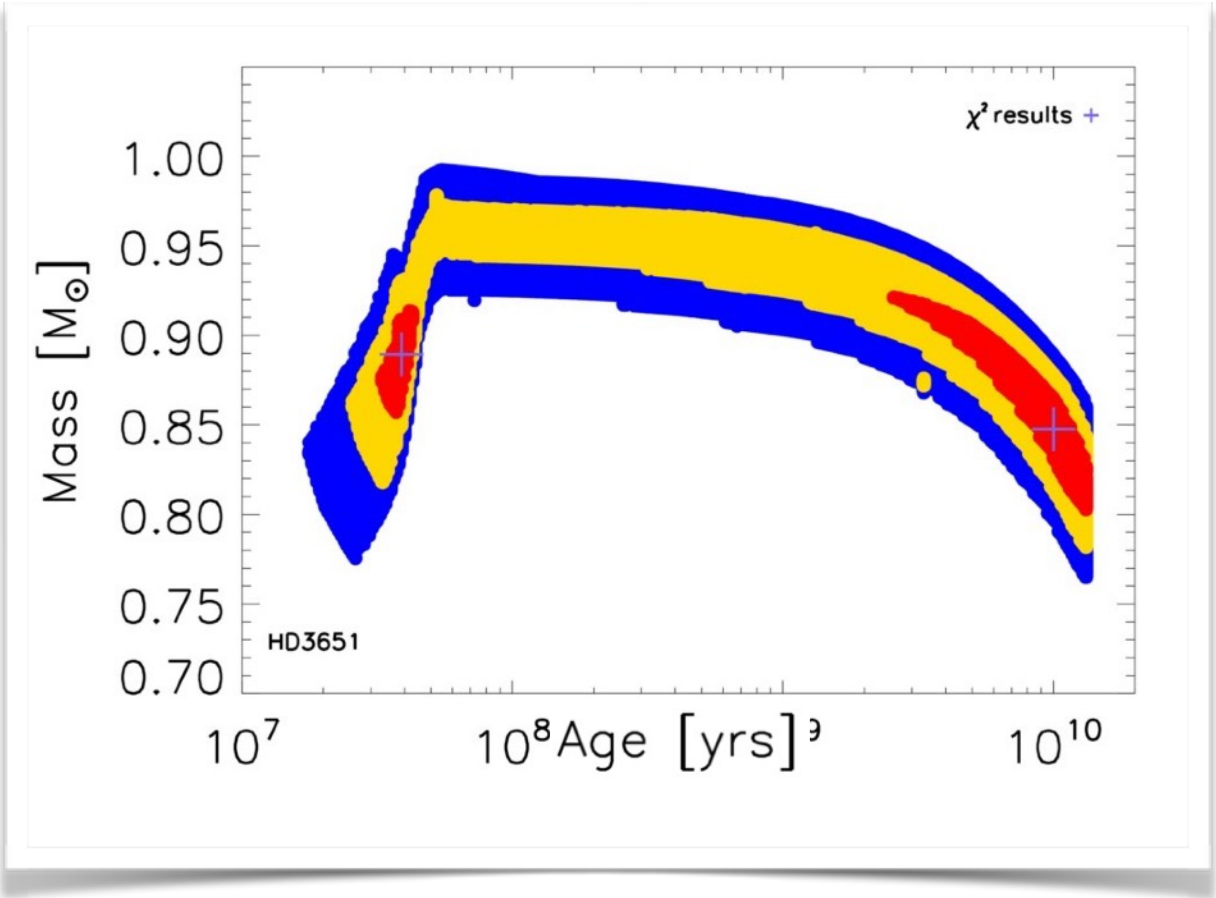

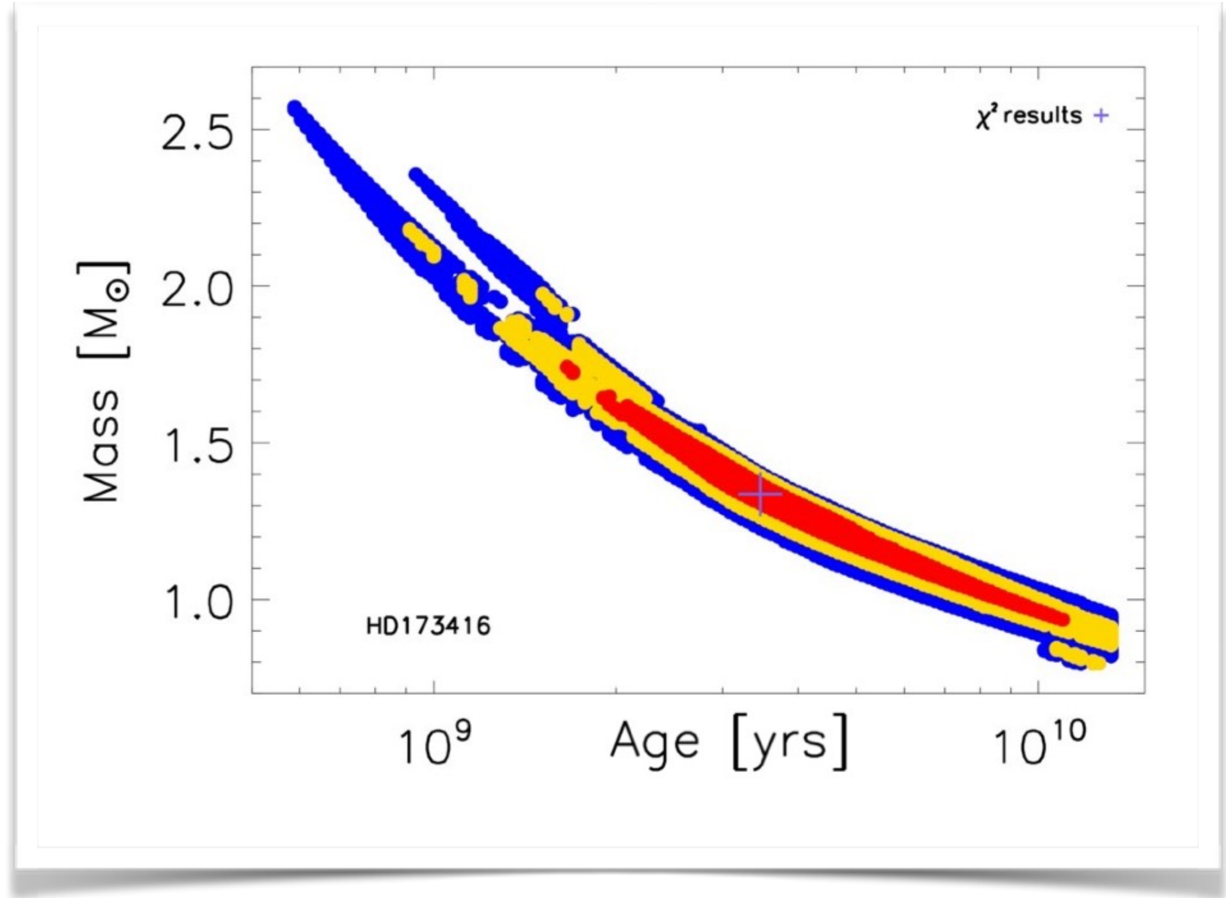

- This corresponds to the approximate likelihood map in the ($M_\star$, age$_\star$) for which each term of the equation $\chi^2 = \frac{(L - L_\star)^2}{{\sigma_{L_\star}}^2} + \frac{(T_{\rm eff} - T_{{\rm eff},\star})^2}{{\sigma_{T_{{\rm eff},\star}}}^2} + \frac{([{\rm M/H}] - [{\rm M/H}]_\star)}{{\sigma_{[{\rm M/H}]_\star}}^2}$ is less than 1, 2, 3.
- Then, least squares to give a value.

DETERMINATION OF STELLAR MASSES AND AGES

Method: Interpolation of PARSEC stellar models (*Bressan et al. 2012*).

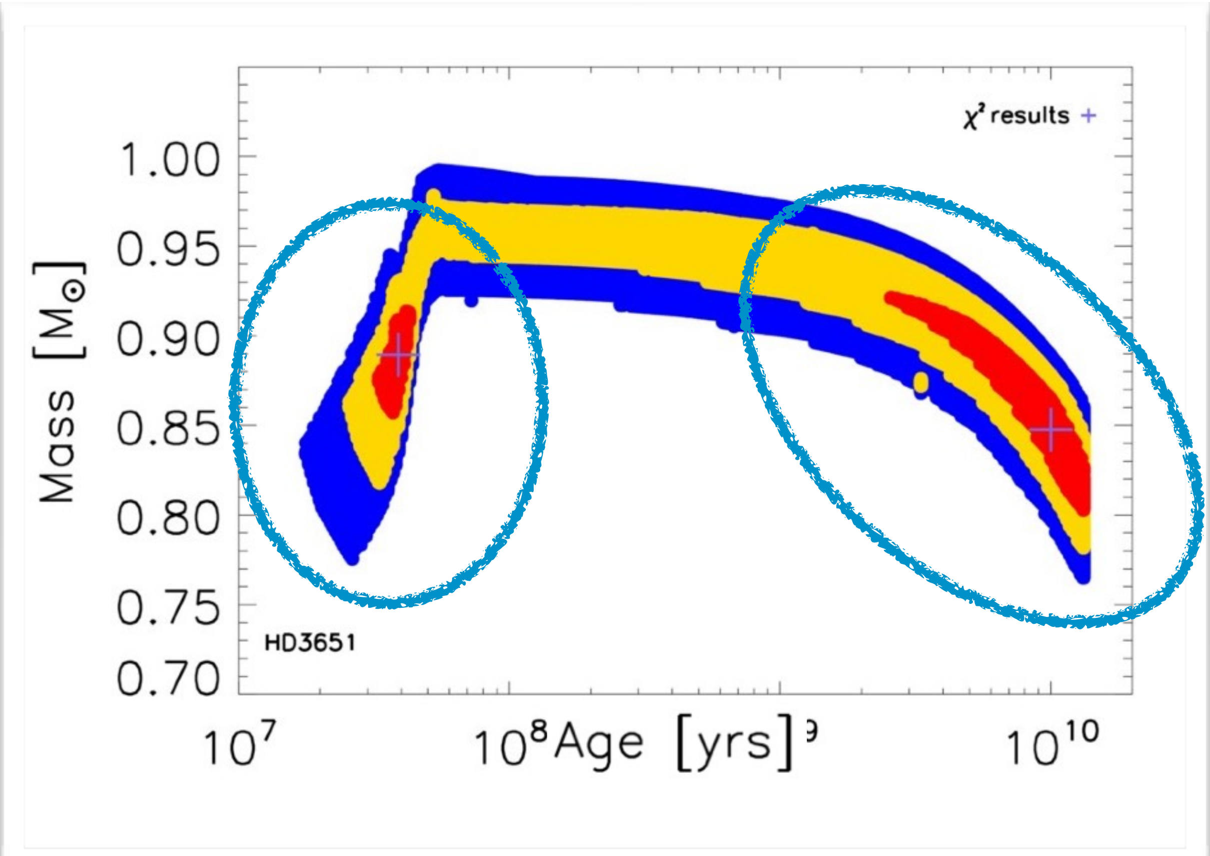

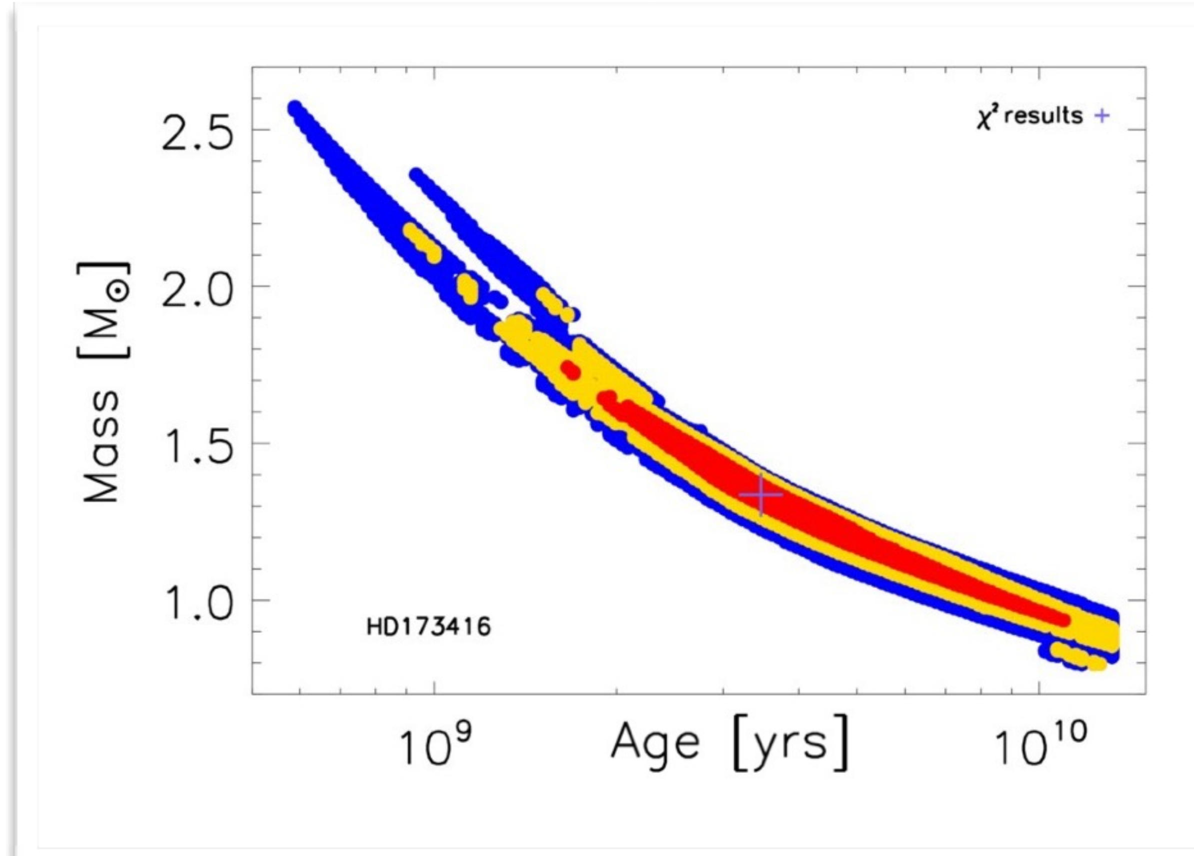

- $\mathcal{L}$ shows 2 different peaks for many MS stars:
  an old solution: > 400 Myrs
  a young solution: < 400 Myrs

→ Need additional stellar properties (gyrochronology, chromospheric activity, Lithium abundance...) to validate the age.

- $M_\star$ and $age_\star$ are not independent
- Clear negative correlation for the old solution

DETERMINATION OF STELLAR MASSES AND AGES

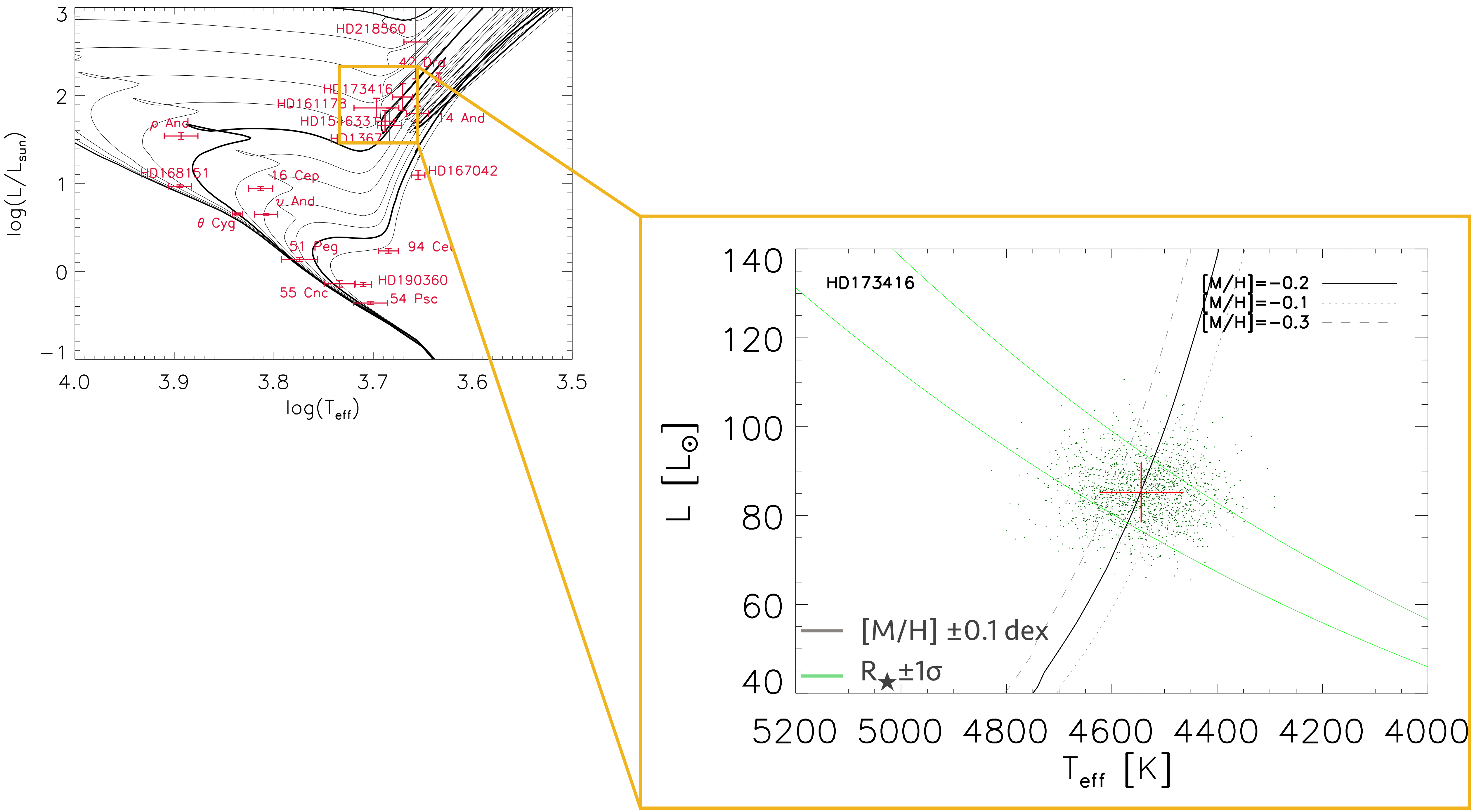

DETERMINATION OF STELLAR MASSES AND AGES

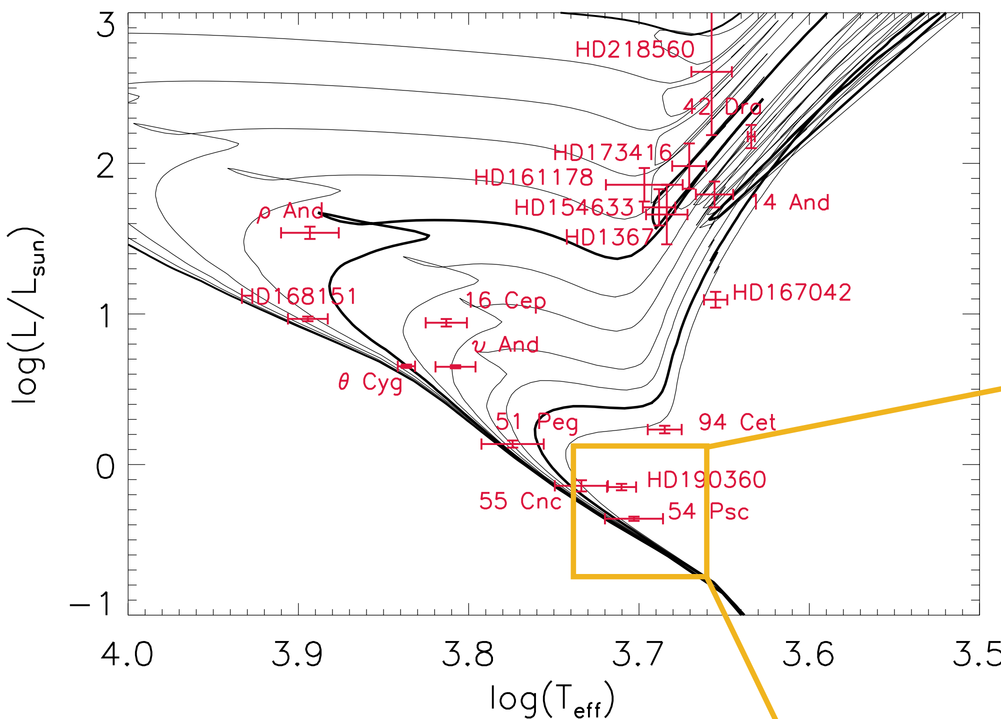

Accuracy on ages: ~ Myrs and Gyrs

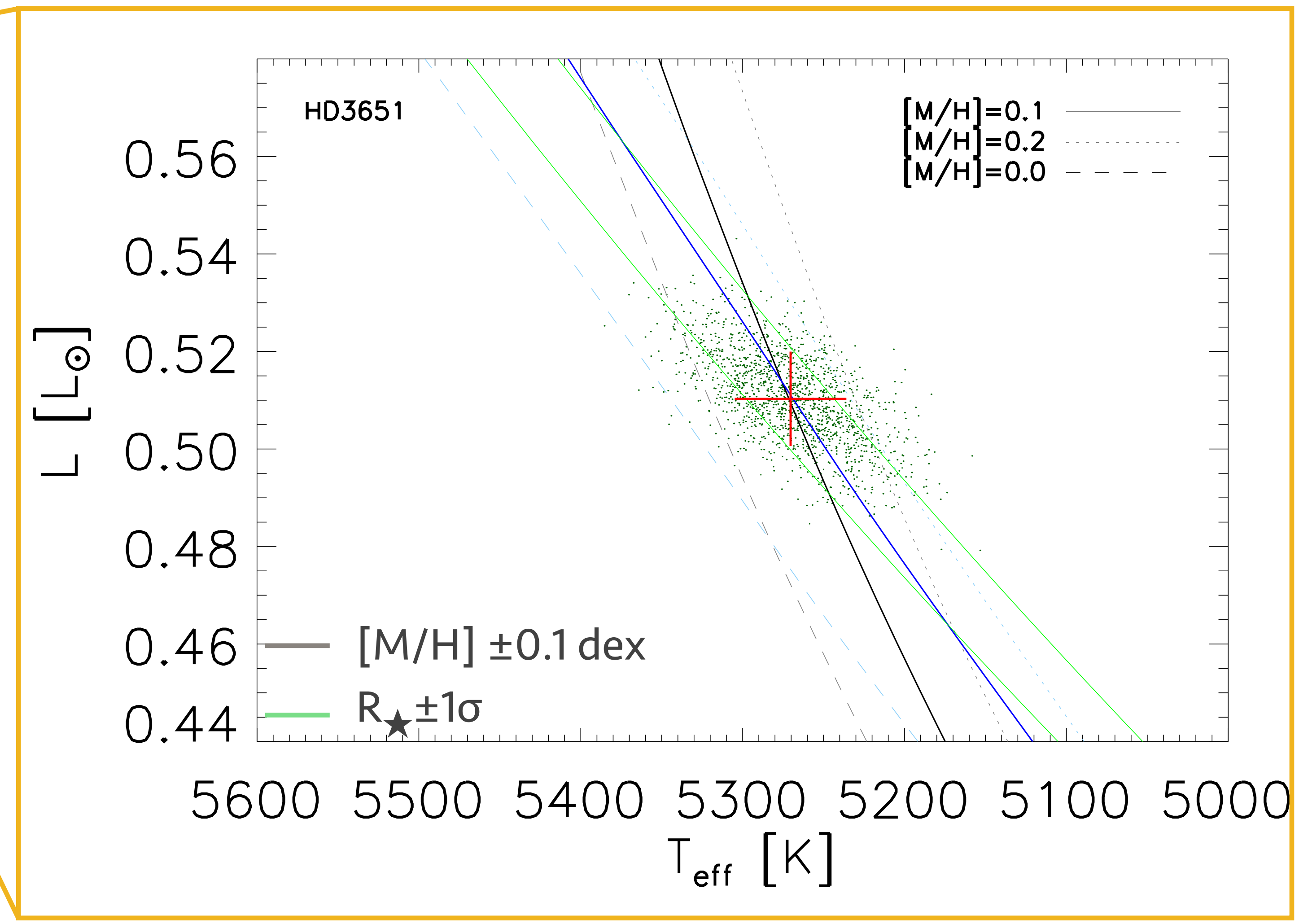

Average accuracy on masses:

- 7.6% for old solutions
- 10% for young solutions

FROM STELLAR PARAMETERS TO EXOPLANET PROPERTIES

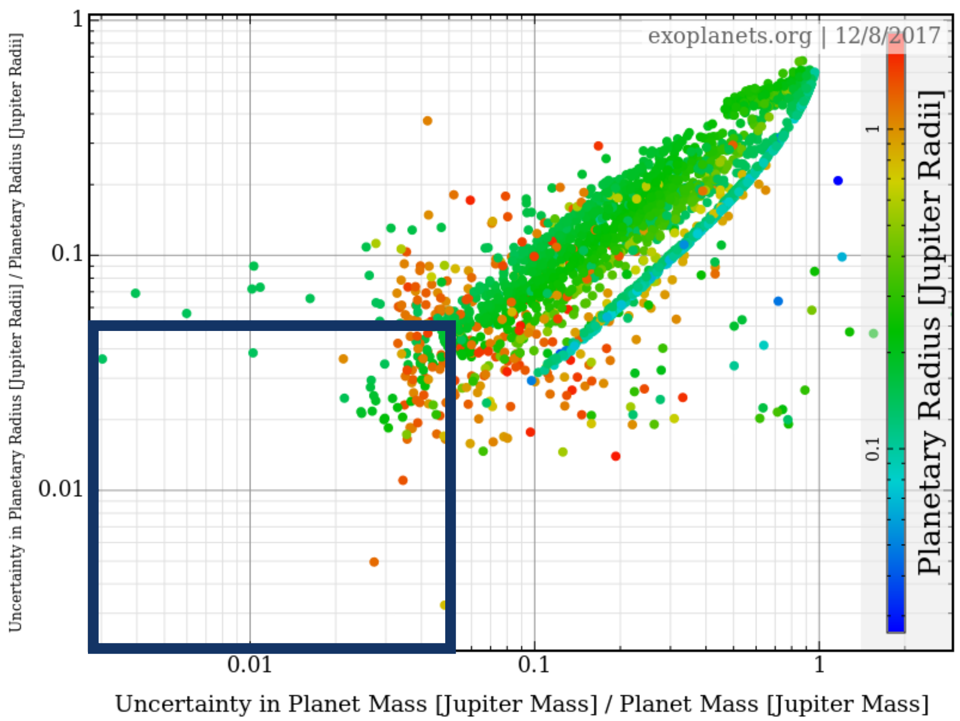

- Usually: Radial Velocity (RV) detections
- Thus we obtain $m_p\sin(i)$ from RV and stellar masses:

$$m_\mathrm{p}\sin(i) = \frac{M_\star^{2/3}P^{1/3}K(1-e^2)^{1/2}}{(2\pi G)^{1/3}}$$

- Habitable Zone (HZ) (*Jones et al. 2006*) $\propto L_\star/T_{\mathrm{eff},\star}^2$
- Semi-major axis $\propto M_\star^{1/3}$

→ New estimations of HZ, semi-major axis (au) and $m_p\sin(i)$ from our measurements.

FROM STELLAR PARAMETERS TO EXOPLANET PROPERTIES

New determinations:
- semi-major axis *a*,
- habitability zone,
- $m_p\sin(i)$

Decrease the uncertainties for 18 exoplanets

Transiting exoplanet 55 Cnc e

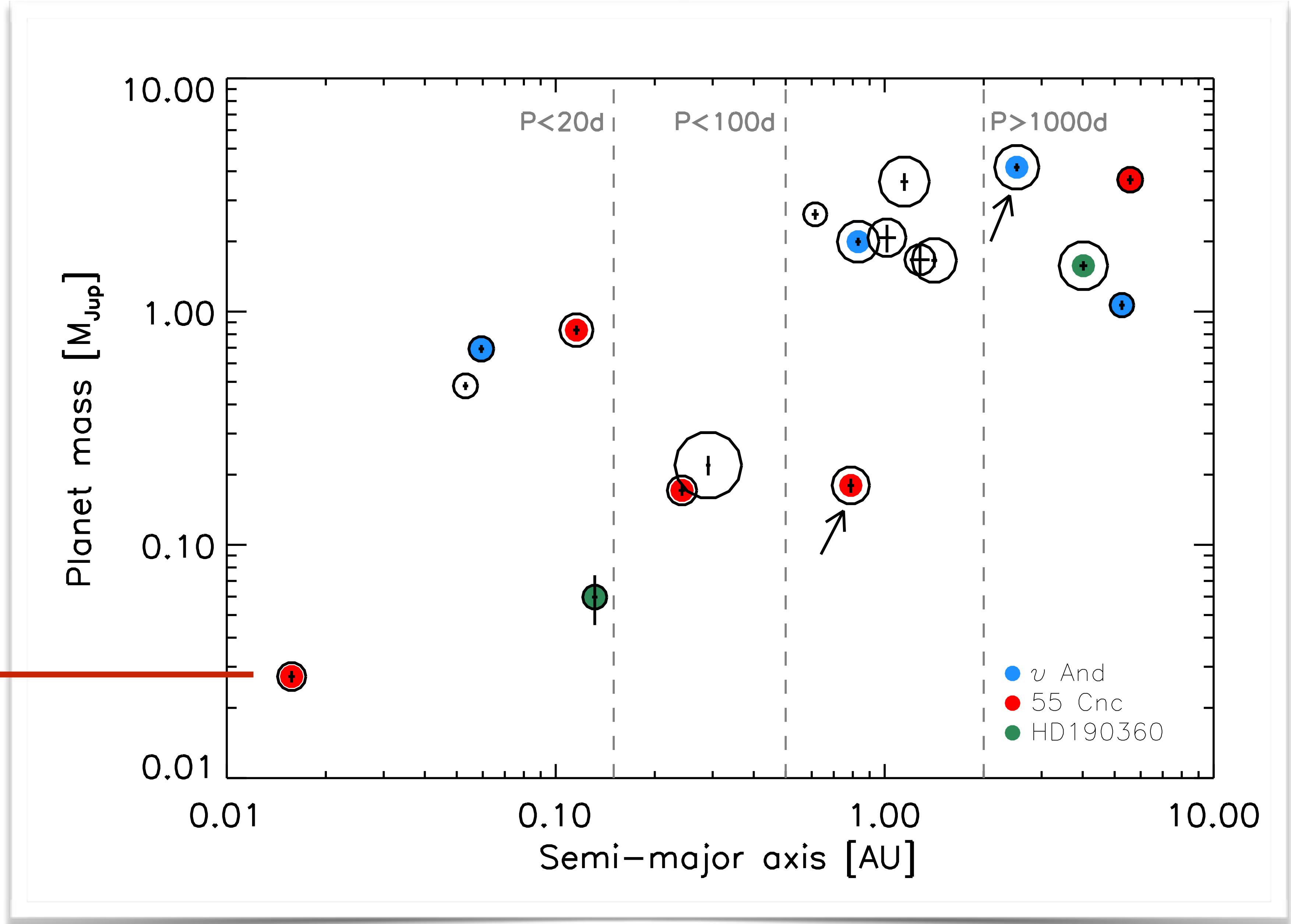

Only doable with a combinations of methods: interferometry, photometry, spectroscopy, models

Ligi et al. (2012a, 2012b, 2016)

OUTLINE

- Introduction: from the formation to the characterisation of exoplanets

- Characterisation of exoplanetary systems with interferometry

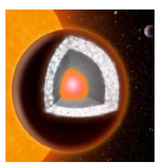

- Getting the most out of it: 55 Cnc

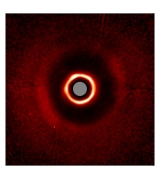

- Detection of exoplanets with direct imaging: insights in the system of HD169142

- Formation mechanisms: the challenging case of GJ504

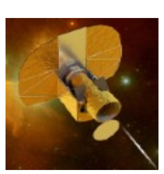

- Conclusion and perspectives

55 CNC AND ITS TRANSITING EXOPLANET

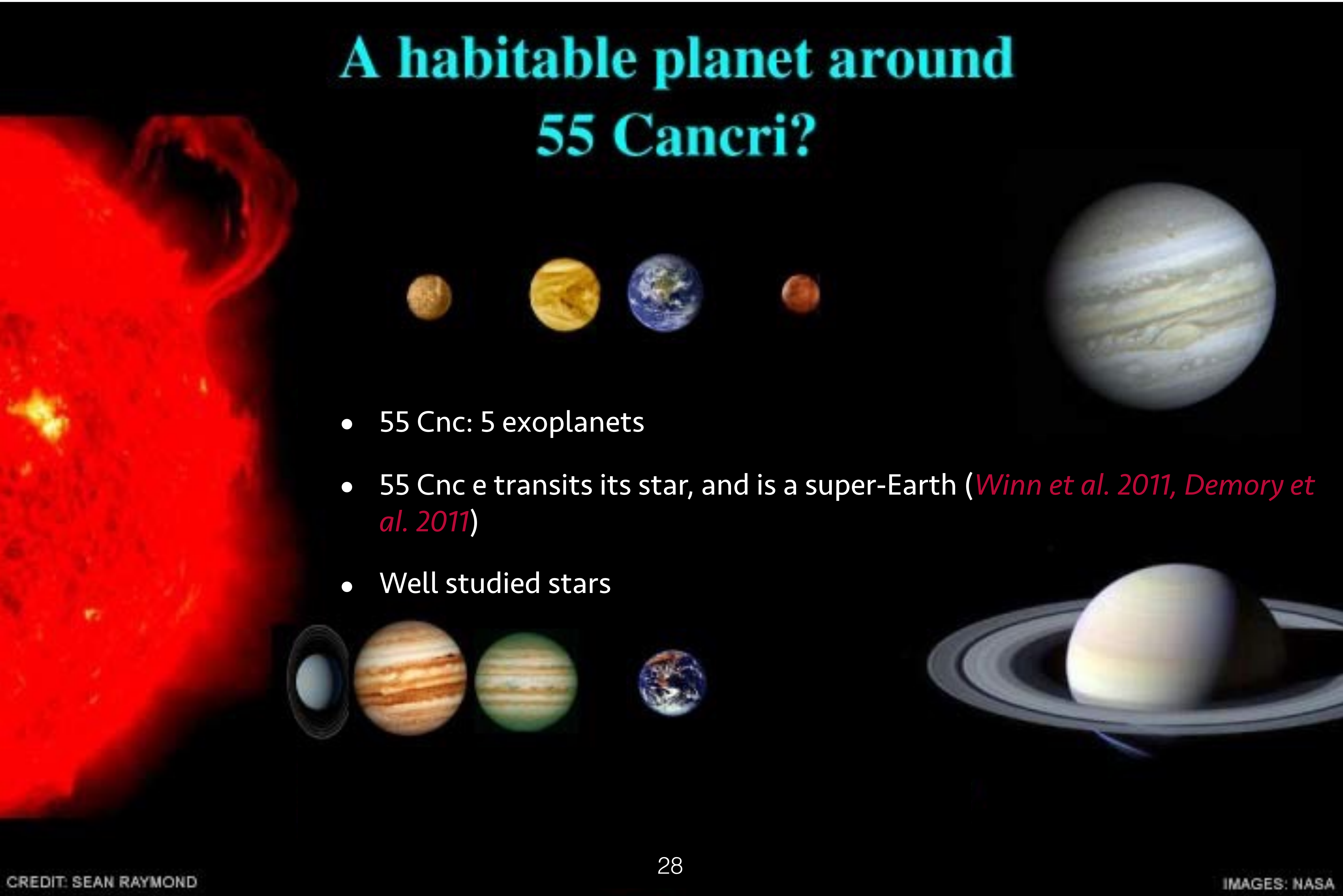

- 55 Cnc: 5 exoplanets
- 55 Cnc e transits its star, and is a super-Earth (*Winn et al. 2011, Demory et al. 2011*)
- Well studied stars

55 CNC AND ITS TRANSITING EXOPLANET

Stellar Results

Transit duration: $T=2R_\star/a\Omega$

Period: $P = 2\pi/\Omega$

→

$P/T^3 = (\pi^2 G/3)\,\rho_\star$

measure of stellar density $\rho_\star$ (Maxted et al. 2015, Seager & Mallén-Ornelas 2003)

Measure of $R_\star$ by interferometry → $M_\star=(4\pi/3)R_\star{}^3\rho_\star$ (Ligi et al. 2016)

55 CNC AND ITS TRANSITING EXOPLANET

Stellar Results

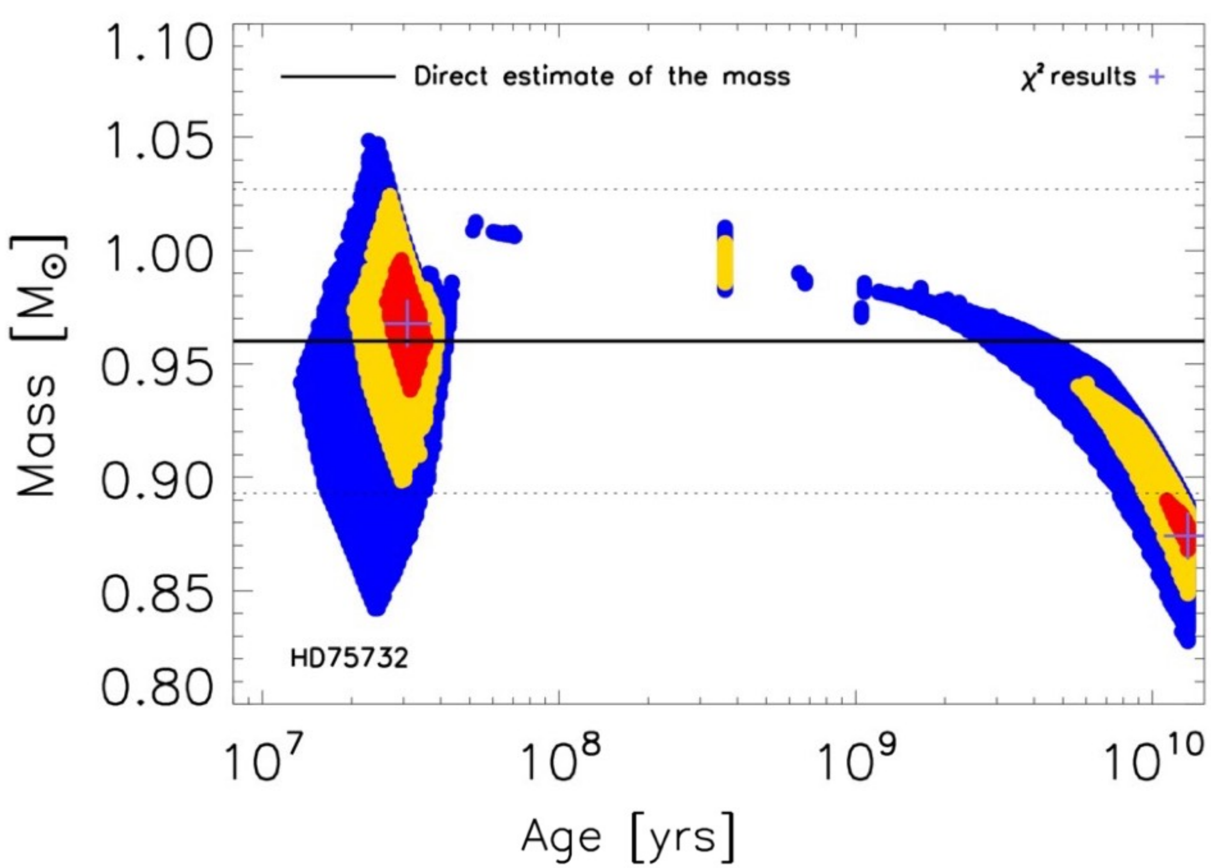

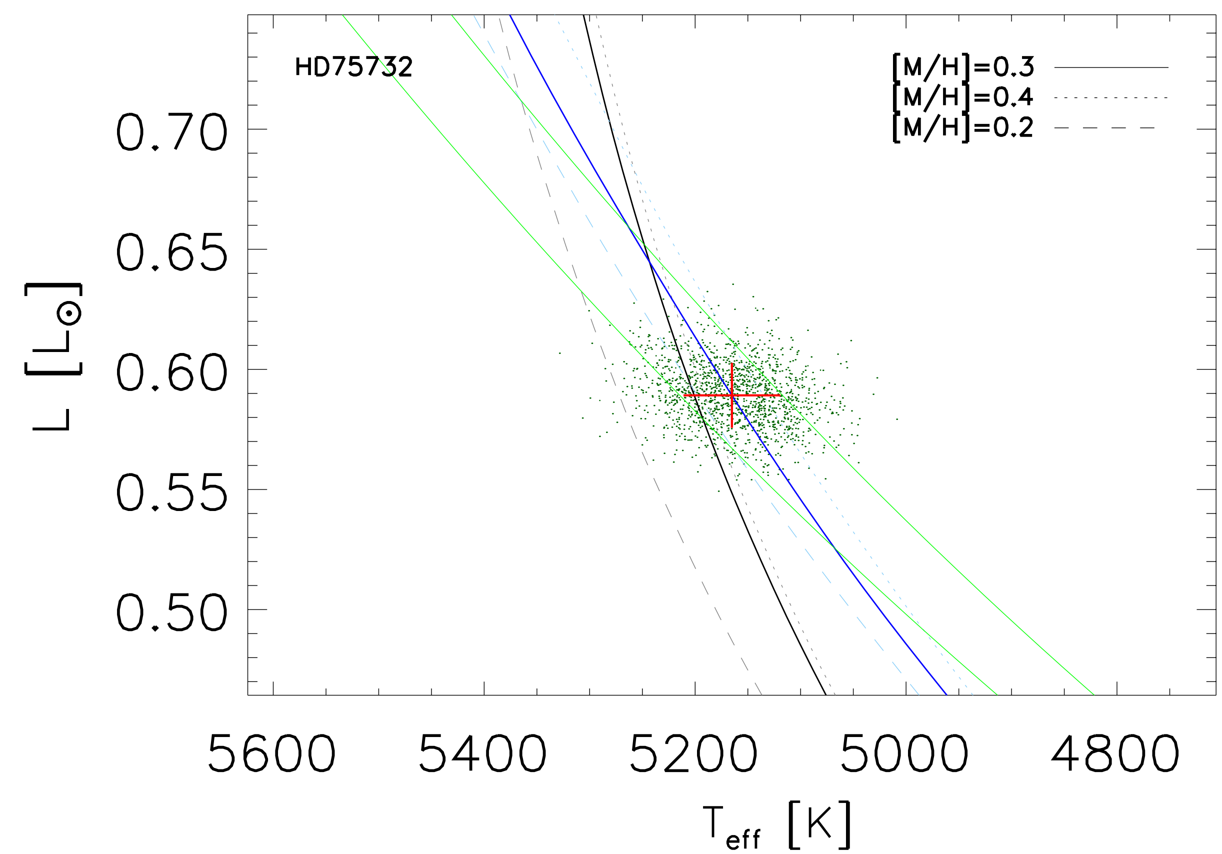

- Using the stellar density: $M_\star = 0.96 \pm 0.067\ M_\odot$

- From isochrones: 2 solutions
  - **Young solution**: $M_\star = 0.968 \pm 0.018\ M_\odot$, 30.0 ± 3.028 Myrs
  - **Old solution**: $M_\star = 0.874 \pm 0.013\ M_\odot$, 13.19 ± 1.18 Gyrs

55 CNC AND ITS TRANSITING EXOPLANET

Planetary Results

Transit duration: $T = 2R_\star / a\Omega$

Period: $P = 2\pi/\Omega$

→ $P/T^3 = (\pi^2 G/3)\ \rho_\star$

measure of stellar density $\rho_\star$ (Maxted et al. 2015, Seager & Mallén-Ornelas 2003)

Measure of $R_\star$ by interferometry → $M_\star = (4\pi/3) R_\star^3 \rho_\star$ (Ligi et al. 2016)

Transit light curve:

$R_p = R_\star \times \sqrt{TD}$

RV measurements:

$m_p \sin(i) = M_\star\ K\ (P/2\pi G M_\star)^{1/3}$

sin(i)

R_p

m_p

ρ_p

Some calculation to decrease the error bar…

$$\rho_p = \frac{3^{1/3}}{2\pi^{2/3} G^{1/3}} \rho_\star^{2/3}\ R_\star^{-1}\ TD^{-3/2}\ P^{1/3}\ K\,(1-e^2)^{1/2}$$

55 CNC AND ITS TRANSITING EXOPLANET

Planetary Results

Planet	a [au]	$m_p \sin(i)$ [M_{Jup}]
b	0.1156 ± 0.0027	0.833 ± 0.039
c	0.2420 ± 0.0056	0.1711 ± 0.0089
d	5.58 ± 0.13	3.68 ± 0.17
e	0.01575 ± 0.00037	8.66 ± 0.50* $M_\oplus$
f†	0.789± 0.018	0.180 ± 0.012

55 Cnc e	
R_p [$R_\oplus$]	$2.031^{+0.091}_{-0.088}$
M_p [$M_\oplus$]	8.631 ± 0.495
ρ_p [g.cm^{-3}]	$5.680^{+0.709}_{-0.749}$

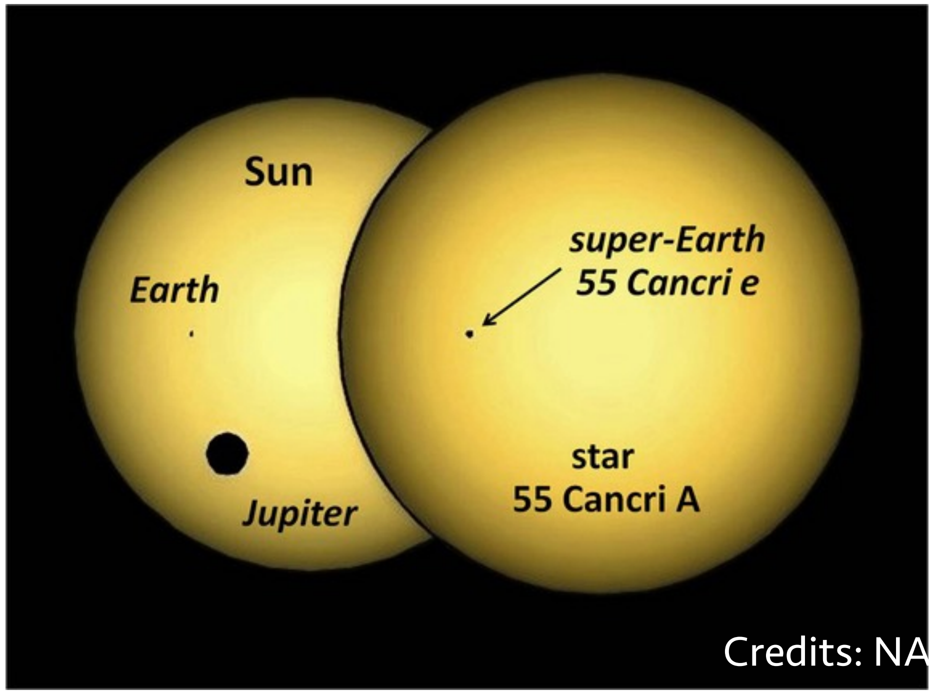

- Super-Earth
- All stellar parameters come from direct measurements
- Better accuracy on the density: compared to *Winn et al. (2011)* and *Demory et al. (2011)*
  ~25% → 12%
  more accurate thanks to direct measurement of $R_\bigstar$ and $\rho_\bigstar$

Error on ρ_p dominated by error on TD.
55 Cnc e has a terrestrial density!

55 CNC AND ITS TRANSITING EXOPLANET

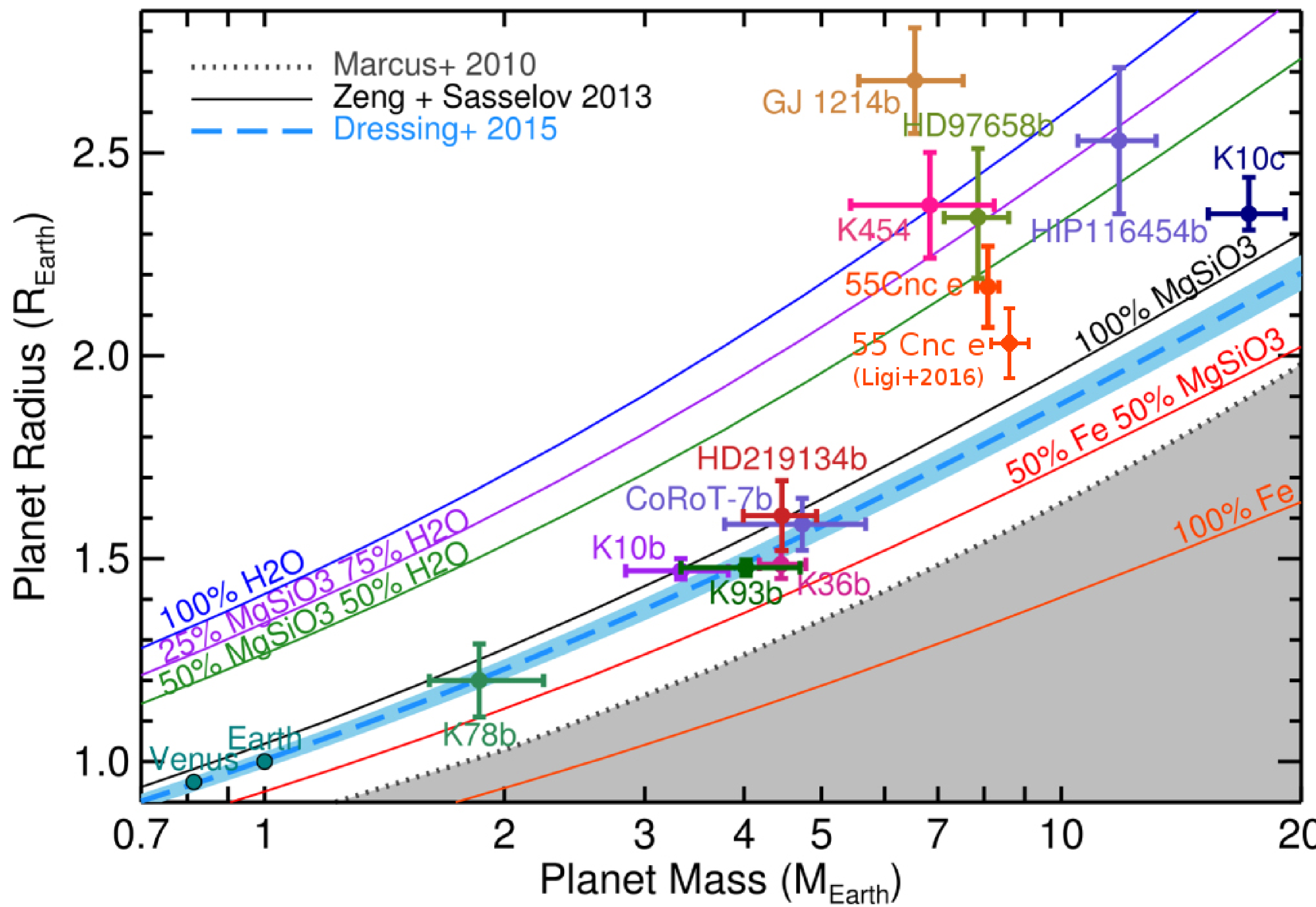

Gettel et al. 2016, ApJ, 816, 95, adapted

→ Different composition?

BUT WE CAN DO BETTER !

55 CNC: A BAYESIAN APPROACH

Crida, Ligi, Dorn & Lebreton, subm.
Crida & Ligi, EPSC 2017

Observations: θ, Π (parallax), m → F_{bol}, the bolometric flux.

$L = 4\,F_{bol}\,(1_{[pc]}\,/\,\Pi)^2$
$T_{eff} = (4\,F_{bol}\,/\,\sigma_{SB}\,\theta\,)^{1/4}$

} Likelihood (analytic) →

$$\mathcal{L}_{HR}(L,T) = \frac{4\sqrt{\pi/\sigma_{SB}}}{L^{3/2}T^3} \times \tag{3}$$
$$\int_0^{+\infty} t \times f_{F_{bol}}(t) \times f_{\Pi}\left(\sqrt{\frac{4\pi t}{L}}\right) \times f_{\theta}\left(\sqrt{\frac{4\,t}{\sigma_{SB}\,T^4}}\right)\,dt\,.$$

Prior: density of stars in the HR diagram of the Hipparcos sample (color).

↓ level curves

Interferometry is precise !
The prior does not bring much.

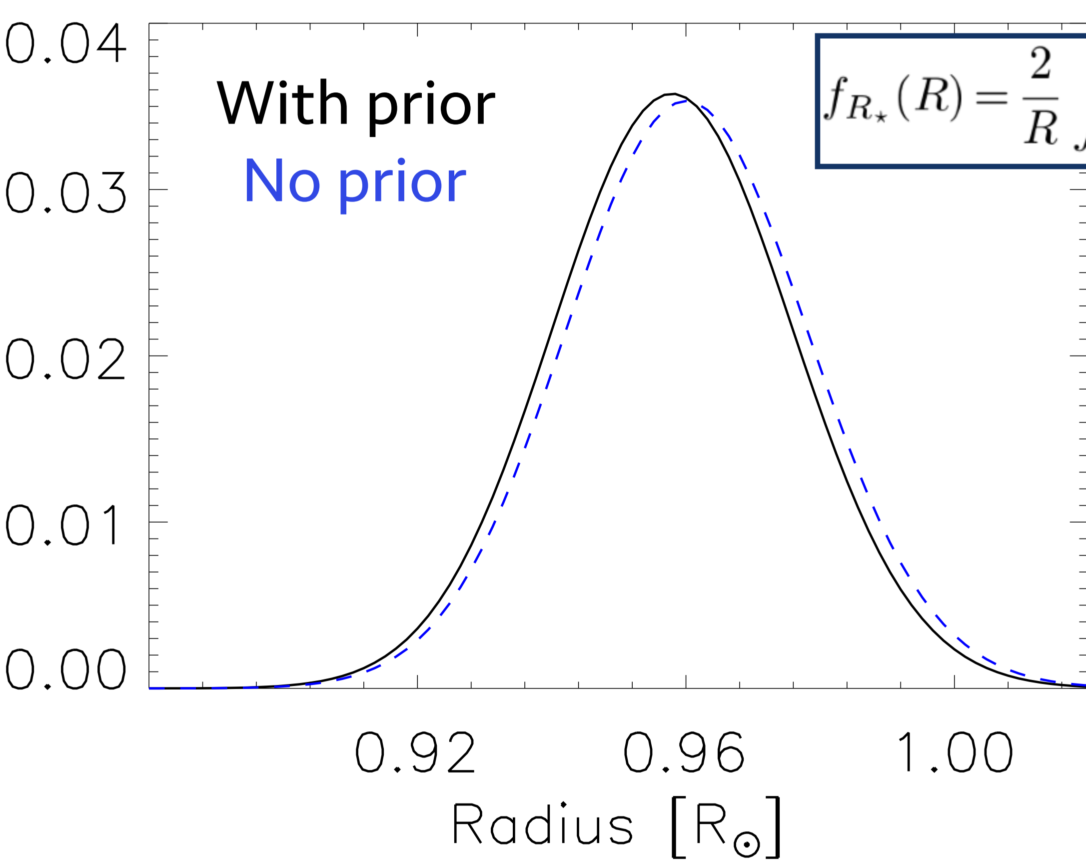

$$f_{R_\star}(R) = \frac{2}{R}\int_{t=0}^{\infty} L_{(R,t)}\, f_{HR}(L_{(R,t)},t)\;dt$$

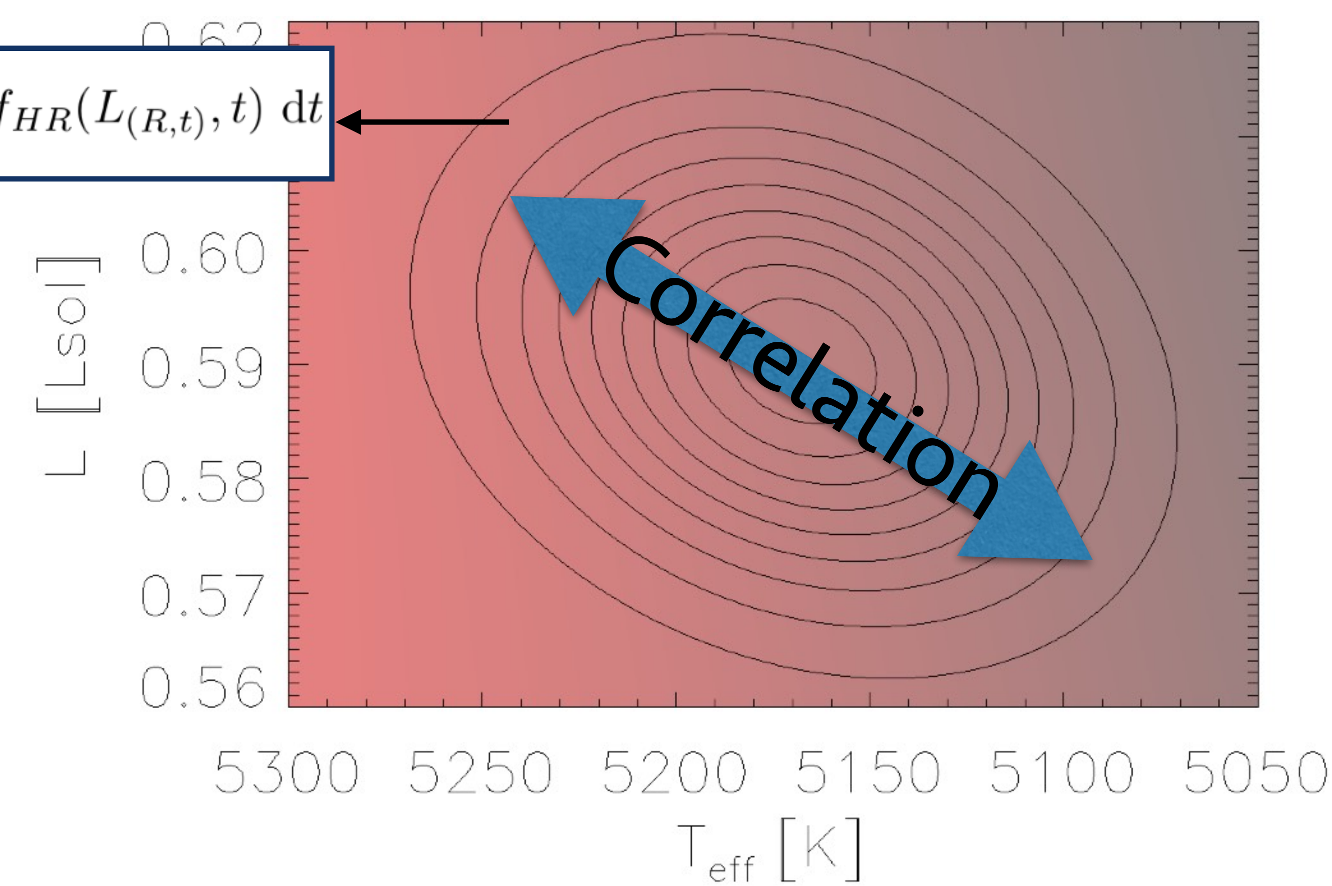

55 CNC: A BAYESIAN APPROACH

Results:

- Bayesian or not: 2 solutions
- But Lithium detection rules out the old solution! Consistent with young solution (age and mass) of Ligi et al. 2016.
- Still, different parameters in the model → different, inconsistent masses for the young solution: CES2MO (Lebreton & Goupil 2014) gives $M_\star$ from 0.950 ± 0.015 to 0.989 ± 0.020 $M_\odot$

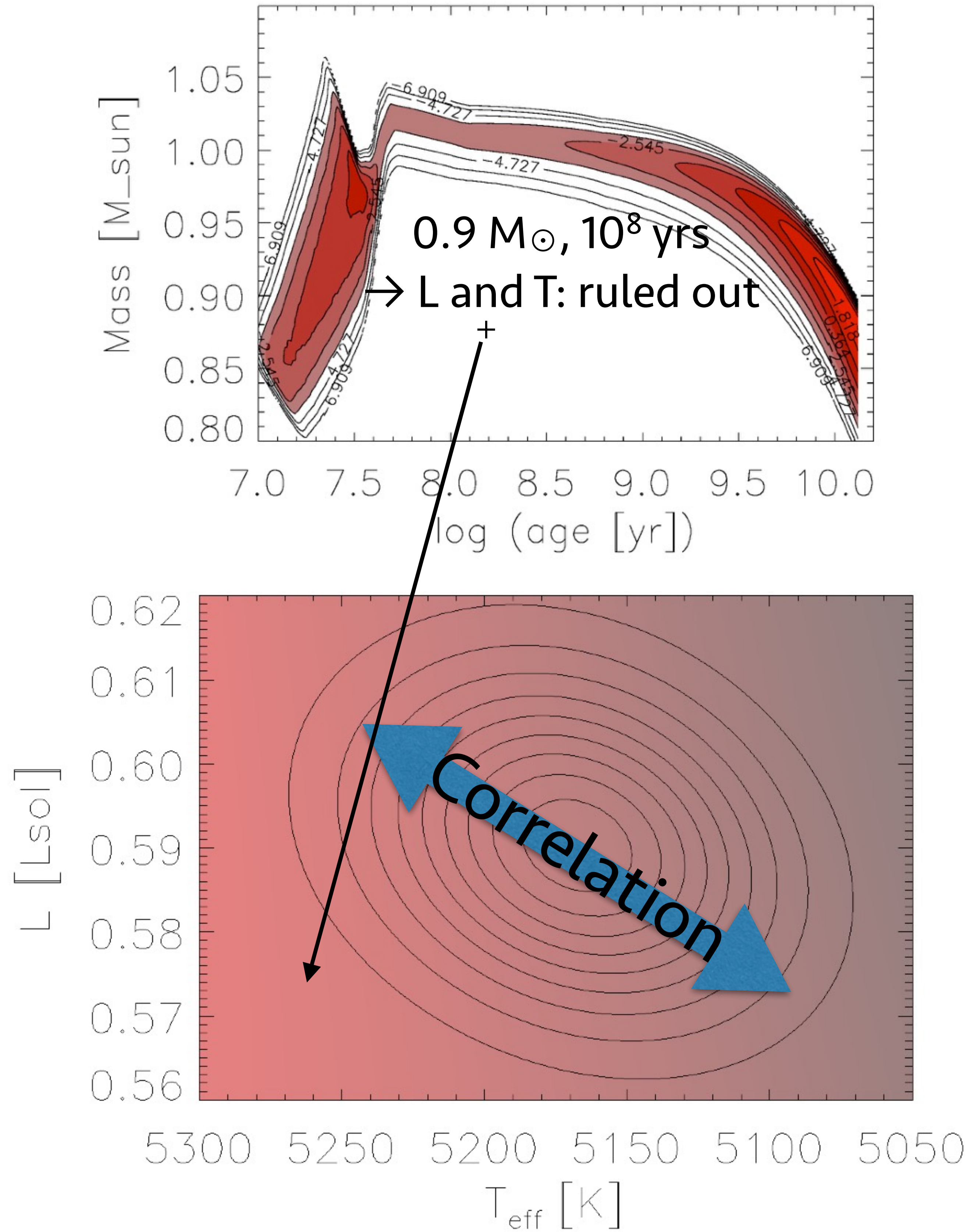

USING STELLAR DENSITY AND ANGULAR DIAMETERS

Transit duration: $T=2R_\star/a\Omega$

Period: $P = 2\pi/\Omega$

→

$P/T^3 = (\pi^2 G/3)\,\rho_\star$

measure of stellar density $\rho_\star$ (Maxted et al. 2015, Seager & Mallén-Ornelas 2003)

Measure of $R_\star$ by interferometry → $M_\star=(4\pi/3)R_\star^3\rho_\star$ (Ligi et al. 2016)

From the PDF of $R_\star$ and $\rho_\star$,

analytic joint PDF of $M_\star$ - $R_\star$.

$$\mathcal{L}_{MR\star}(M,R) = \frac{3}{4\pi R^3} \times f_{R_\star}(R) \times f_{\rho_\star}\left(\frac{3M}{4\pi R^3}\right)$$

→ Strong correlation (0.85) !

→ Different $M_\star$ than von Braun et al. (2011) based on isochrones.

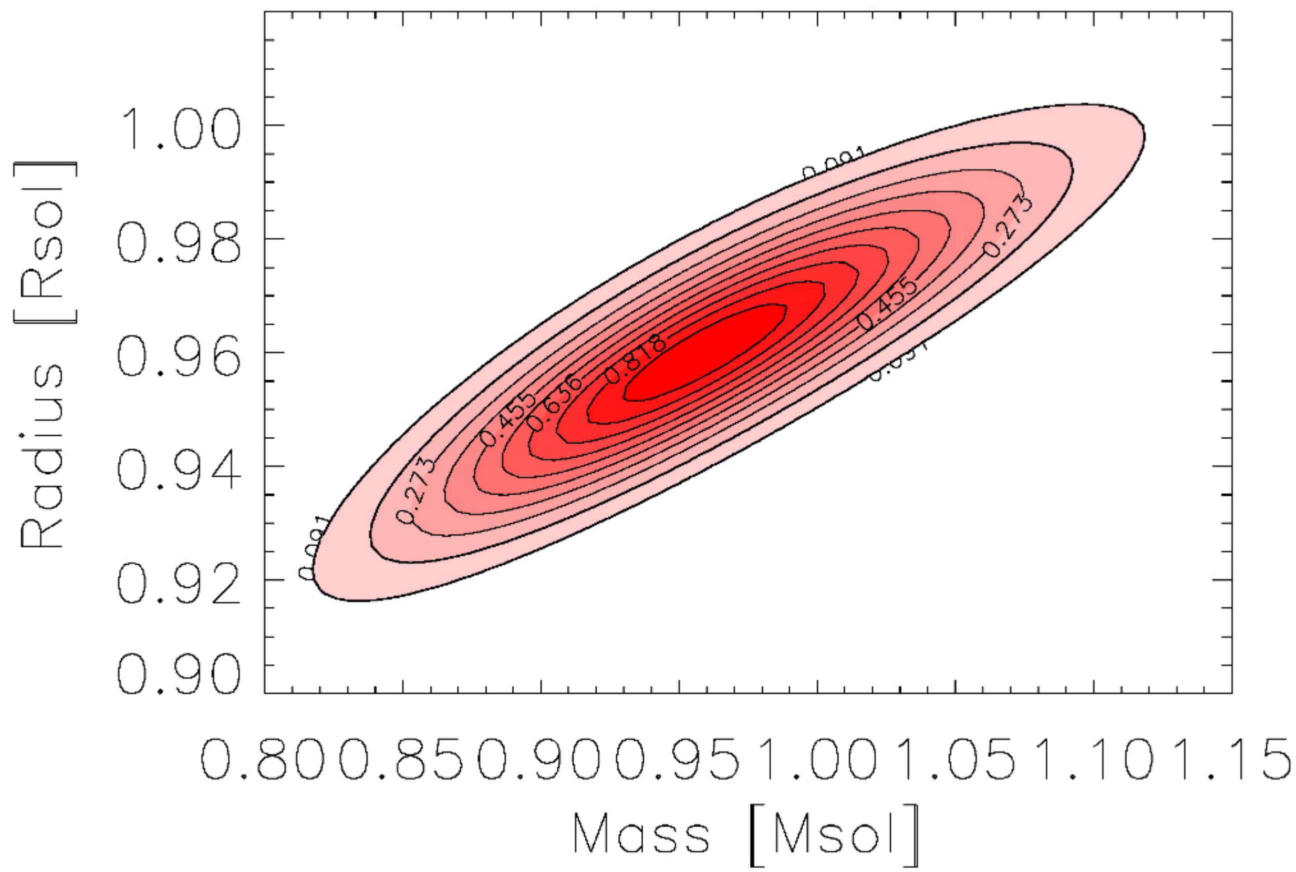

USING STELLAR DENSITY AND ANGULAR DIAMETERS

Transit duration: $T = 2R_\star/a\Omega$

Period: $P = 2\pi/\Omega$

→ $P/T^3 = (\pi^2 G/3)\,\rho_\star$

measure of stellar density $\rho_\star$ (Maxted et al. 2015, Seager & Mallén-Ornelas 2003)

Measure of $R_\star$ by interferometry → $M_\star = (4\pi/3) R_\star^3 \rho_\star$ (Ligi et al. 2016)

From the PDF of $R_\star$ and $\rho_\star$,

analytic joint PDF of $M_\star$ - $R_\star$.

$$\mathcal{L}_{MR\star}(M,R) = \frac{3}{4\pi R^3} \times f_{R_\star}(R) \times f_{\rho_\star}\left(\frac{3M}{4\pi R^3}\right)$$

Taking the values of R★ and M★ from Ligi et al. 2016, one gets the large, wrong blue ellipse.

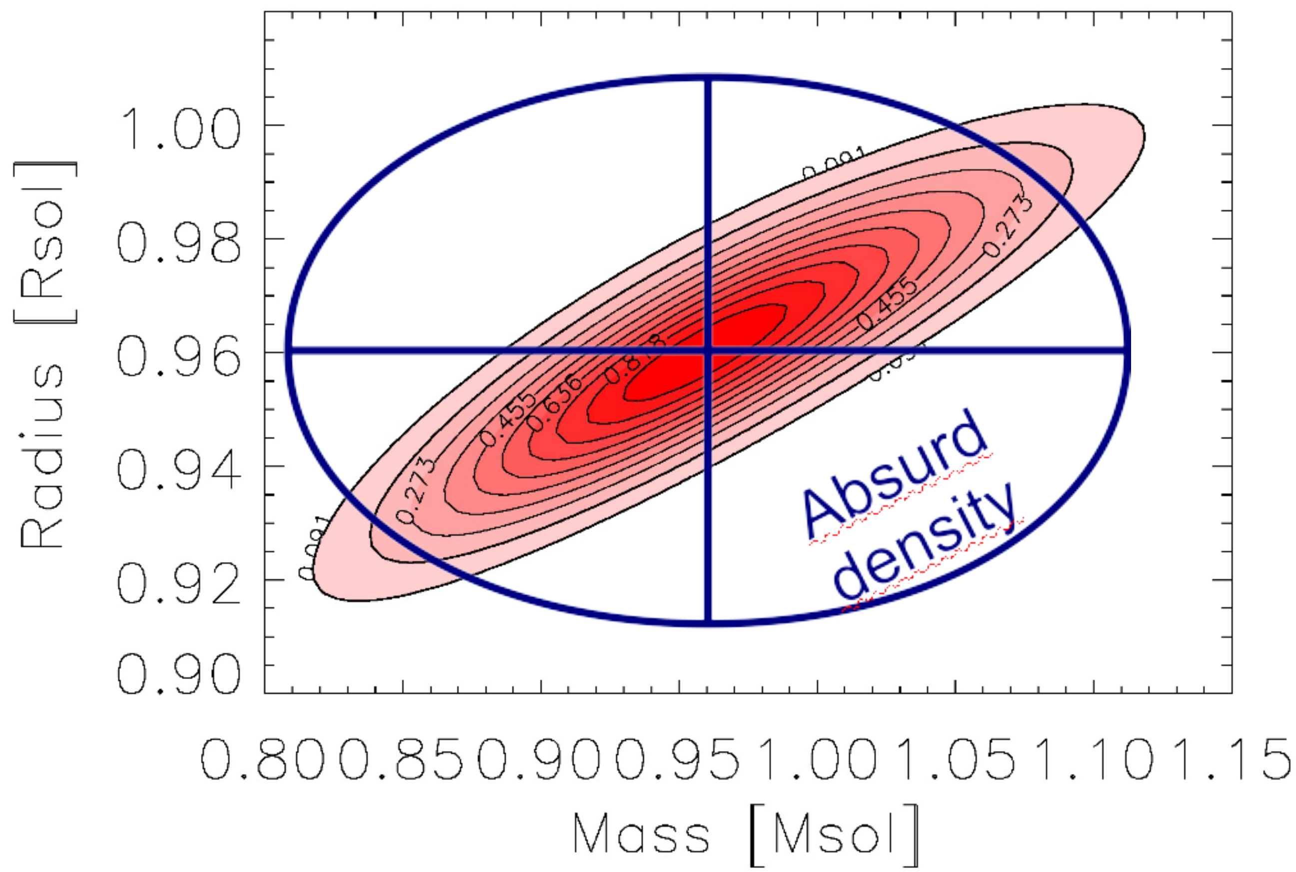

USING STELLAR DENSITY AND ANGULAR DIAMETERS

Planetary Results

Transit duration: $T = 2R_\star / a\Omega$

Period: $P = 2\pi/\Omega$

→ $P/T^3 = (\pi^2 G/3)\, \rho_\star$

measure of stellar density $\rho_\star$ (Maxted et al. 2015, Seager & Mallén-Ornelas 2003)

Measure of $R_\star$ by interferometry → $M_\star = (4\pi/3) R_\star^3 \rho_\star$ (Ligi et al. 2016)

Transit light curve:
$R_p = R_\star \times \sqrt{TD}$

RV measurements:
$m_p \sin(i) = M_\star K (P/2\pi G M_\star)^{1/3}$

→ Analytic PDF of ρ_p

→ Joint PDF of m_p-R_p

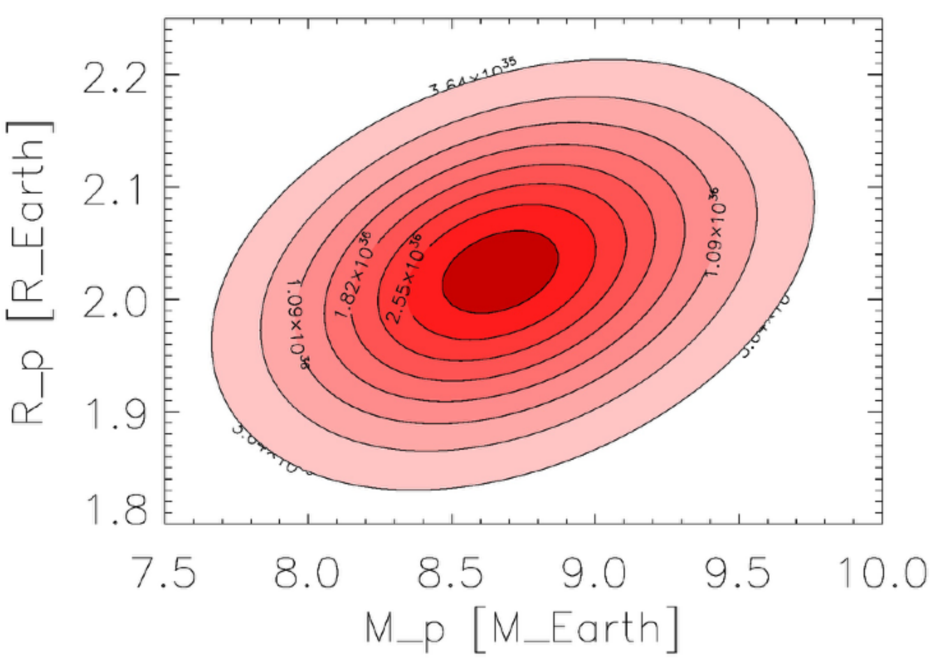

←

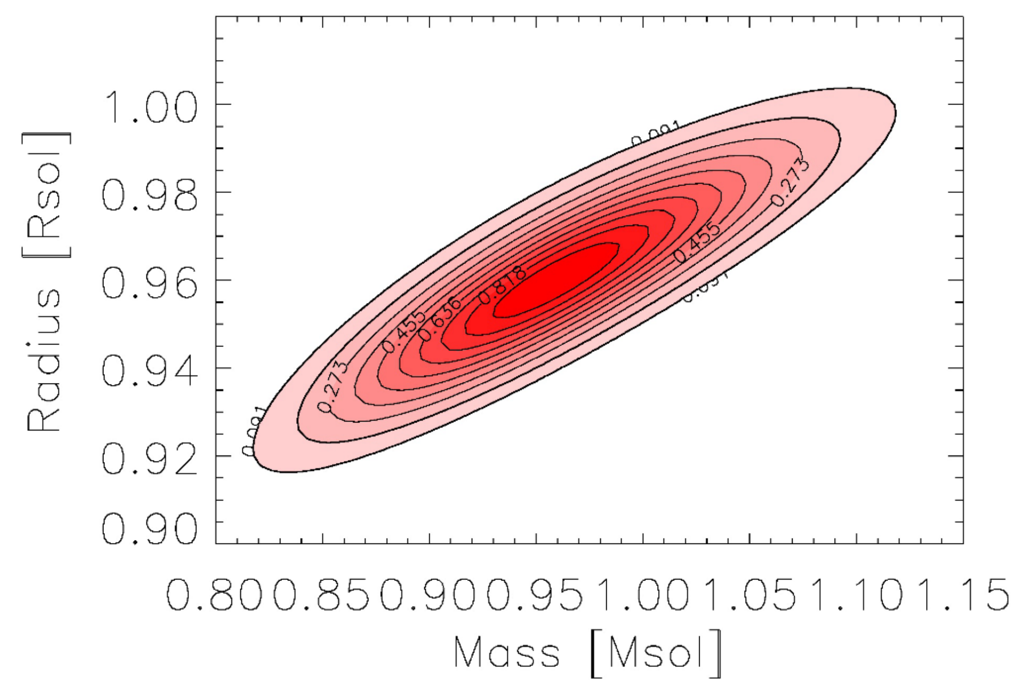

USING STELLAR DENSITY AND ANGULAR DIAMETERS

Planetary Results

Transit duration: $T = 2R_\star / a\Omega$

Period: $P = 2\pi/\Omega$

→ $P/T^3 = (\pi^2 G/3)\, \rho_\star$

measure of stellar density $\rho_\star$ (Maxted et al. 2015, Seager & Mallén-Ornelas 2003)

Measure of $R_\star$ by interferometry → $M_\star = (4\pi/3) R_\star^3 \rho_\star$ (Ligi et al. 2016)

Transit light curve:

$R_p = R_\star \times \sqrt{TD}$

RV measurements:

$m_p \sin(i) = M_\star K (P/2\pi G M_\star)^{1/3}$

→ Analytic PDF of ρ_p

→ Joint PDF of m_p-R_p

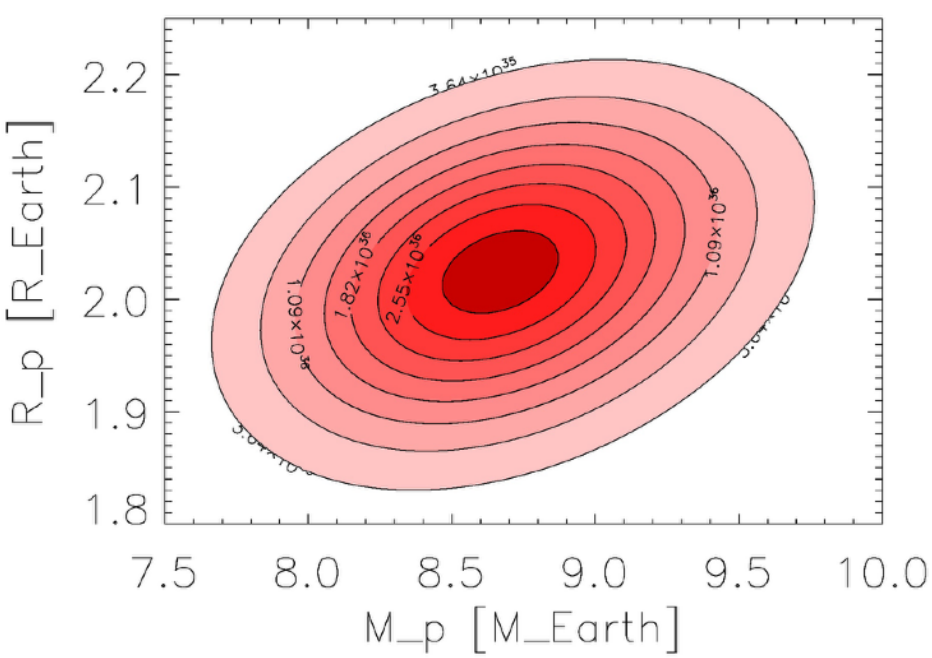

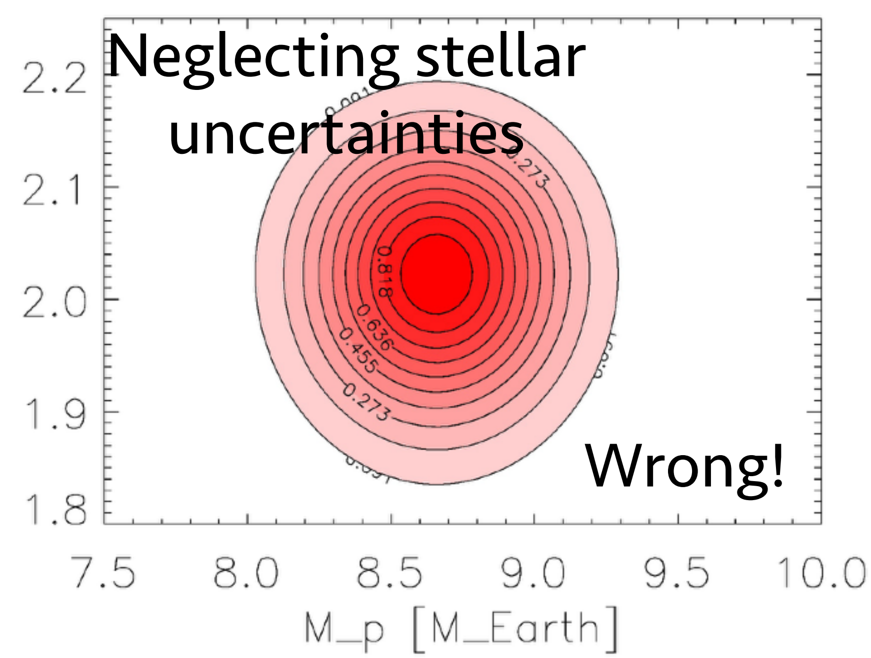

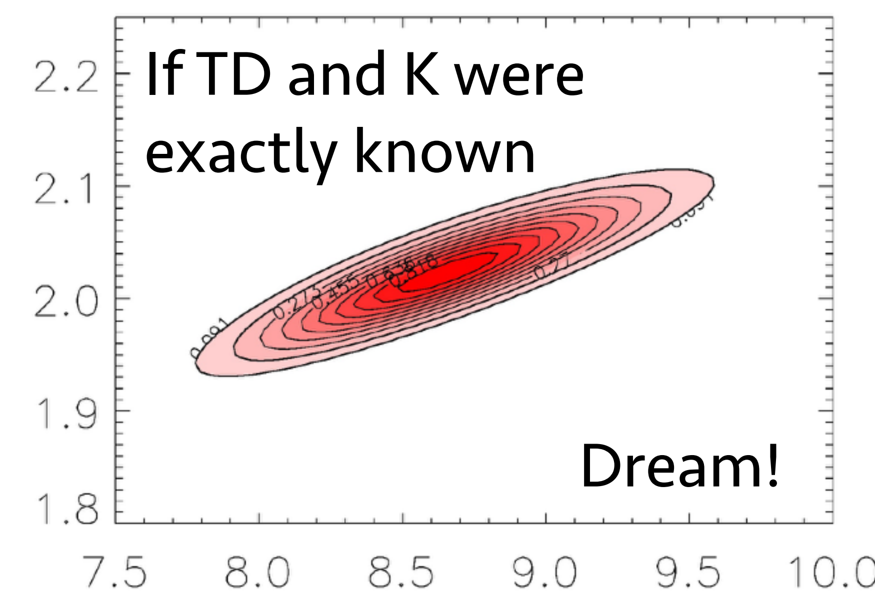

55 CNC E: INTERNAL COMPOSITION

Internal structure model developed by Dorn et al. (2017).

Input :

Original data : m_p, R_p (uncorrelated), a, $L_\star$.
Correlation between m_p and R_p (0.30).
Hypothetical correlation (0.85).
Abundances : stellar Fe/Si, Mg/Si.

Output :

PDF (or CDF) of all the internal parameters.
We test the importance of the various data O, C, H, A.

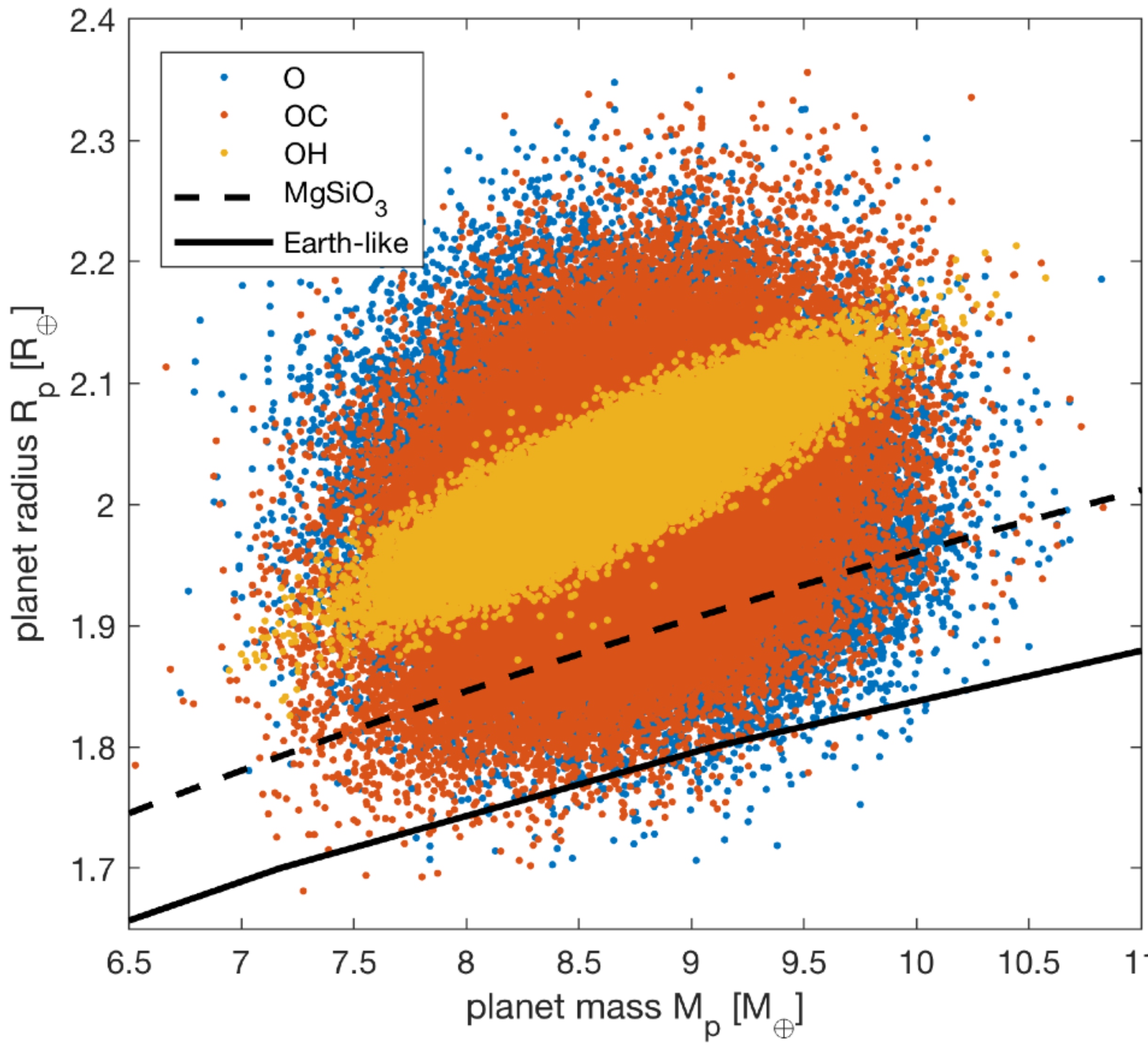

55 CNC E: INTERNAL COMPOSITION

Input :
Original data mp
Correl. mp-Rp (0.30)
Hypothetical corr. (0.85)
Abundances

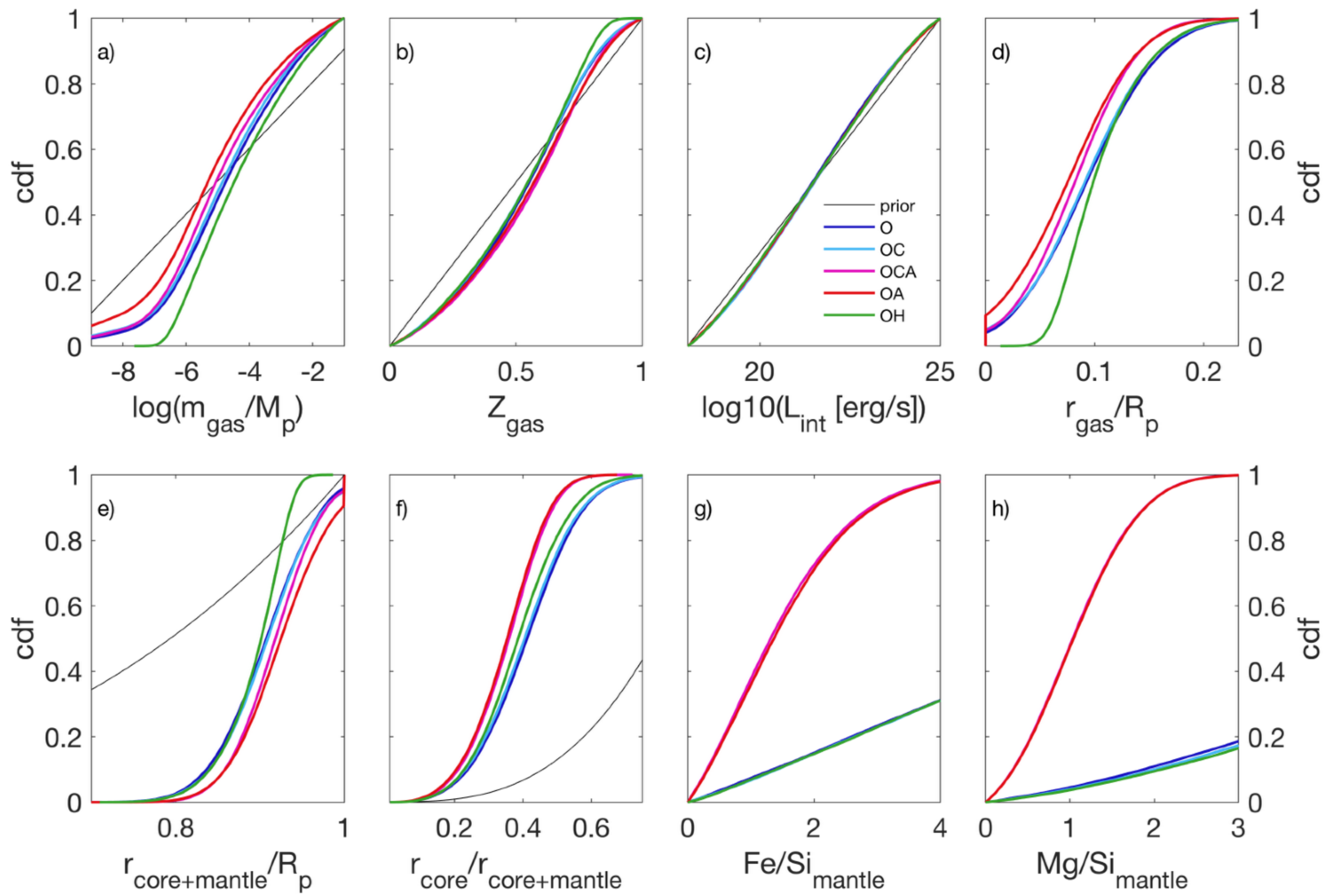

Results :
A → composition of the mantle
C → gas layer
H → could rule out pure solid composition

OCA case: our best constrains on all the parameters.

STELLAR ABUNDANCES?

EPIC-XXXX1451
(Santerne et al., in press)

Model of the planet based on stellar abundances

But composition not compatible with stellar abundances!
➔ Mercury-like planet (transit+RV)

In the future, more discoveries of this type?
R_p and m_p still reliable….

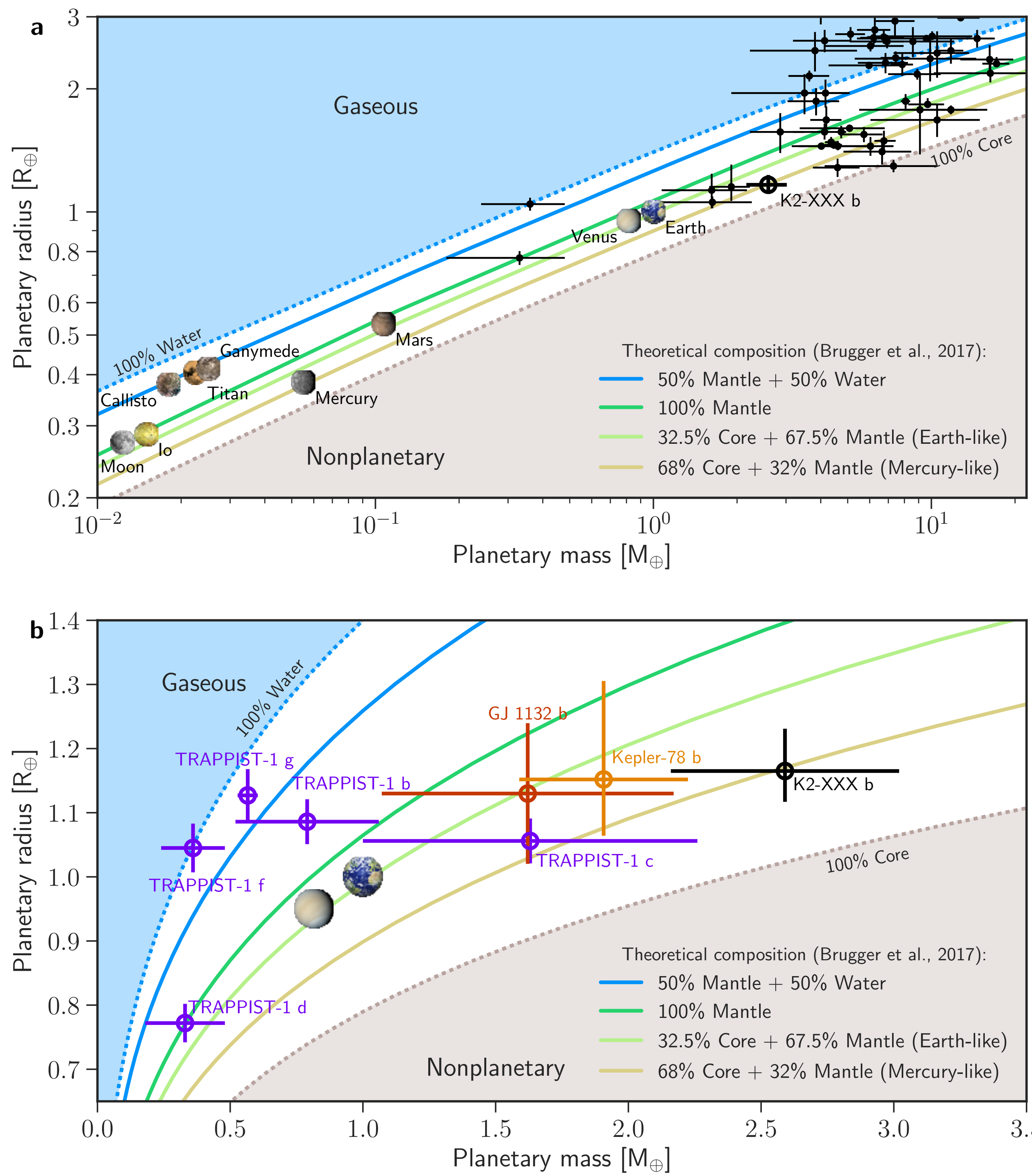

OUTLINE

- Introduction: from the formation to the characterisation of exoplanets

- Characterisation of exoplanetary systems with interferometry

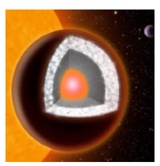

- Getting the most out of it: 55 Cnc

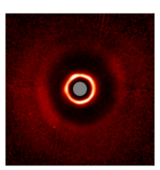

- Detection of exoplanets with direct imaging: insights in the system of HD169142

- Formation mechanisms: the challenging case of GJ504

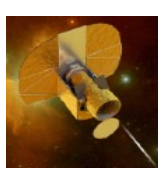

- Conclusion and perspectives

SPHERE/VLT FOR EXOPLANETS AND DISKS DETECTION

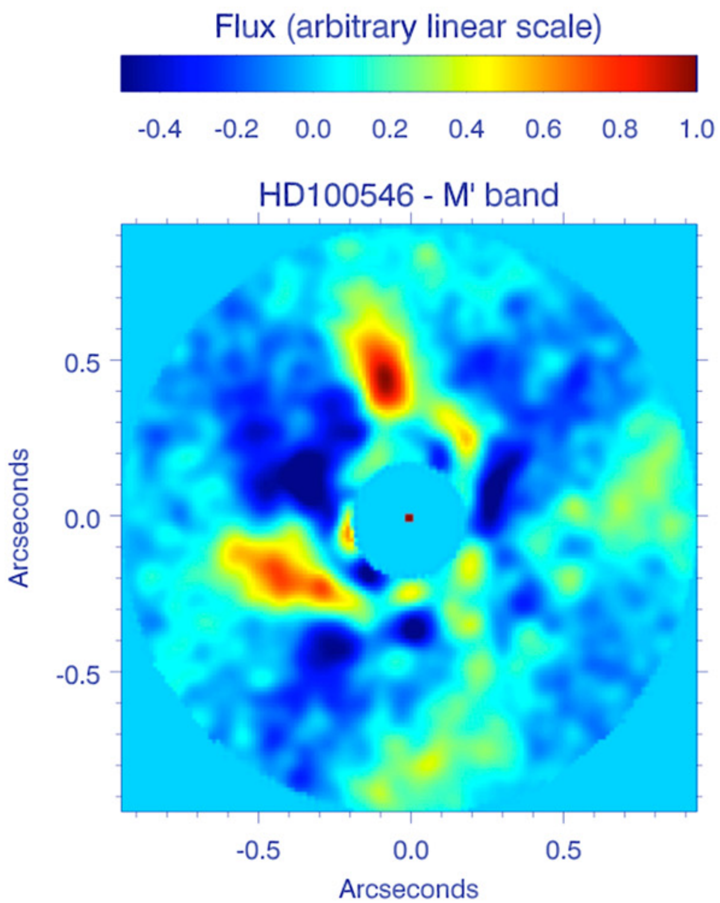

HD100546
(Quanz et al. 2015)

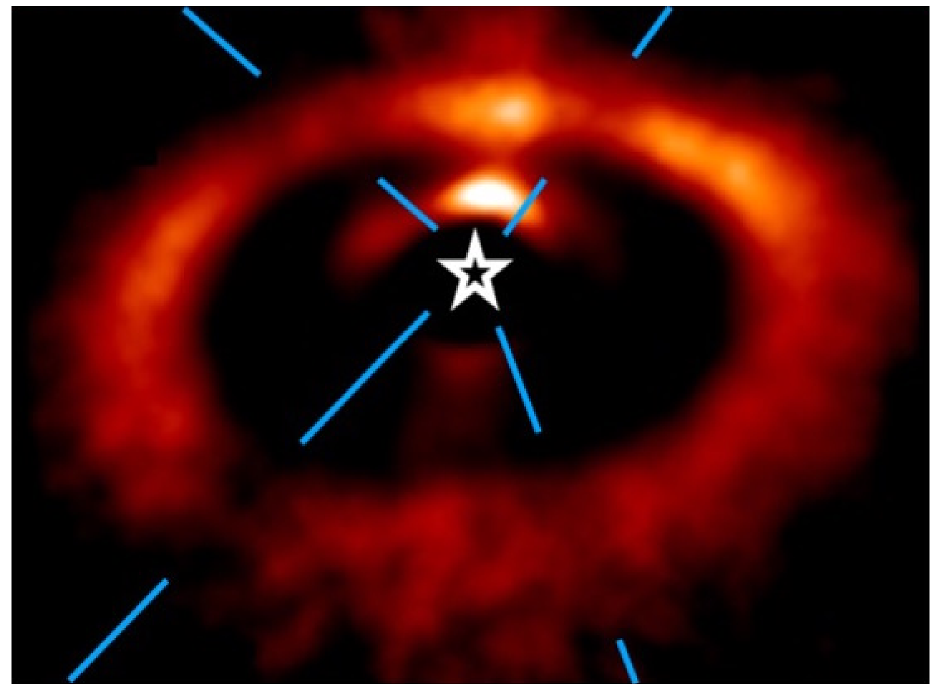

LkCA 15
(Thalmann et al. 2016)

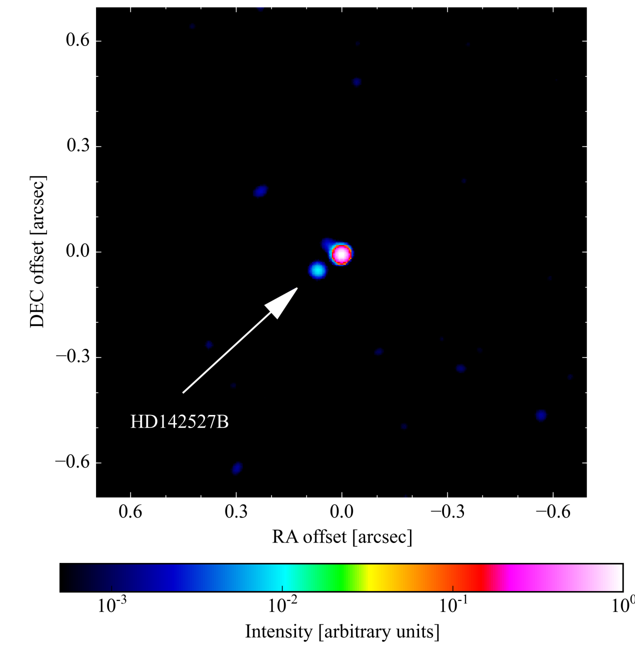

HD142527
(Lacour et al. 2016)

SPHERE/VLT: high-contrast direct imaging

- direct detection and characterisation of exoplanets
- detection of protoplanetary disks, transitional disks
  ➔ important for the comprehension of planetary formation

A PECULIAR CASE...

- Herbig Ae star (d=117 pc, $M_\star$=1.65 $M_\odot$, $L_\star$=10 $L_\odot$)
- Age estimate of ~10 Myr
- Strong infrared excess, variability of NIR/MIR
- Disk close to face-on (i=13°, PA=5°)
- Previous H-/J-band scattered light detections (Momose et al. 2015, Monnier et al. 2017)
- 1.3 mm continuum: double-ring structure (Fedele et al. 2017): ~20-35 au and ~56-83 au

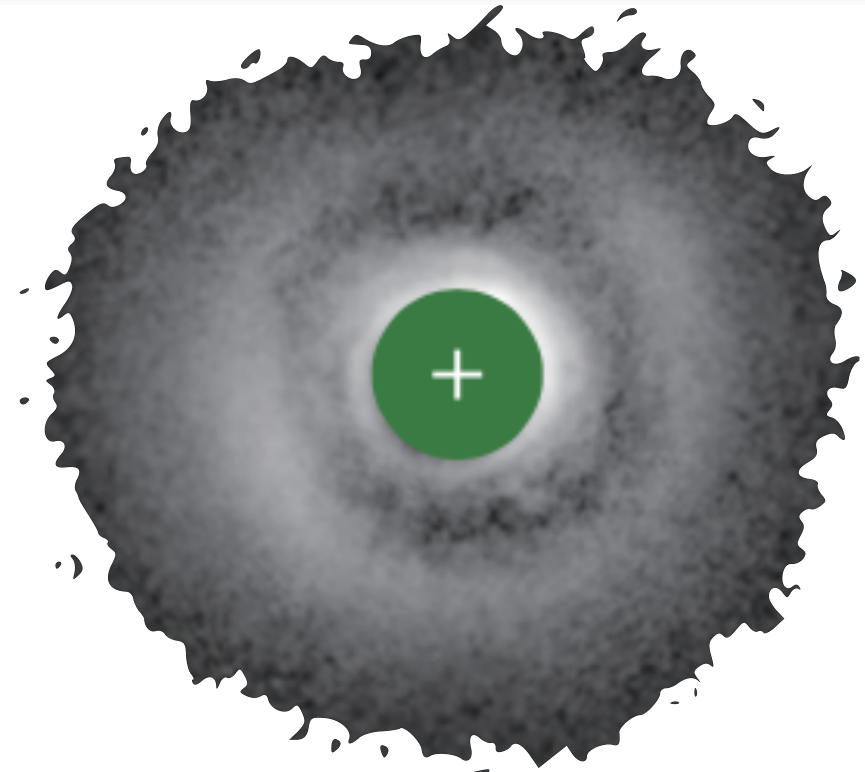

Momose+ 2015

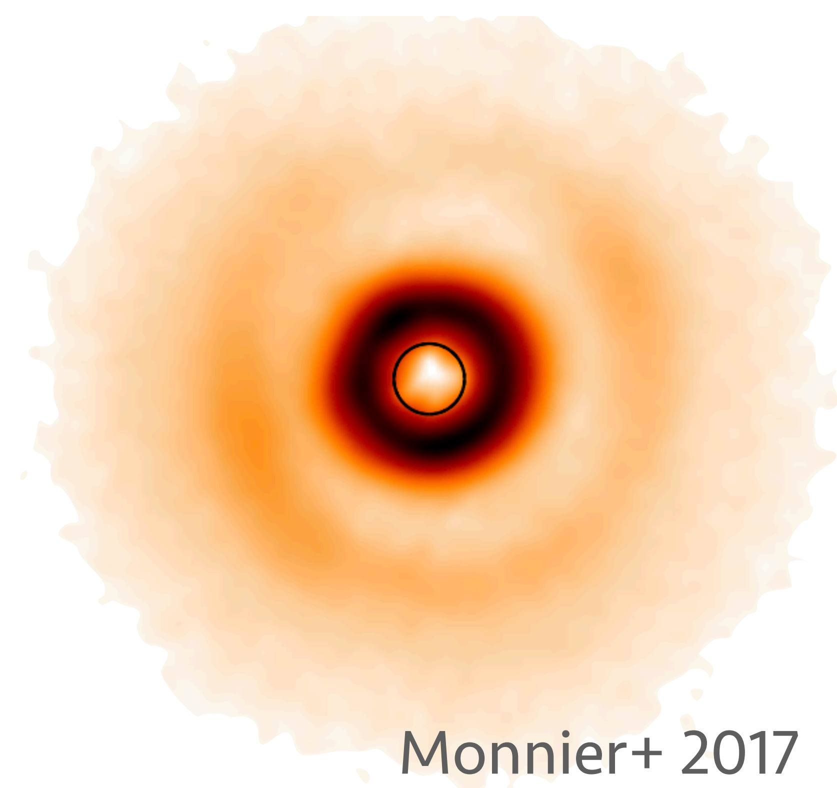

Monnier+ 2017

PREVIOUS DETECTIONS

Biller+ 2014

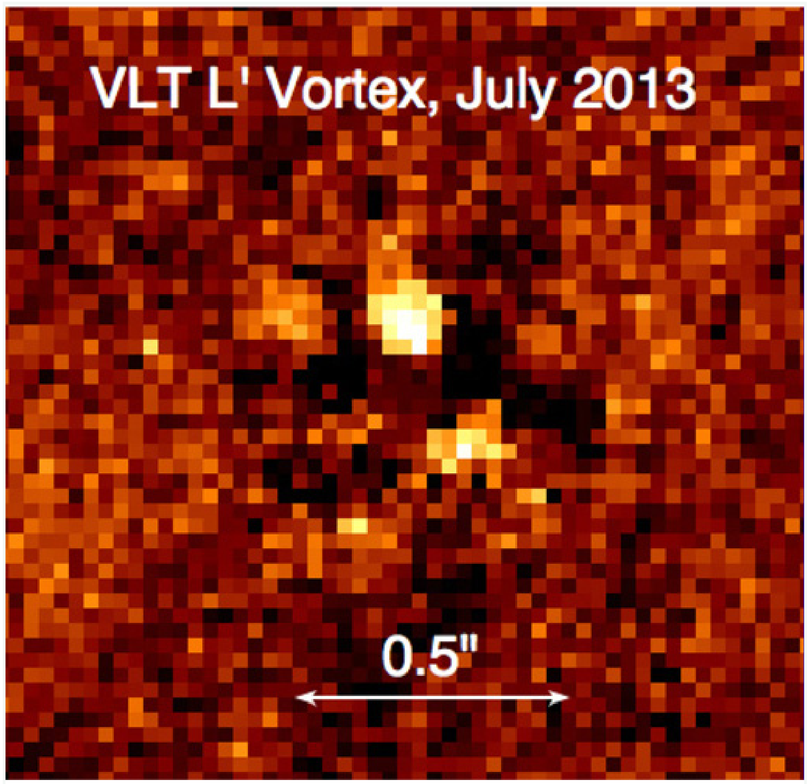

Point-like feature
Δmag=6.4±0.2
sep=0.11±0.03''
PA=0±14°
↓
60-80 M_{Jup}
brown dwarf

Reggiani+ 2014

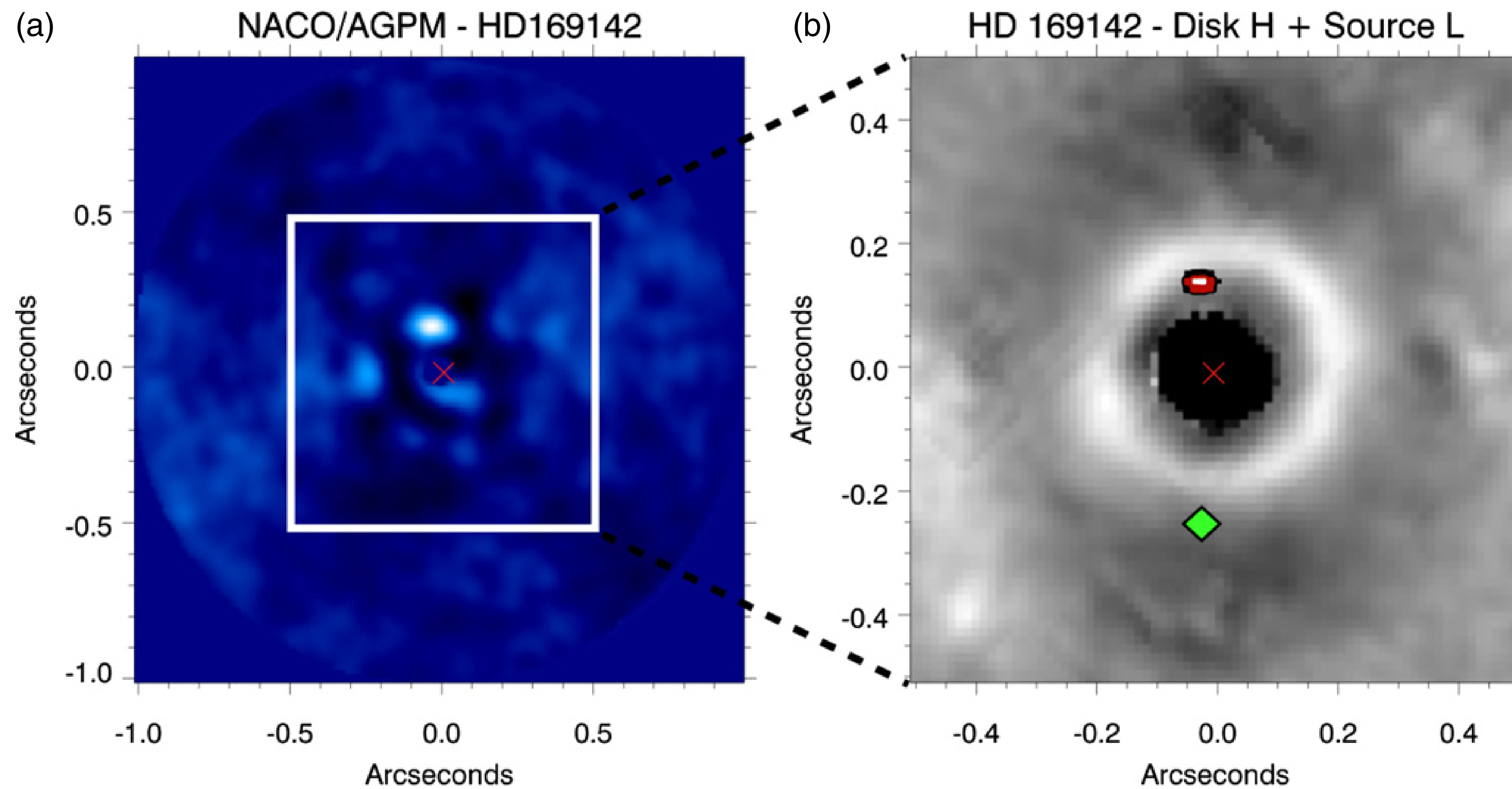

Point-like feature
Δmag=6.5±0.5
sep=0.156±0.032''
PA=7.4±11.3°
in the inner gap cavity
↓
28-32 M_{Jup} companion

PREVIOUS DETECTIONS

Biller+ 2014

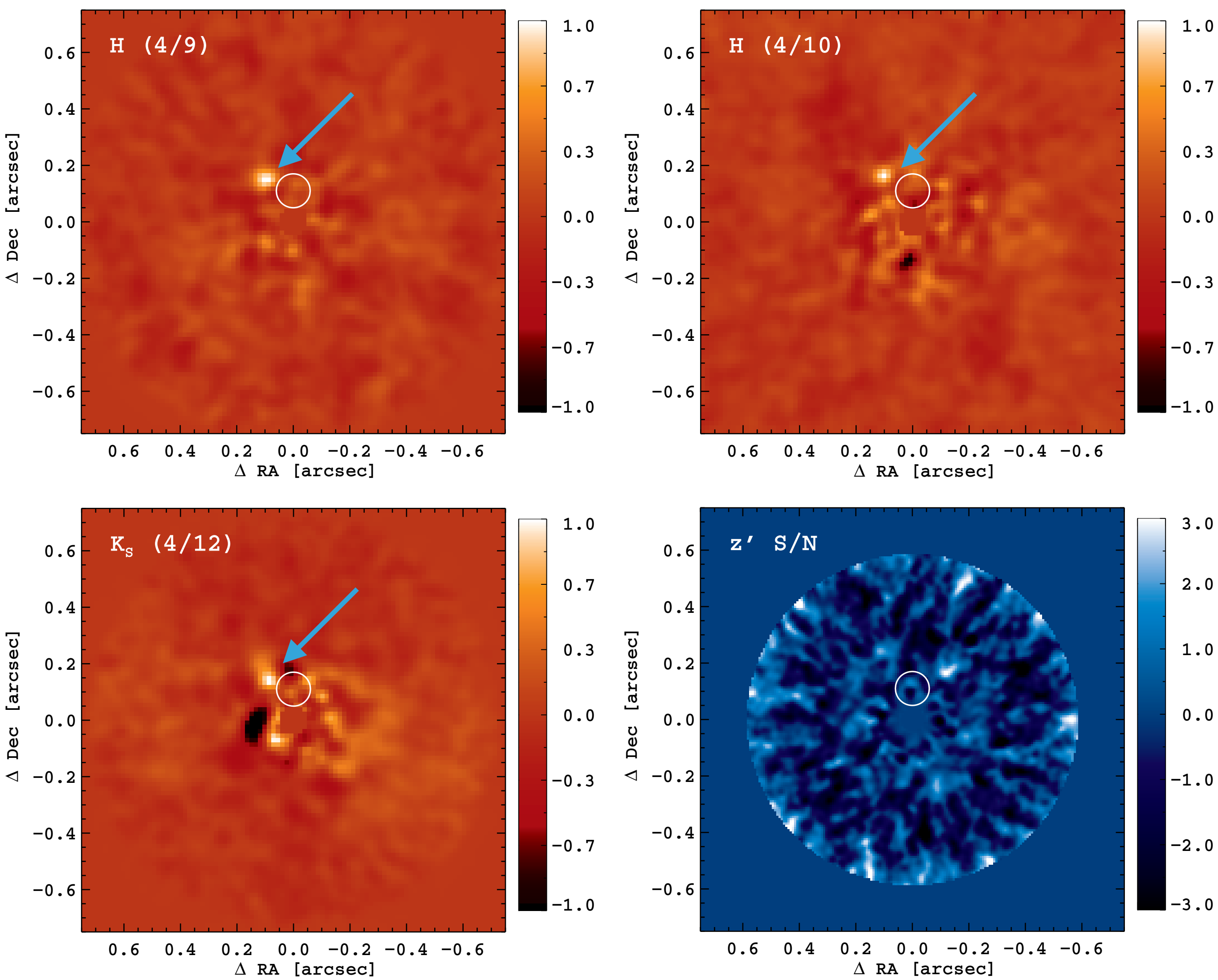

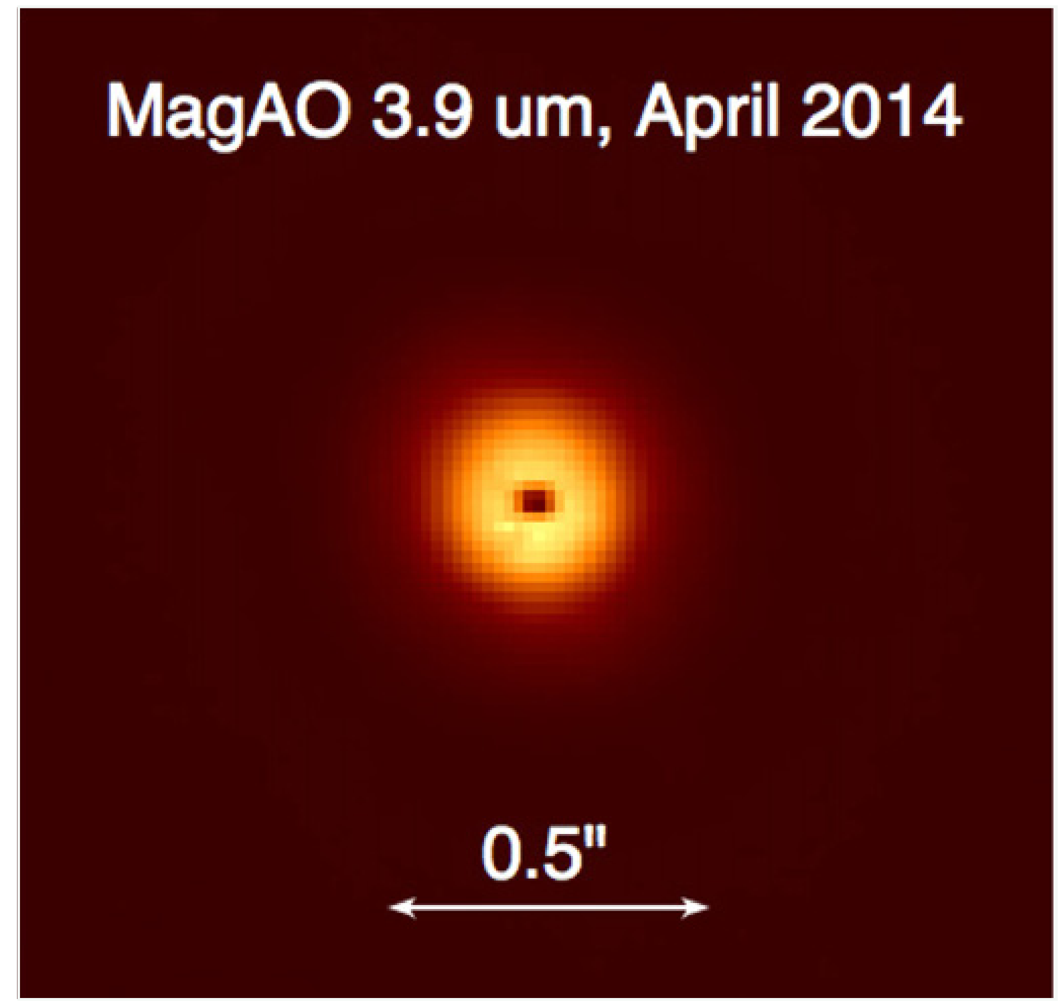

Follow-up observations with MagAO H&K_S:
Additional detection at sep=180 mas, PA=33°
→ 8-15 M_{Jup} planet/substellar companion
(No L' counterpart)

Follow-up observations with MagAO 3.9µm:
No point-like feature

SPHERE/VLT OBSERVATIONS: DISK OR EXOPLANET?

SPHERE/SHINE Survey

Several detections, in particular:

- One structure at sep=0.18'', PA=20°, S/N~2.5-3
- One structure at sep=0.18'', PA=310°
- One structure at sep=0.093'', PA=355°
  - Very red (no background star)
  - S/N~3-4, Δmag=9.3 in H band
  - More extended in the H-band

Ligi et al. (2018)

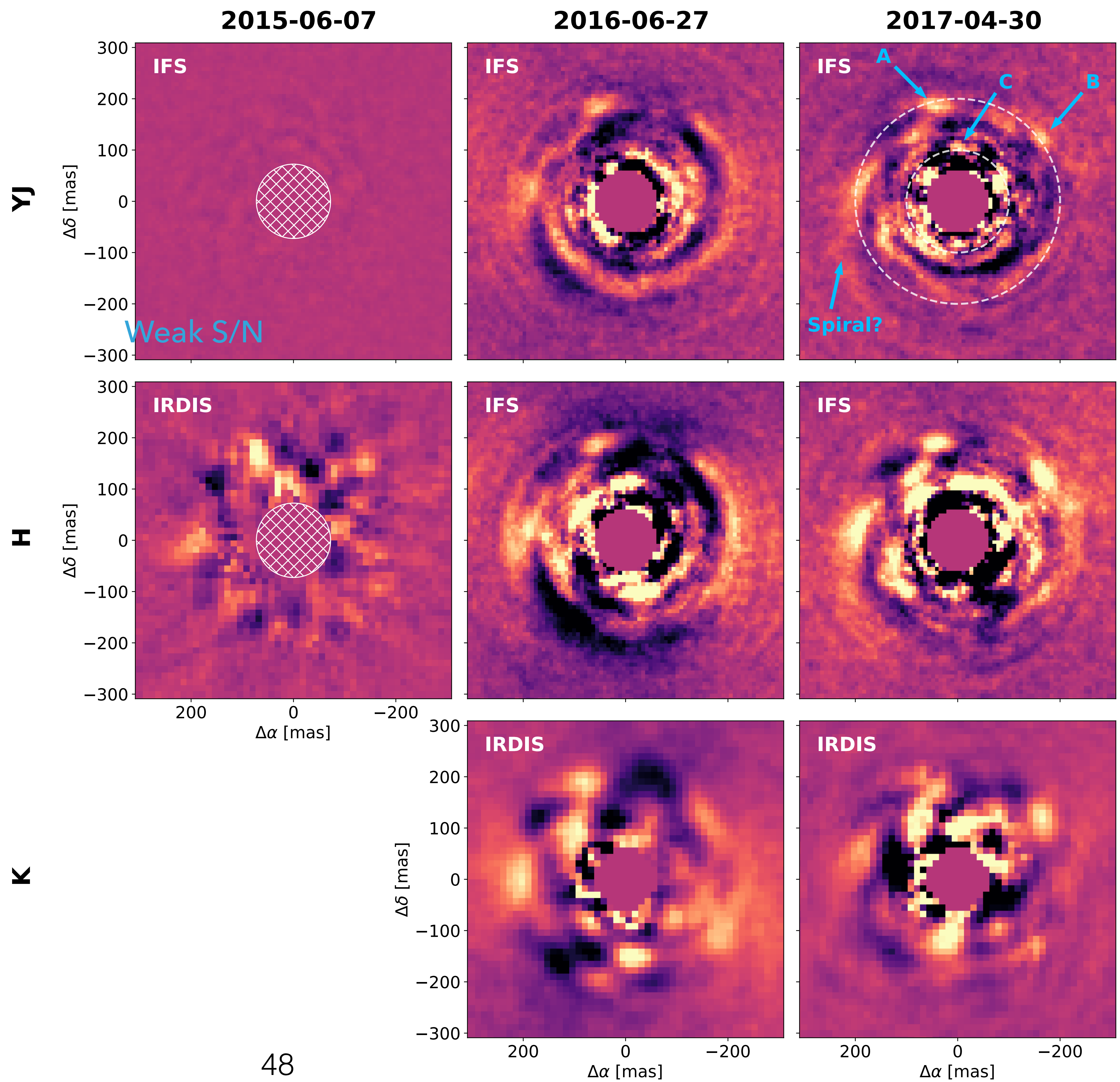

SPHERE/VLT OBSERVATIONS: DISK OR EXOPLANET?

SPHERE/SHINE Survey

Several detections, in particular:

- One structure at sep=0.18'', PA=20°, S/N~2.5-3
- One structure at sep=0.18'', PA=310°
- One structure at sep=0.093'', PA=355°
  - Very red (no background star)
  - S/N~3-4, Δmag=9.3 in H band
  - More extended in the H-band

Ligi et al. (2018)

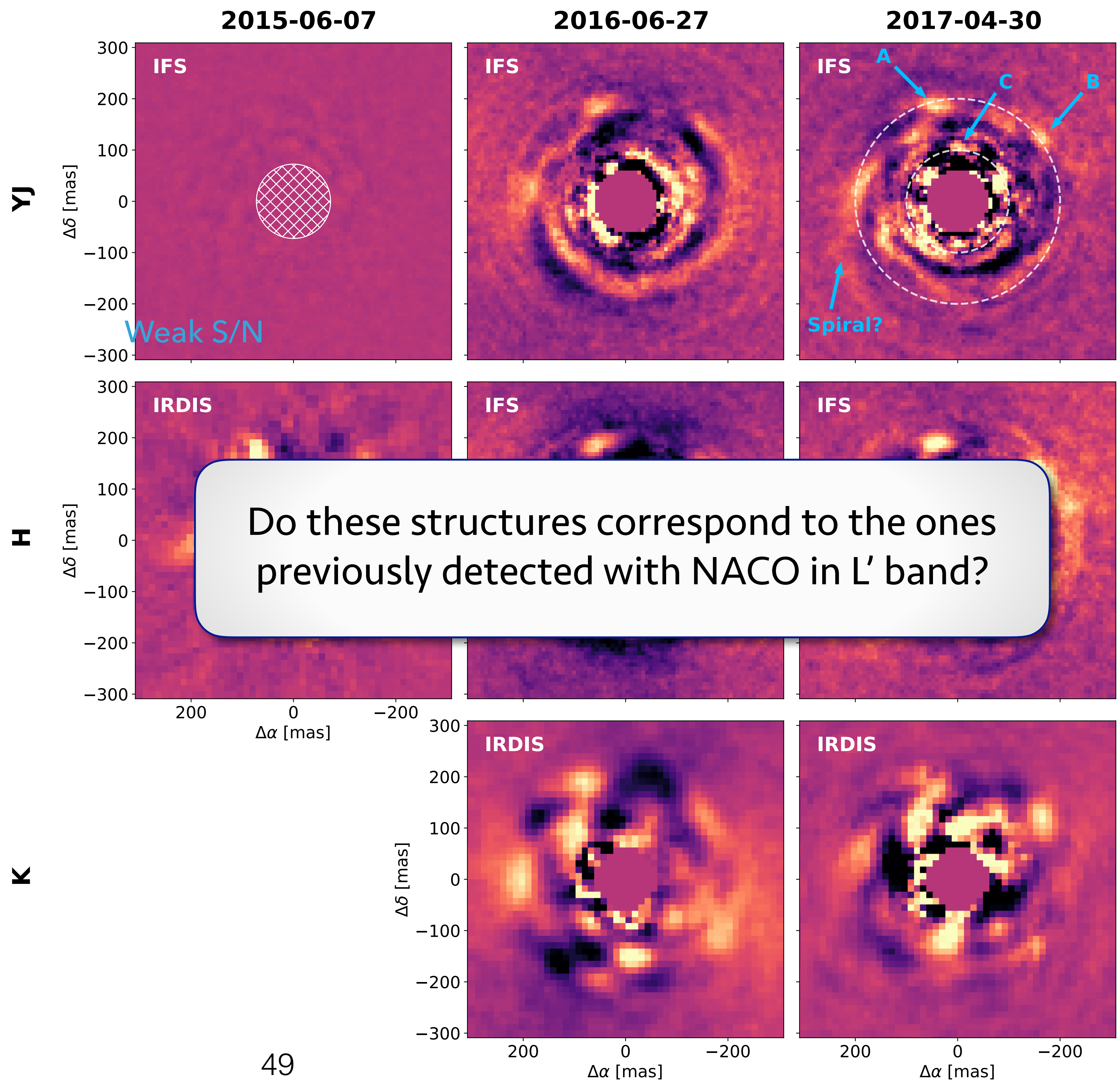

Do these structures correspond to the ones previously detected with NACO in L' band?

SPHERE/VLT OBSERVATIONS: DISK OR EXOPLANET?

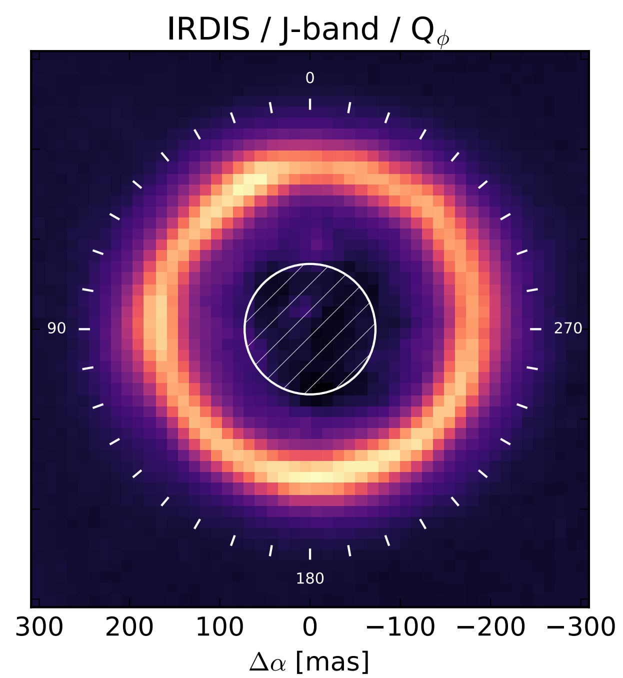

PDI (IRDIS) data (Pohl et al. 2017) and cADI simulation

- create copies of the PDI data and derotate them
- make data treatment as for IRDIS data

SPHERE/VLT OBSERVATIONS: DISK OR EXOPLANET?

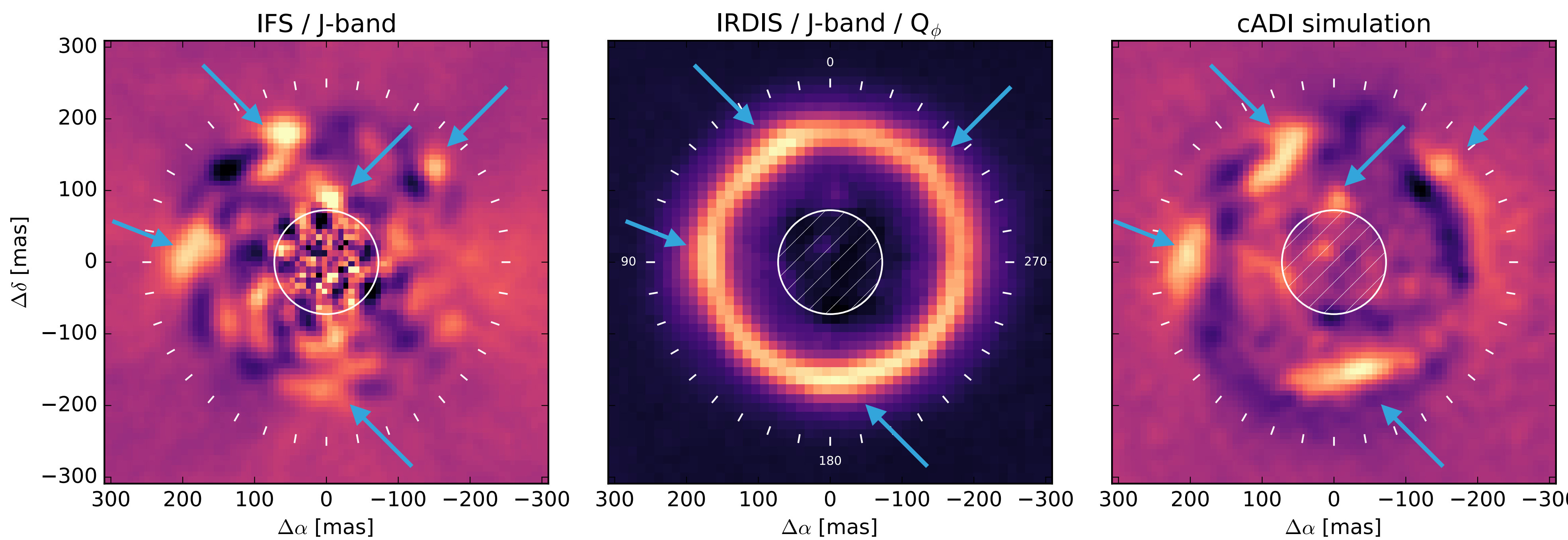

Results

- The bright structures previously detected appear on the resulting image
- the bright structures are polarized light
- detection at 100 mas?

SPHERE/VLT OBSERVATIONS: DISK OR EXOPLANET?

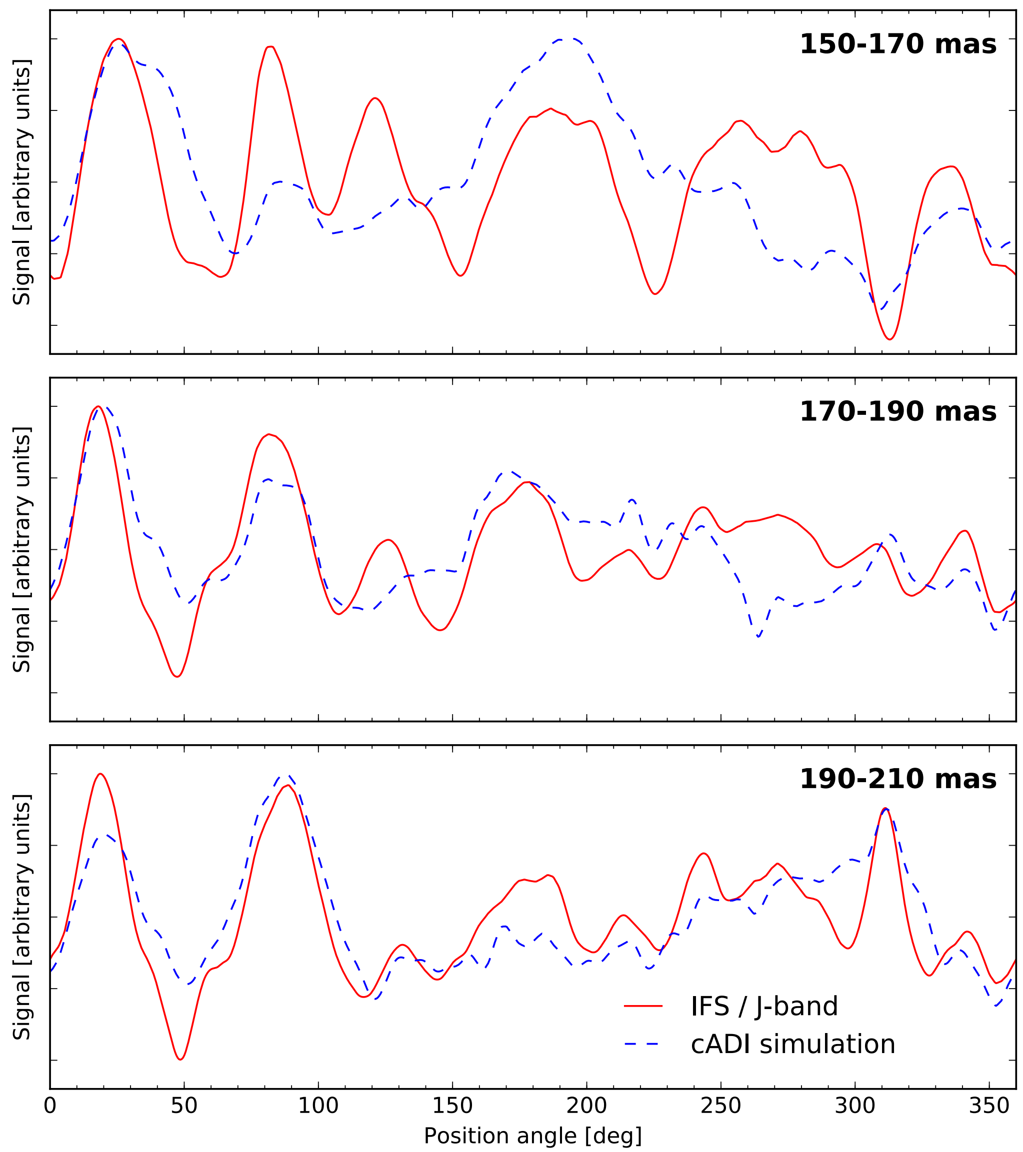

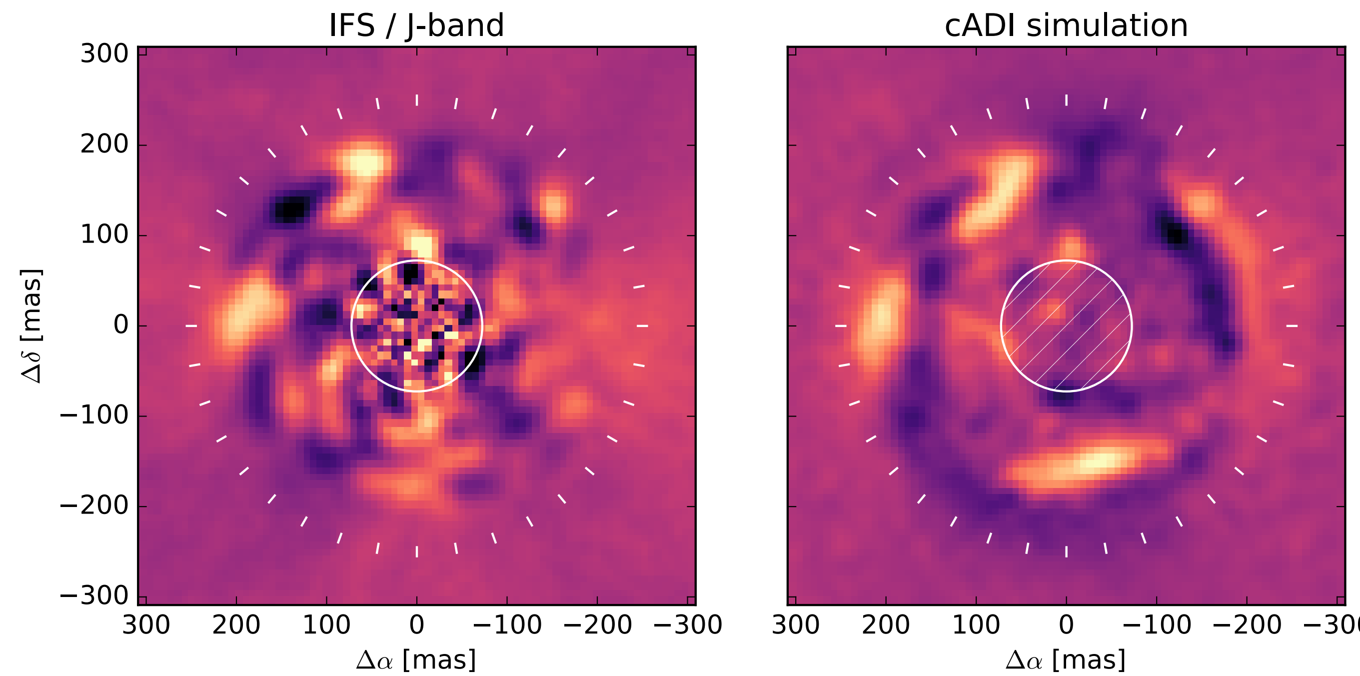

Results

- The bright structures previously detected appear on the resulting image
- the bright structures are polarized light
- detection at 100 mas?

The bright structure at 0.18'' belong to the ring!

SPHERE/VLT OBSERVATIONS: DISK OR EXOPLANET?

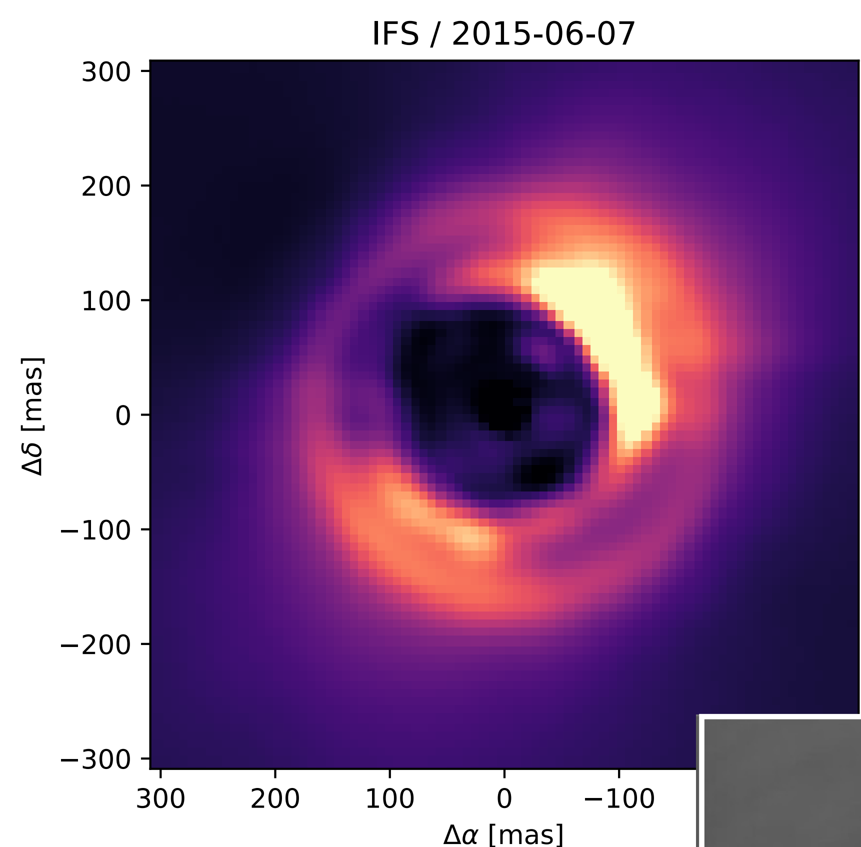

- A ring appears at a separation of ~180 mas
- in every data reduction
- Enhanced brightness structures at positions consistent with the bright blobs detected in ADI and with polarised data
- An additional ring at 100 mas, that does not appear in each reduction

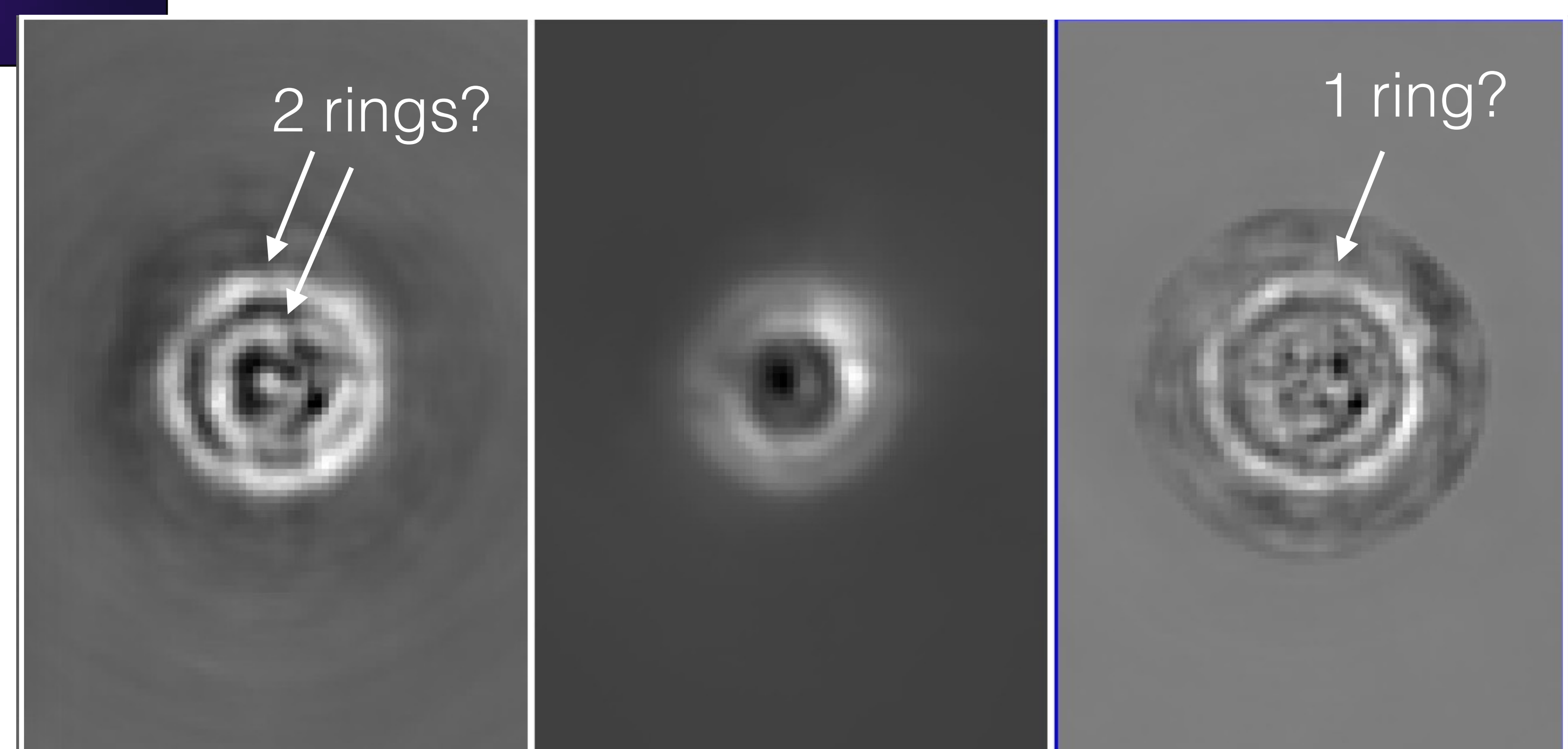

SPHERE/VLT OBSERVATIONS: DISK OR EXOPLANET?

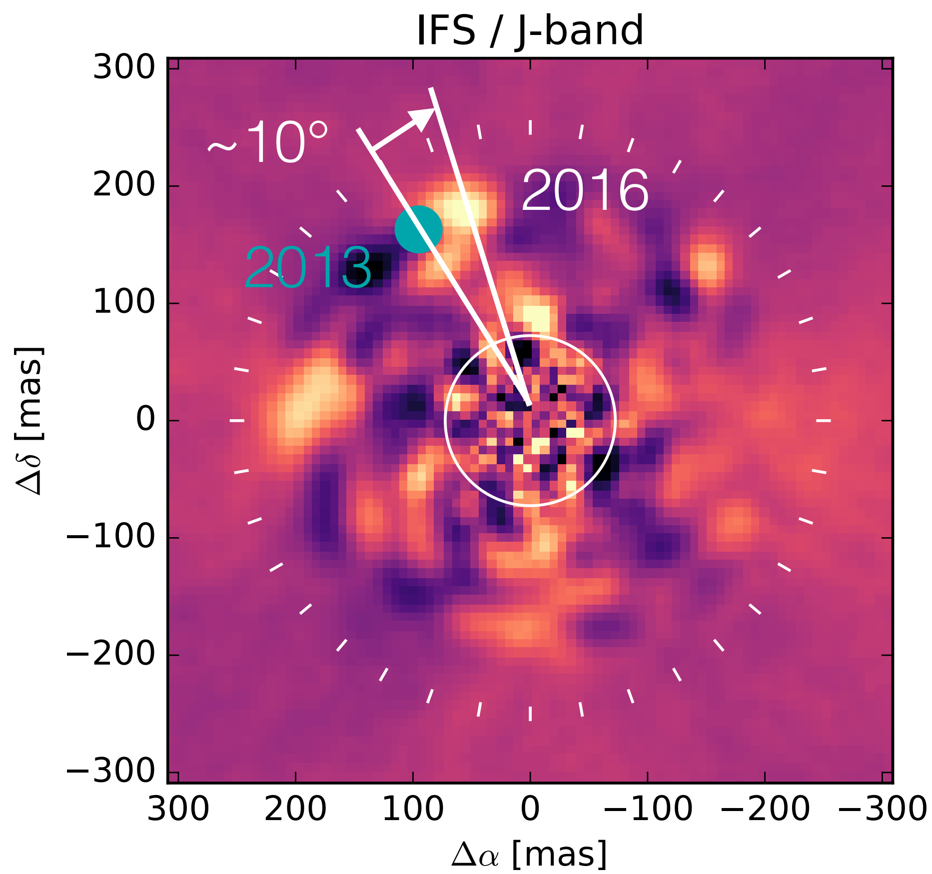

PA=33° in 2013 makes it at ~20° in 2016
→ Keplerian orbit, clockwise motion

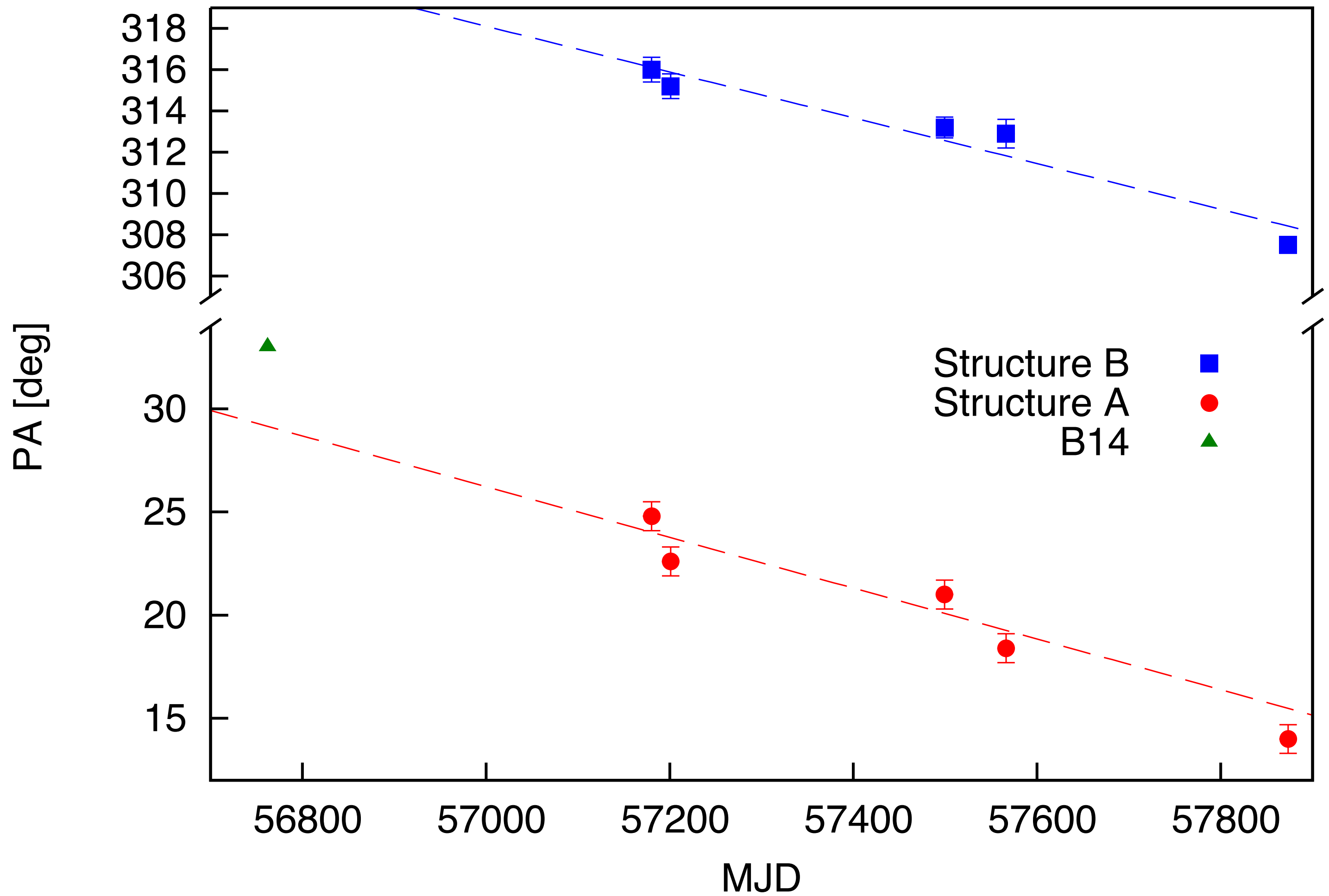

SPHERE/VLT OBSERVATIONS: DISK OR EXOPLANET?

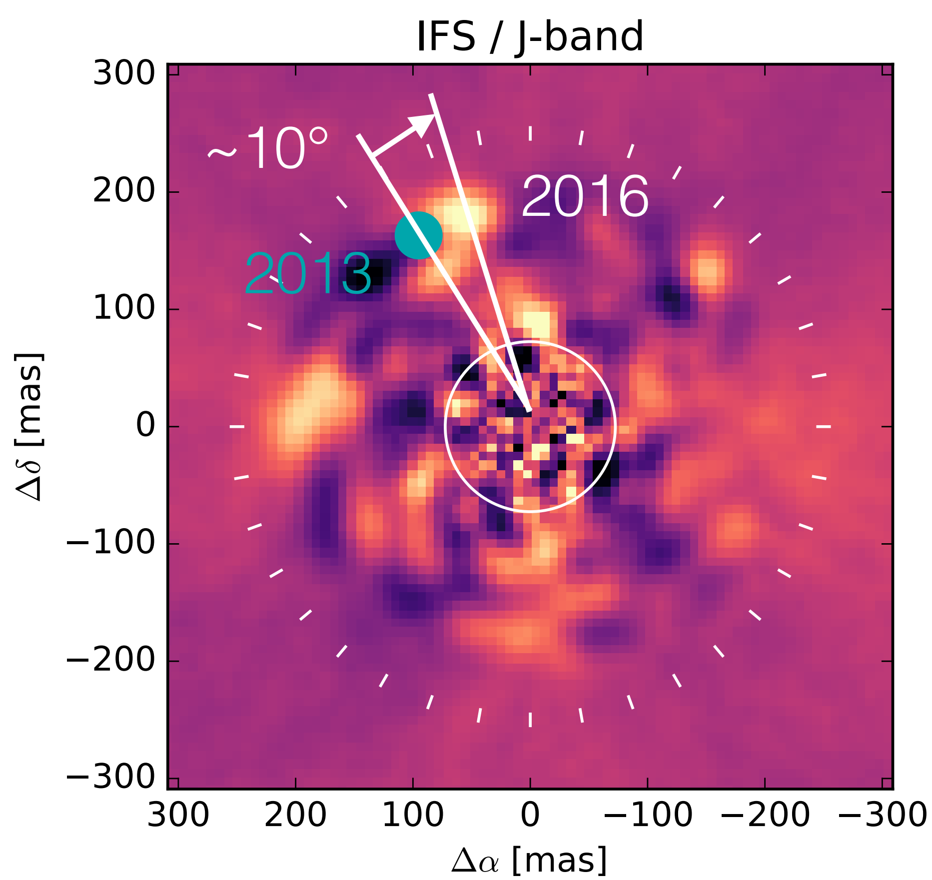

PA=33° in 2013 makes it at ~20° in 2016
→ Keplerian orbit, clockwise motion

Surdensity zones in the disk: origins?
→ Rossby wave instability (vortices)?
If so, could be precursors of forming planets!

SPHERE/VLT OBSERVATIONS: DISK OR EXOPLANET?

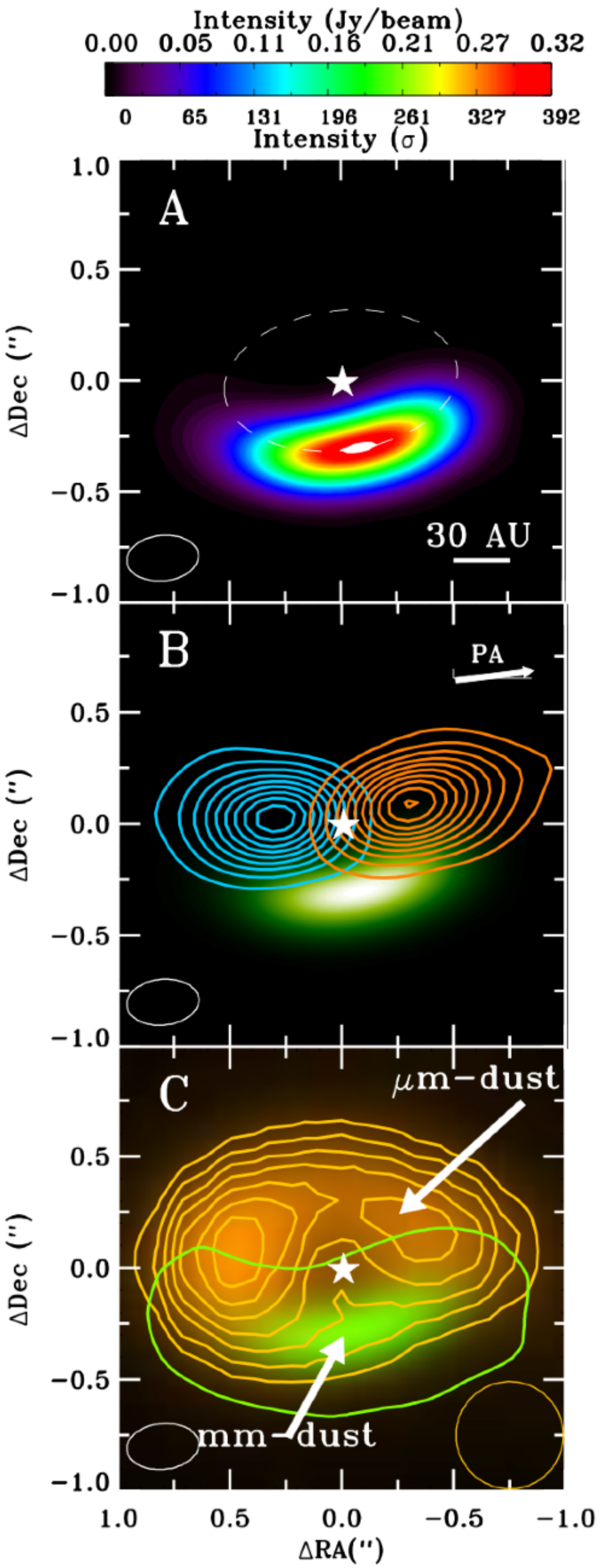

van der Marel+ 2013

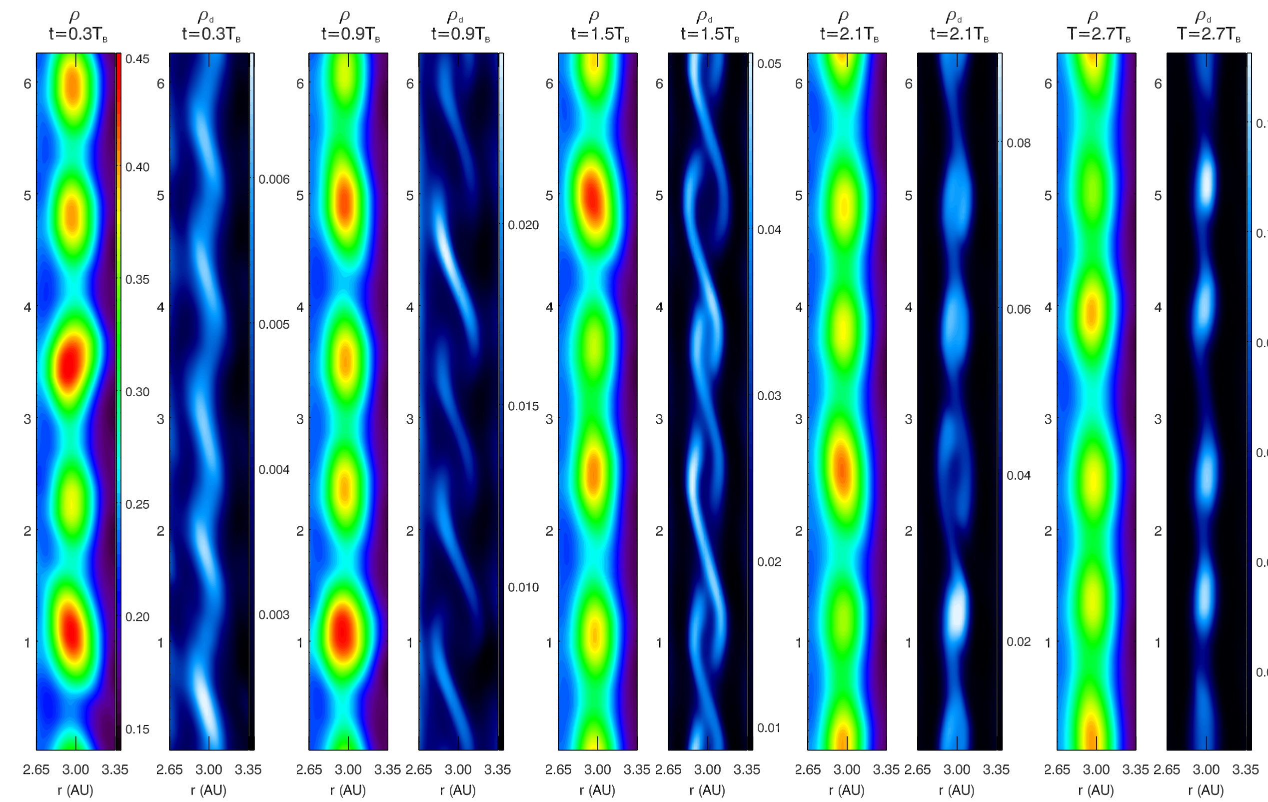

Méheut+ 2012

SPHERE/VLT OBSERVATIONS: DISK OR EXOPLANET?

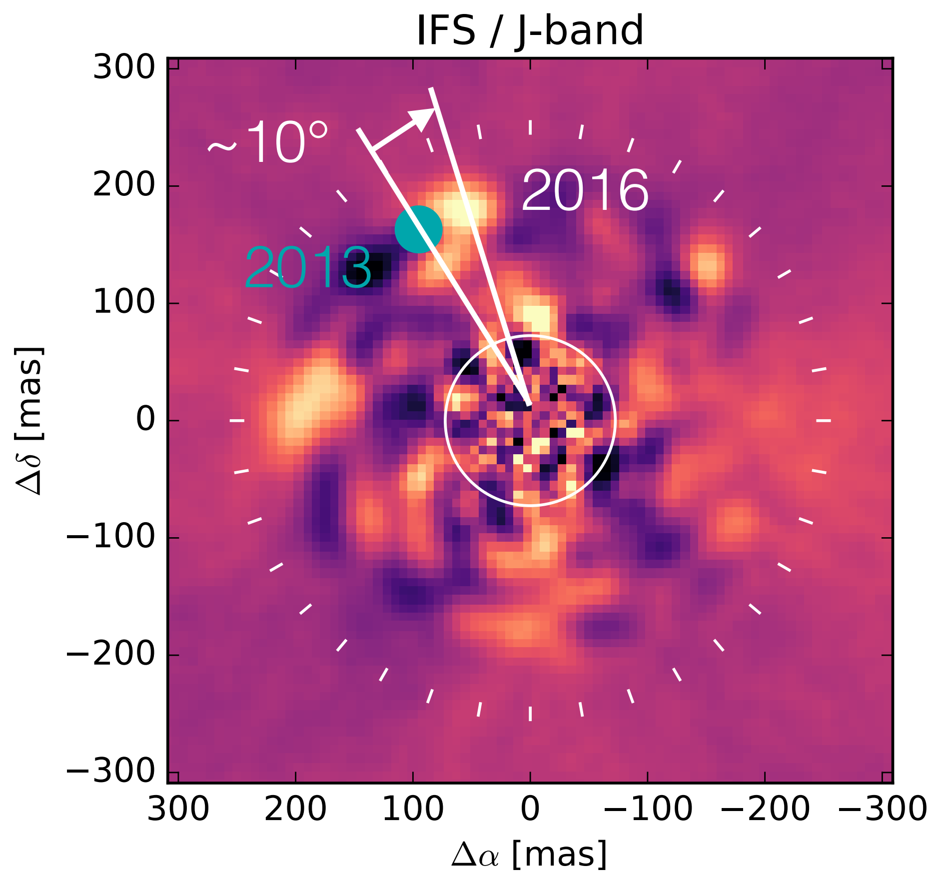

PA=33° in 2013 makes it at ~20° in 2016
→ Keplerian orbit, clockwise motion

Surdensity zones in the disk: origins?
→ Rossby wave instability (vortices)?
If so, could be precursors of forming planets!

→ Inhomogeneous illumination from the inner ring (if real)?
If so, what is the origin of these inner inhomogeneities?

OUTLINE

- Introduction: from the formation to the characterisation of exoplanets

- Characterisation of exoplanetary systems with interferometry

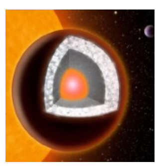

- Getting the most out of it: 55 Cnc

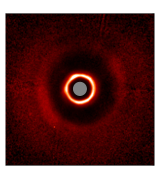

- Detection of exoplanets with direct imaging: insights in the system of HD169142

- Formation mechanisms: the challenging case of GJ504

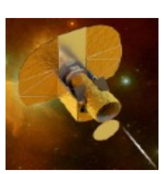

- Conclusion and perspectives

A COMPANION FORMATION DEPENDING ON THE STELLAR AGE

GJ504
G0V bright star
High metallicity
High activity

One companion detected at 43.5 au (SEEDS survey)

Mass of the companion?
Strongly depends on the age of the star!

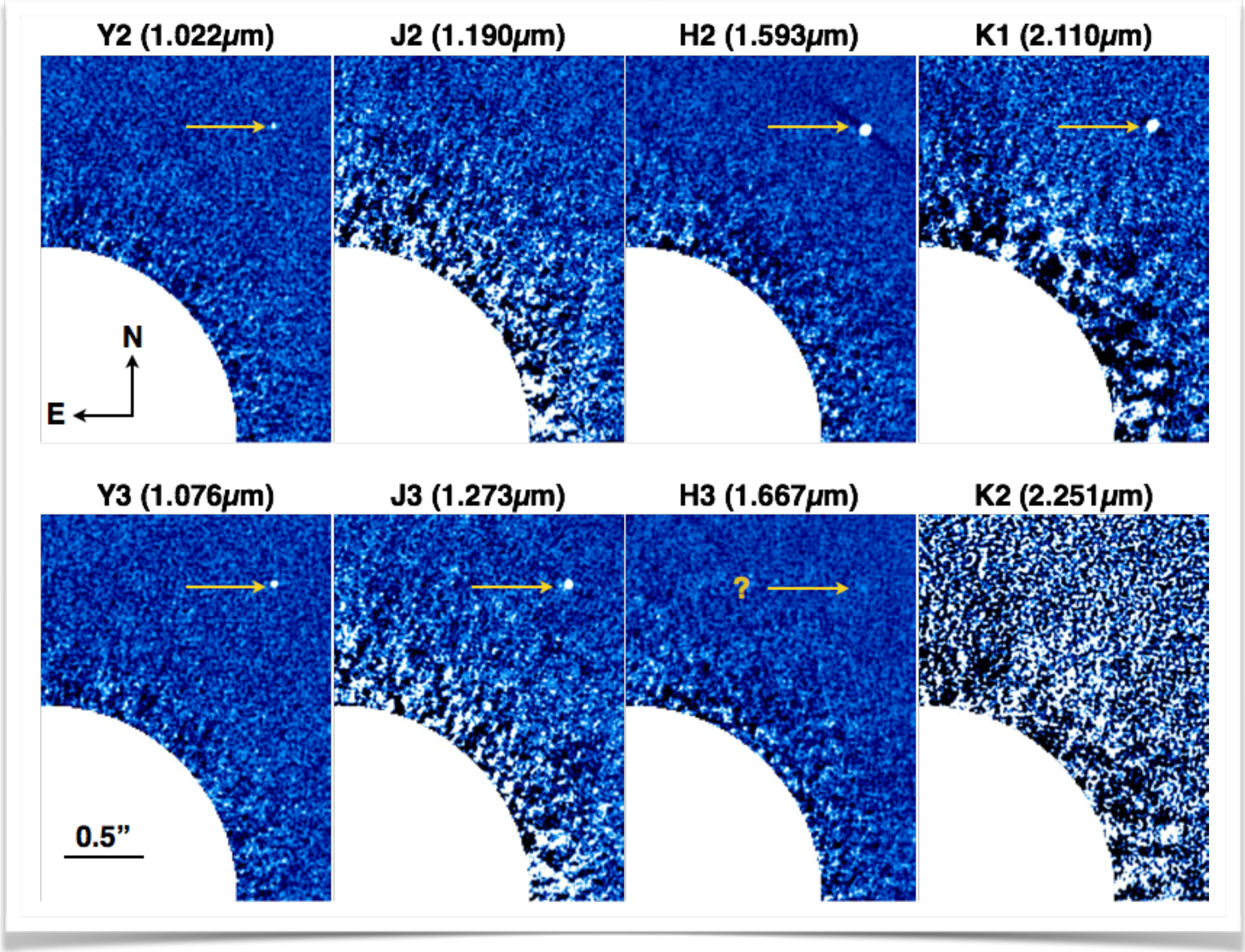

IRDIS & IFS images (SPHERE/VLT), SHINE survey
Bonnefoy et al. (in prep.)

A COMPANION FORMATION DEPENDING ON THE STELLAR AGE

Kazuhara et al. (2013)
➔ 4 M_{Jup}, 160 Myr
(rotational period, activity)

Fuhrmann & Chini (2015)
➔ 25 M_{Jup}, 4.5 Gyr
(high-resolution spectroscopy)

d'Orazi et al. (2017)
➔ BD, 2.5 Gyr
(differential spectroscopy)

etc.

~25 M_{Jup} ↑ 4.5 Gyr (Fuhrmann & Chini 2015)

~4 M_{Jup} ↑ 160 Myr (Kuzuhara et al. 2013)

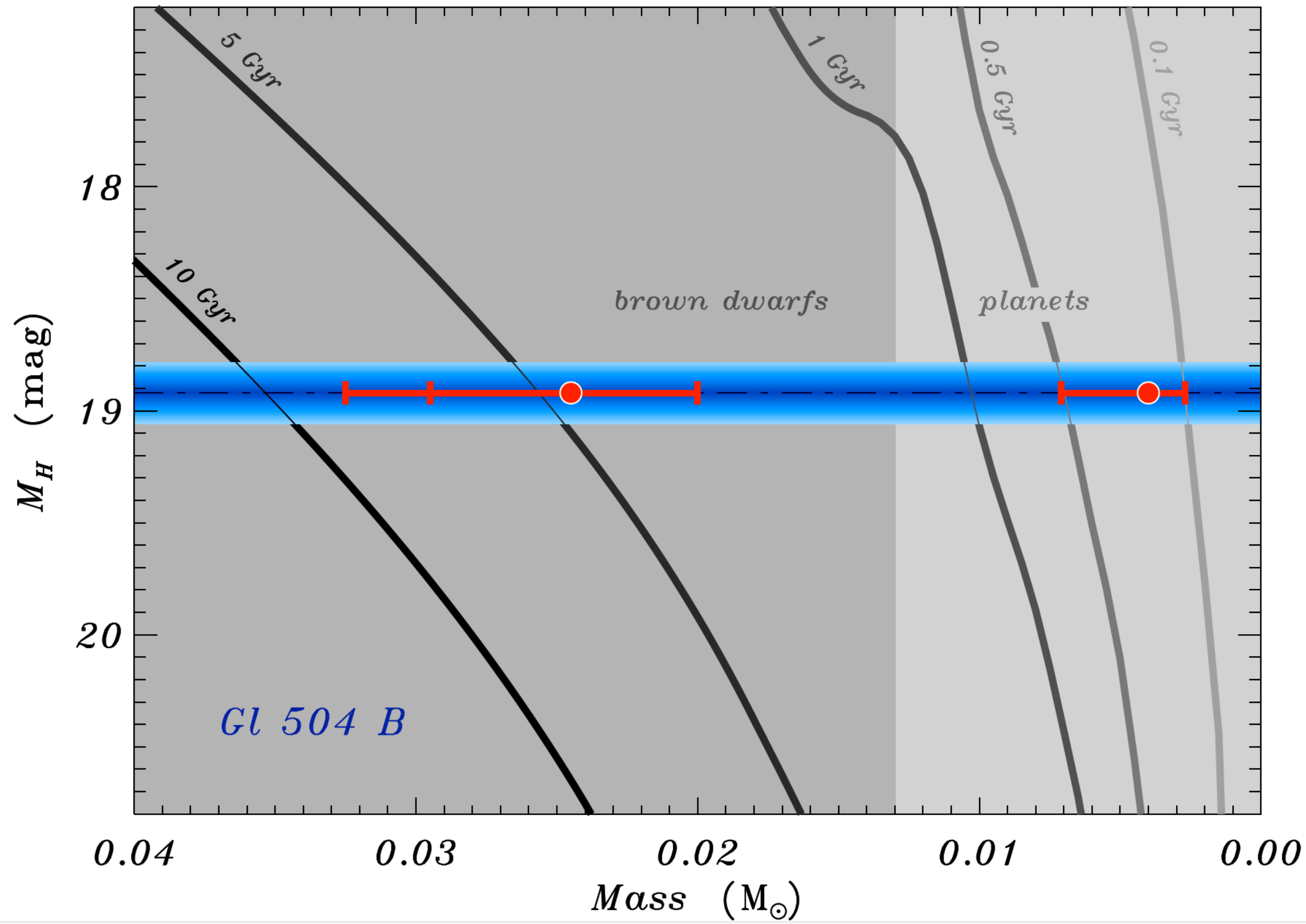

Fuhrmann & Chini (2015)

A COMPANION FORMATION DEPENDING ON THE STELLAR AGE

Different masses call different formation mechanisms:

Skemer et al. (2016)

➔ $T_{eff,c}$ = 543±11 K

➔ T/Y transition and high metallicity

➔ low surface gravity

(imaging, LBT/LMIRCam)

SPHERE SED

➔ T8-T9.5 object with a peculiar SED

Compatible with low surface gravity

(➔ young age) or/and super-solar metallicity, thus core accretion mechanism

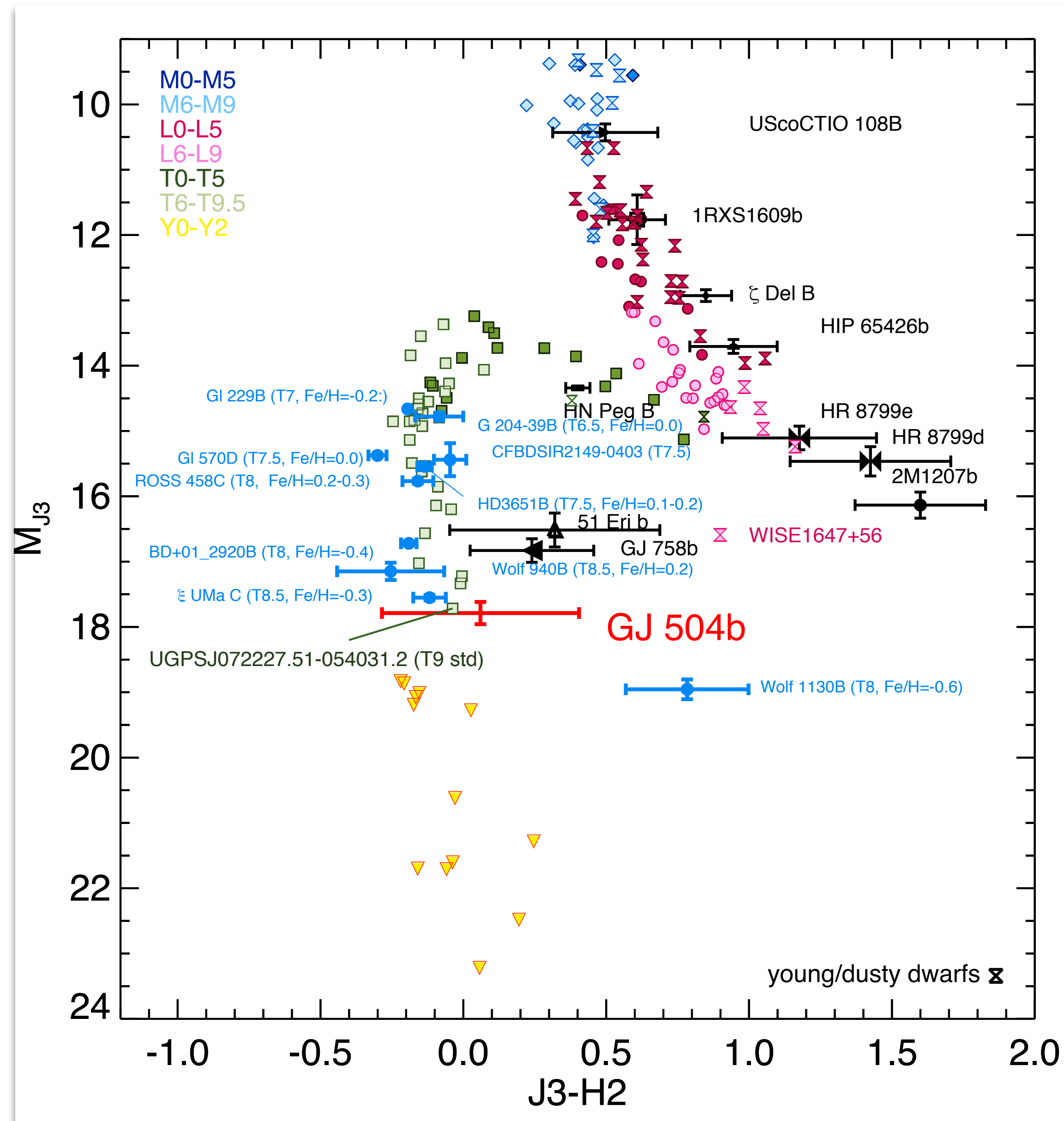

Bonnefoy et al. (in prep.)

A COMPANION FORMATION DEPENDING ON THE STELLAR AGE

Different masses call different formation mechanisms:

Furhmann et al. (2013)

High metallicity

3.3 days rotation period

high chromospheric activity,

➔ merging scenario of a second companion

D'Orazi et al. (2017)

➔ engulfment scenario if <3 M_{Jup} at 0.03 au

Driven by the Kozai-Lidov effect

Would explain the spin-orbit misalignment proposed by Bonnefoy et al. (in prep.).

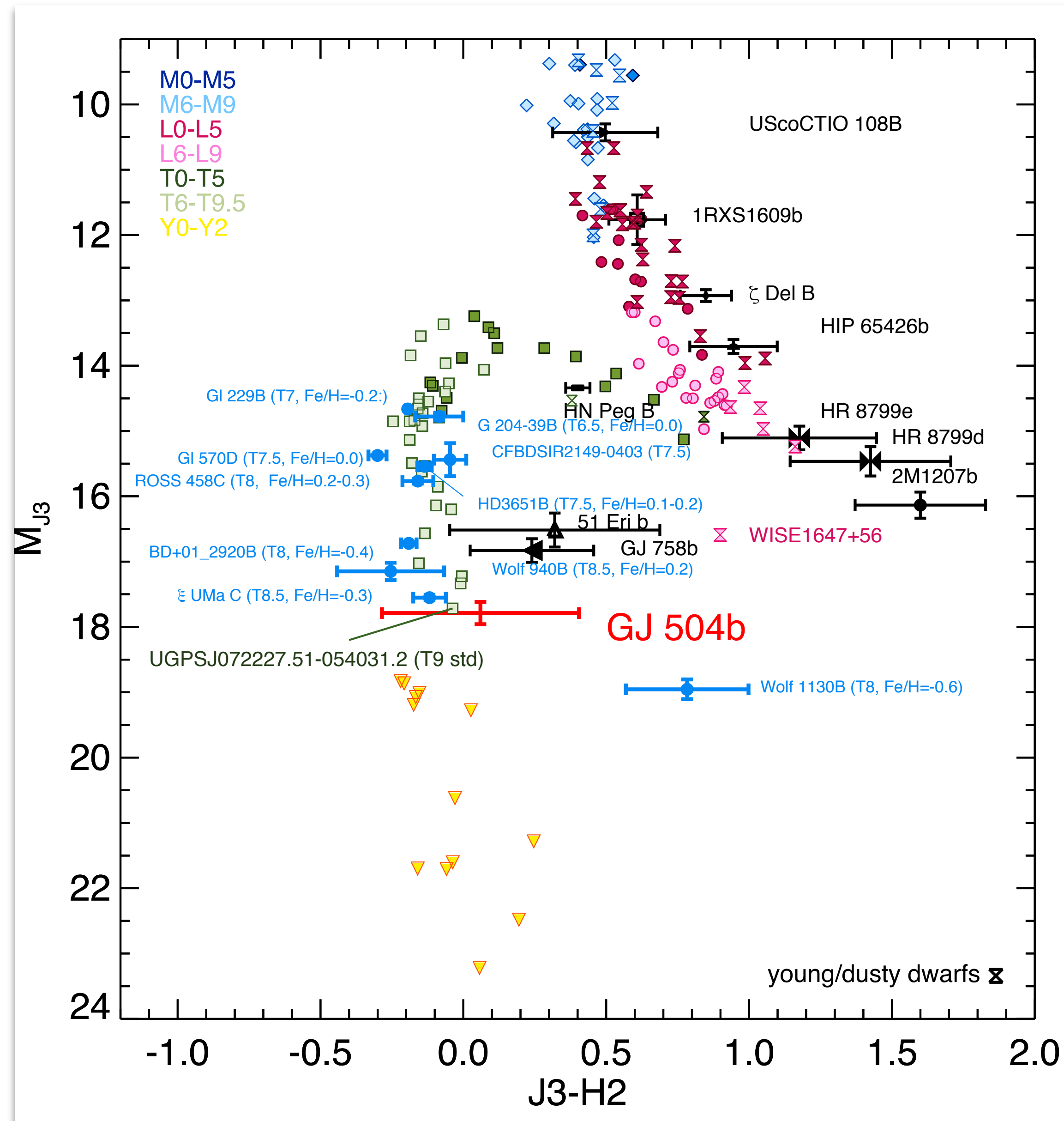

Bonnefoy et al. (in prep.)

BRINGING NEW CONSTRAINS

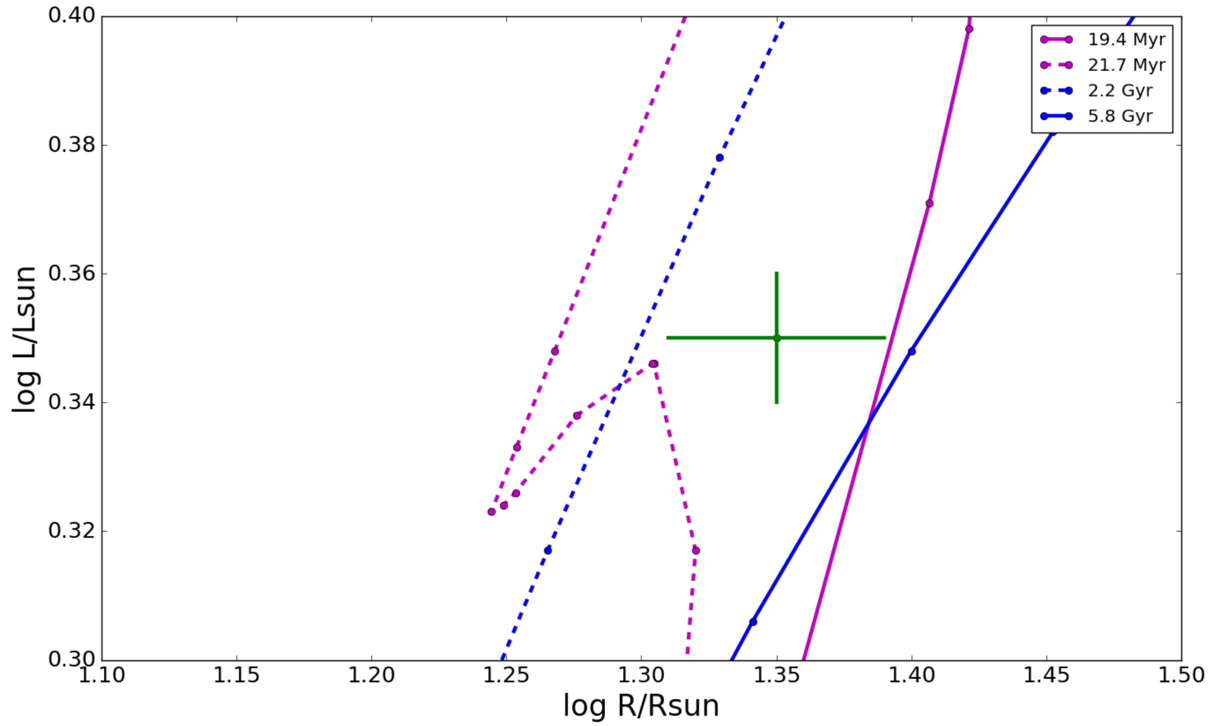

Interferometric measurements
to refine the isochronal age:
VEGA/CHARA
0.71±0.02 mas

But still compatible with **2 isochronal ages**:
21±2 Myr
4.0±1.8 Gyr

Combining SPHERE+RV+model

BD + old system:
Gravitational instability + inward migration

Planet + young system:
core accretion but challenging given the system properties

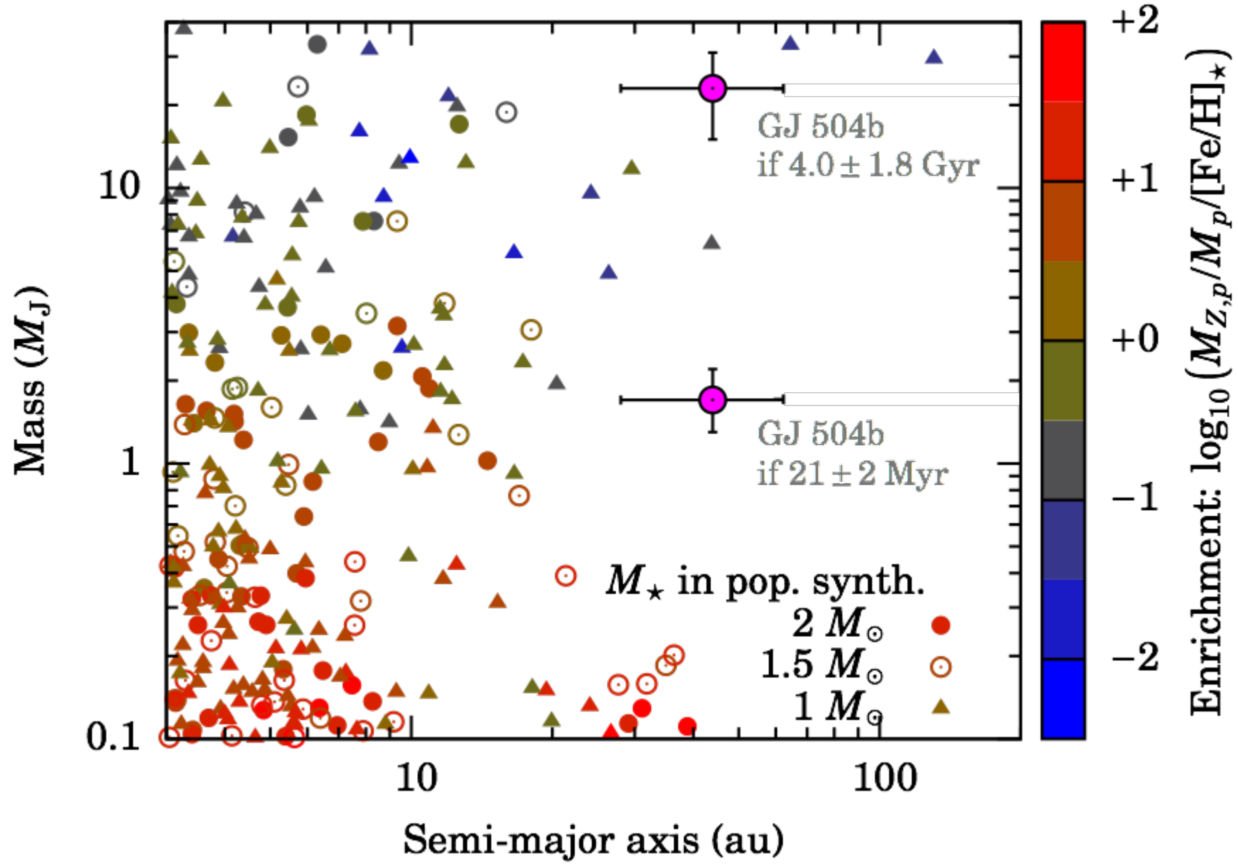

Bonnefoy et al. (in prep.)

BRINGING NEW CONSTRAINS

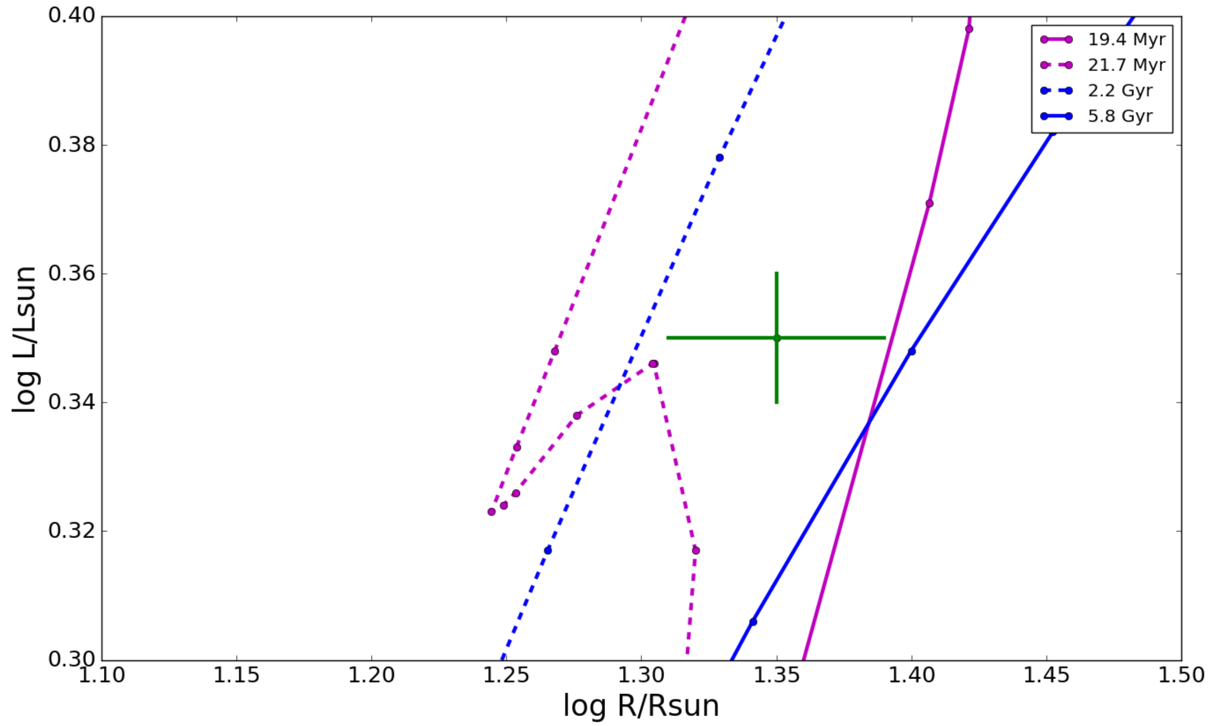

Interferometric measurements to refine the isochronal age:
VEGA/CHARA
0.71±0.02 mas

But still compatible with **2 isochronal ages**:
21±2 Myr
4.0±1.8 Gyr

Combining SPHERE+RV+model

BD + old system:
Gravitational instability + inward migration

Planet + young system:
core accretion but challenging given the system properties

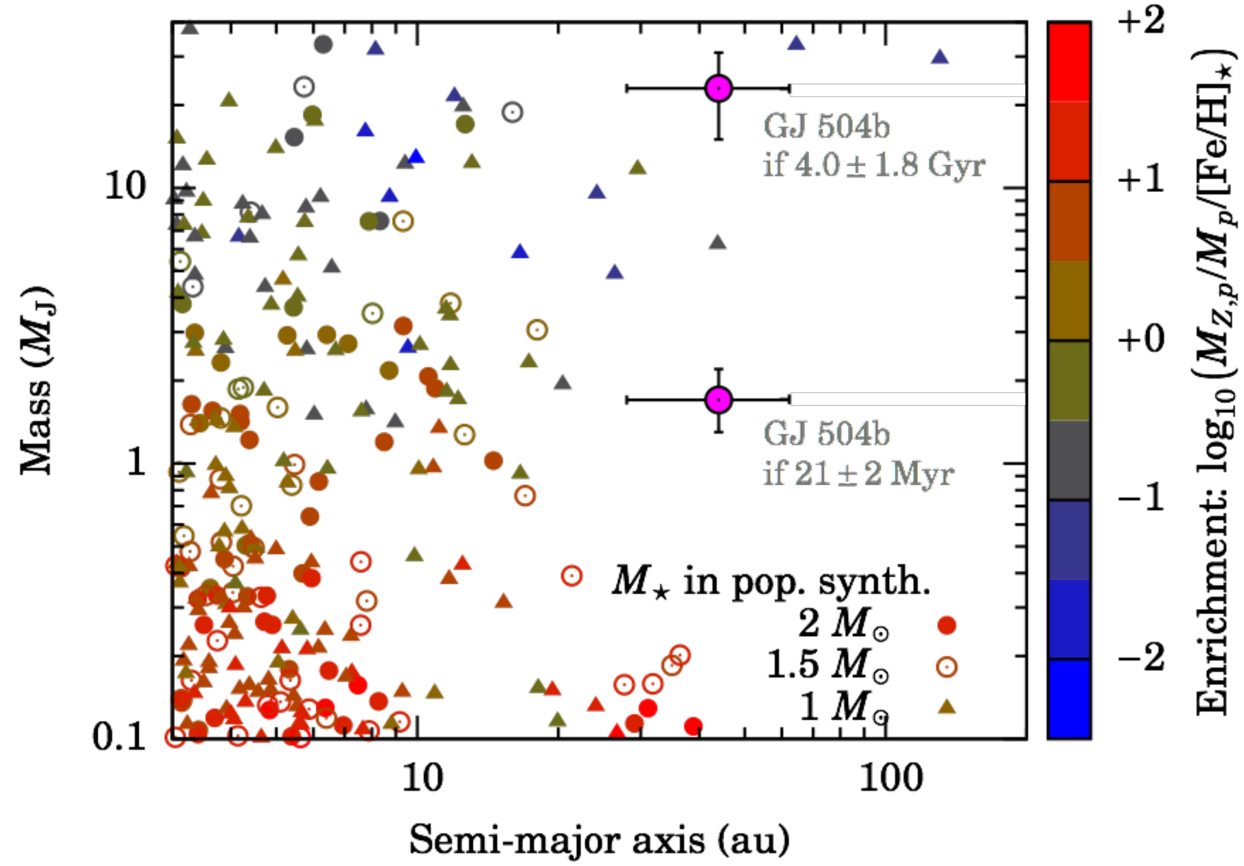

Bonnefoy et al. (in prep.)

To be continued…

OUTLINE

- Introduction: from the formation to the characterisation of exoplanets

- Characterisation of exoplanetary systems with interferometry

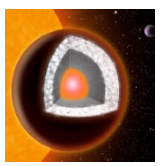

- Getting the most out of it: 55 Cnc

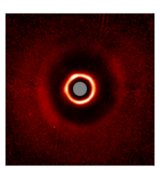

- Detection of exoplanets with direct imaging: insights in the system of HD169142

- Formation mechanisms: the challenging case of GJ504

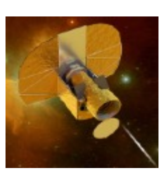

- Conclusion and perspectives

INTERFEROMETRY FOR FAINTER STARS

Stars harbouring transiting exoplanets

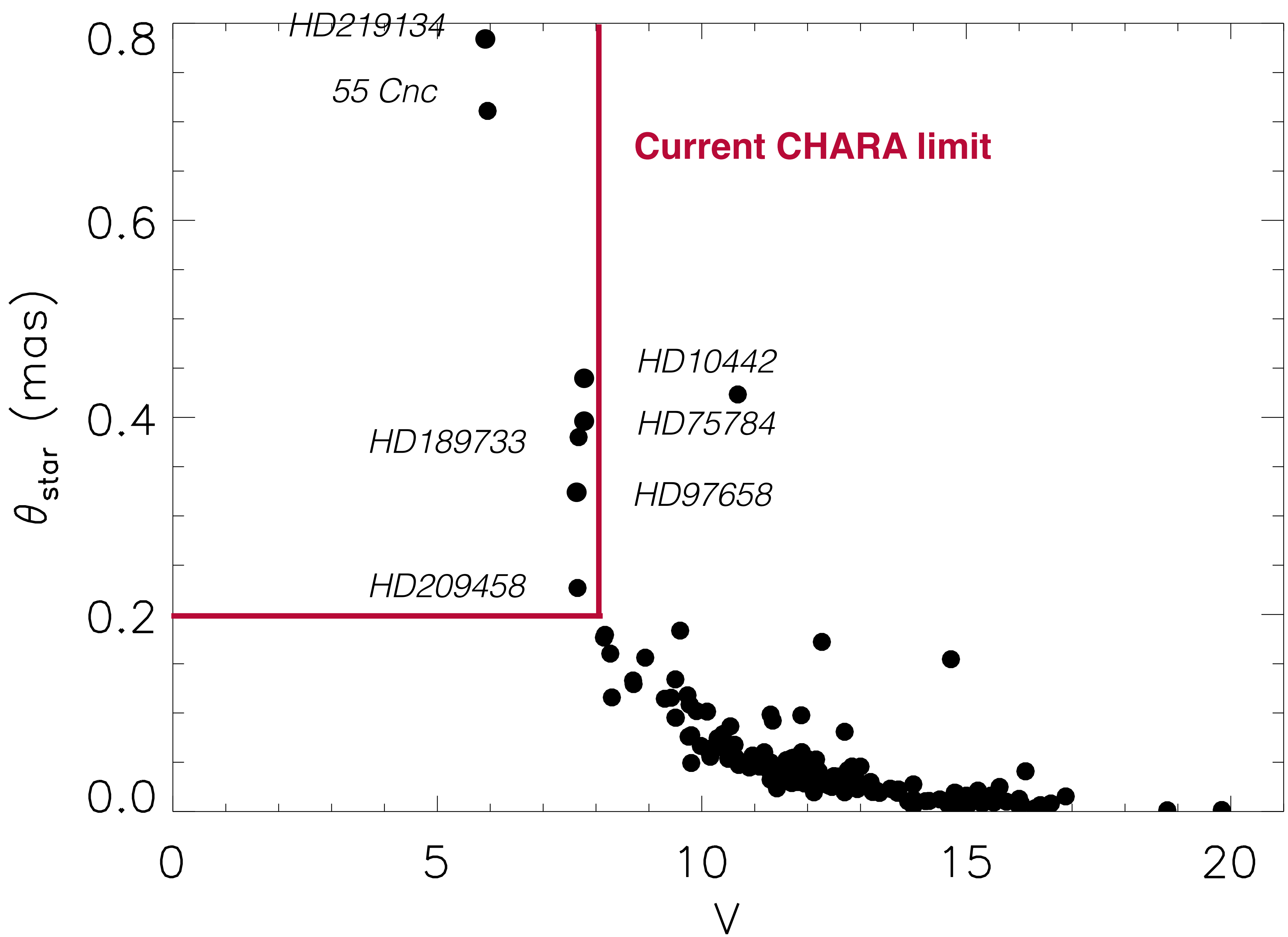

INTERFEROMETRY FOR FAINTER STARS

Stars harbouring transiting exoplanets

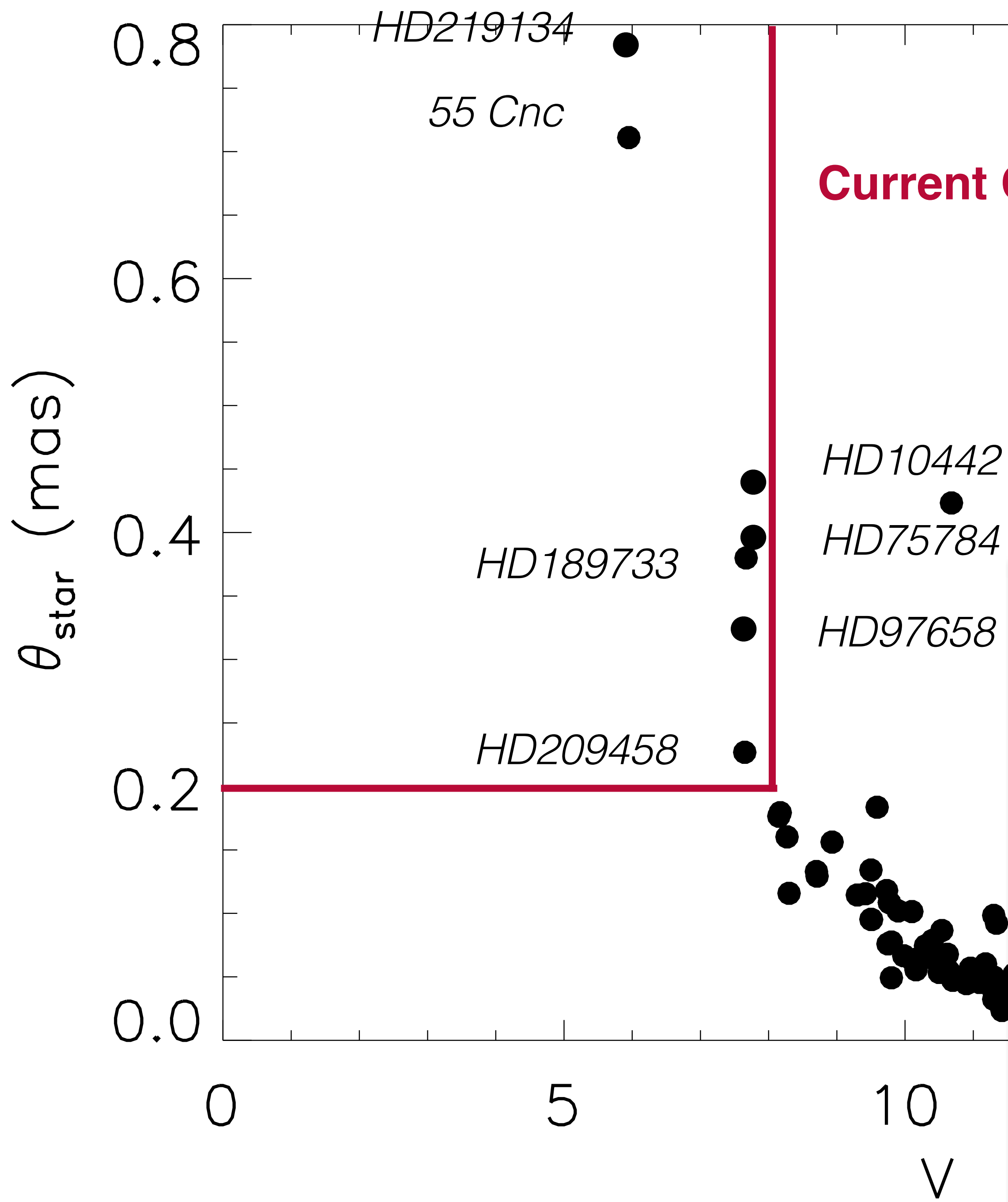

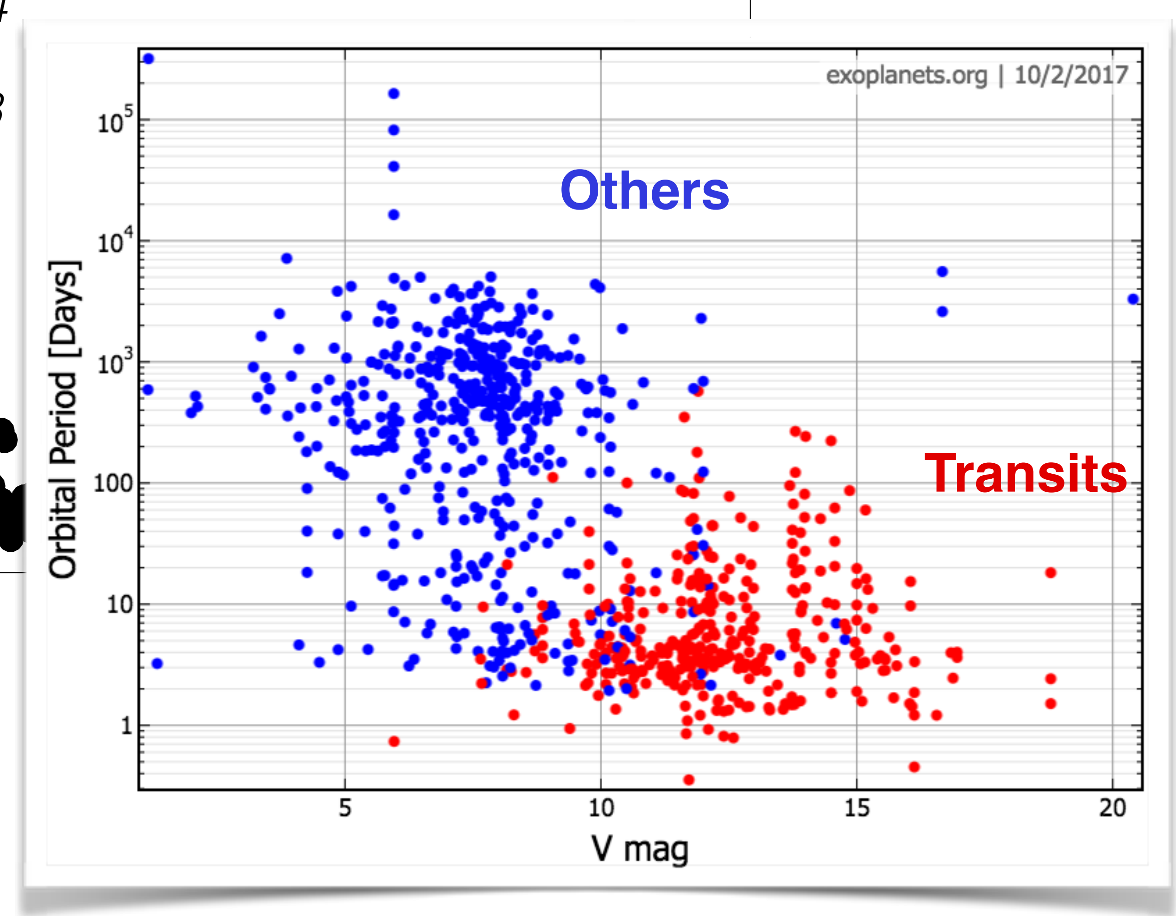

PLATO, TESS, CHEOPS…

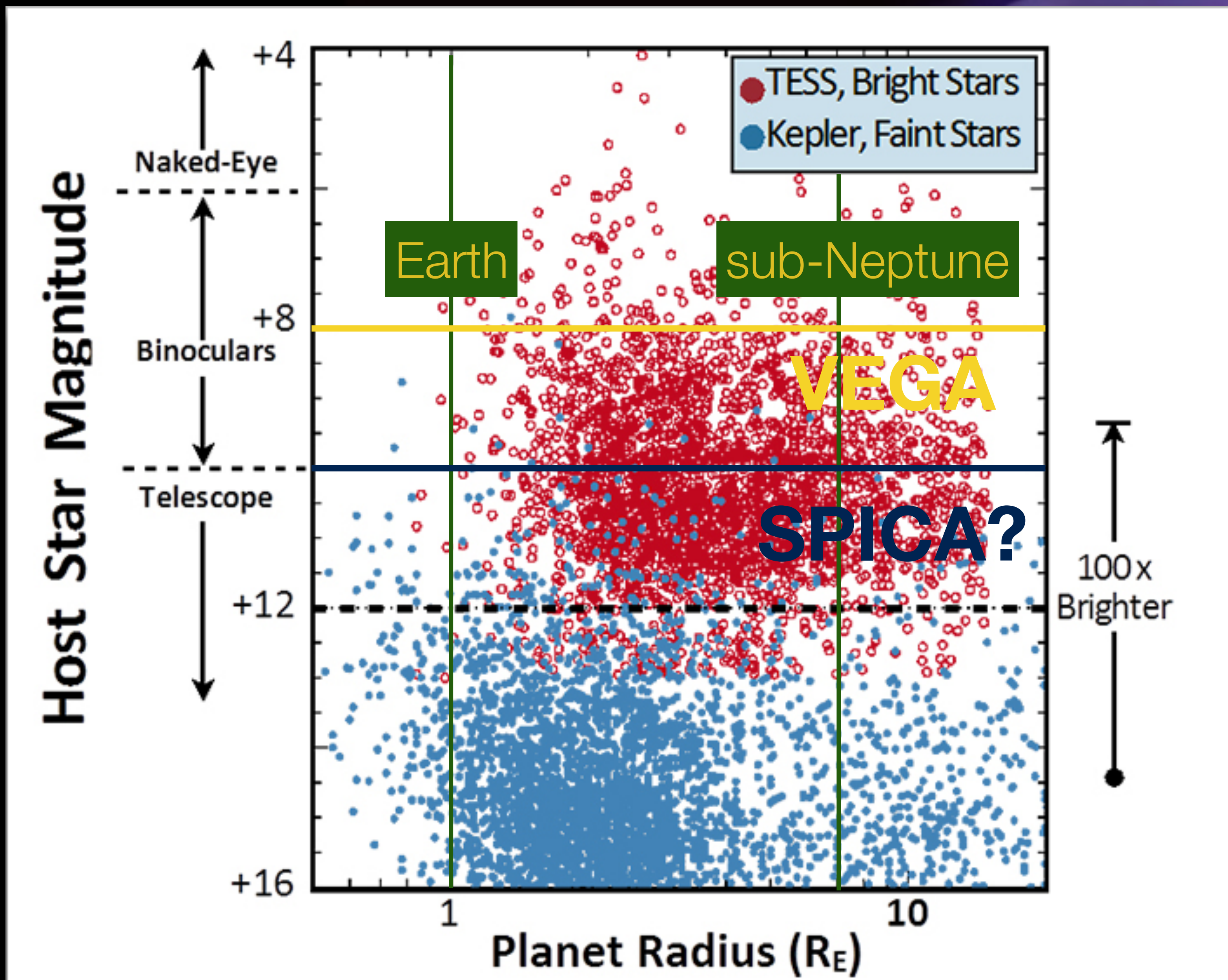

Impression

PLATO, TESS, CHEOPS...

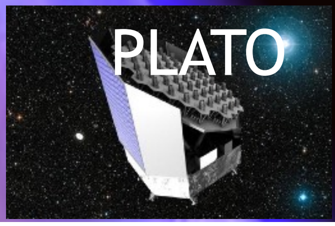

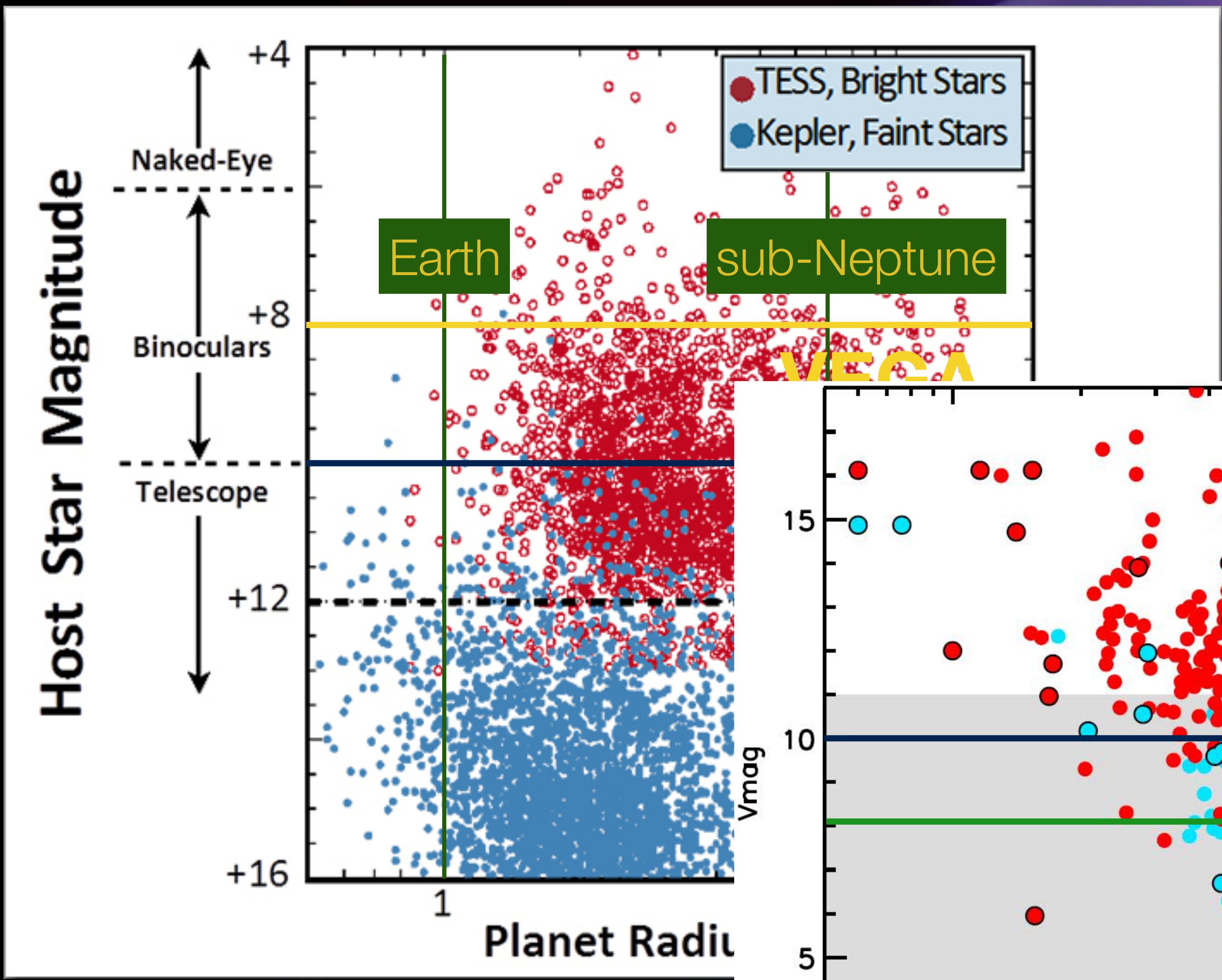

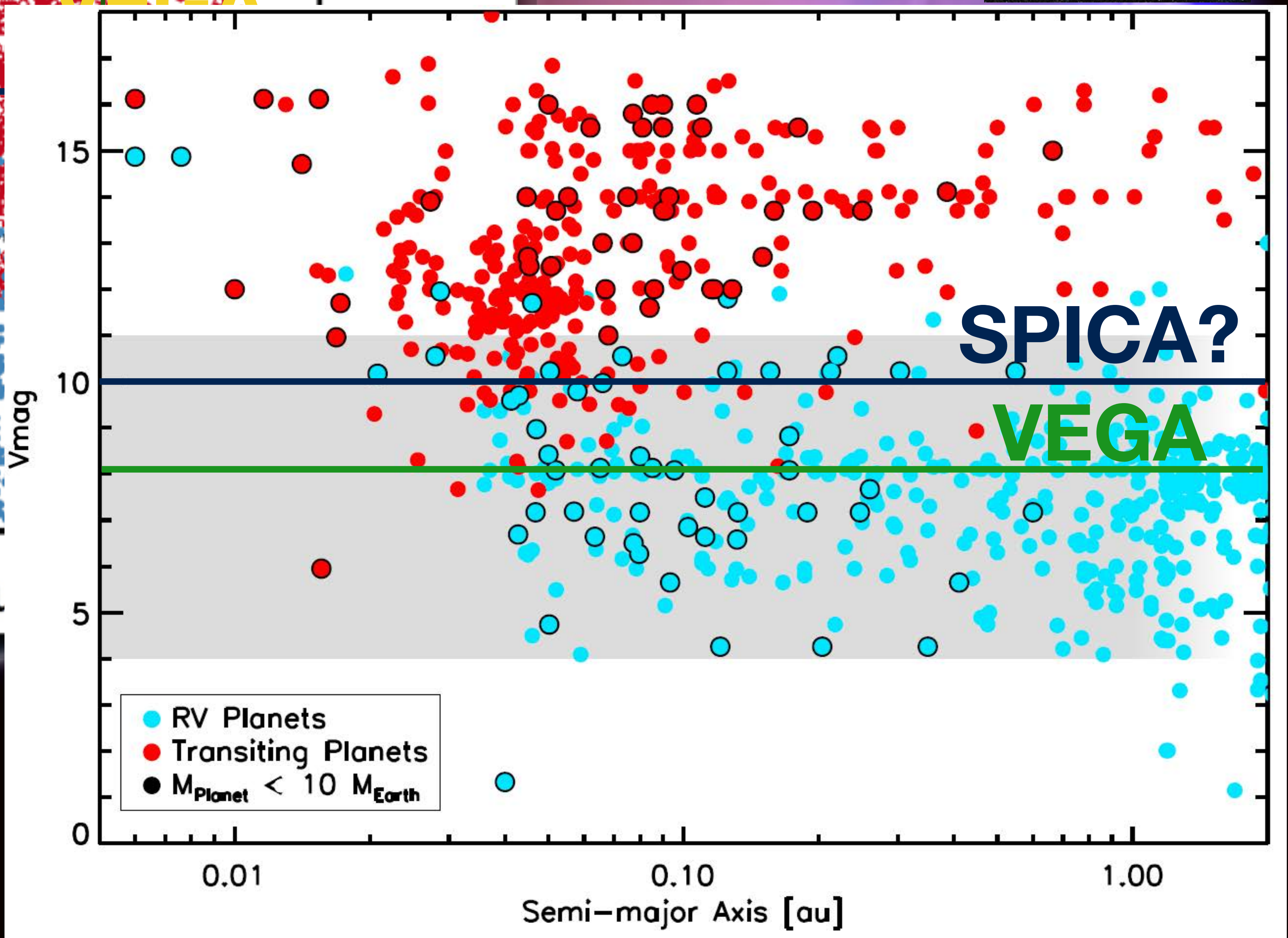

Impression

PLATO, TESS, CHEOPS...

In the (near) future...

More targets

Complementarity between instruments/missions

➔ Better characterisation case by case: composition, habitability.

➔ Better global view: link between planetary parameters and formation mechanisms

➔ Still some stars too faint: refine empirical relations

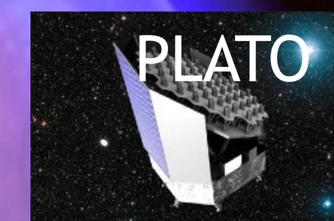

...

THANK YOU
FOR YOUR ATTENTION!